TECHNISCHE UNIVERSITÄT MÜNCHEN

Lehrstuhl für Chemisch-Technische Analyse und
Chemische Lebensmitteltechnologie

In Vitro Toxicokinetics of Ethylene and Ethylene Oxide in Mice, Rats, and Humans

Qiang Li

Vollständiger Abdruck der von der Fakultät Wissenschaftszentrum Weihenstephan für Ernährung, Landnutzung und Umwelt der Technischen Universität München zur Erlangung des akademischen Grades eines

Doktors der Naturwissenschaften

genehmigten Dissertation.

Vorsitzender: Univ.-Prof. Dr. K.-H. Engel

Prüfer der Dissertation:

1. Univ.-Prof. Dr. Dr. h. c. H. Parlar
2. apl. Prof. Dr. J. G. Filser
3. Priv.-Doz. Dr. M. Coelhan

Die Dissertation wurde am 05.03.2012 bei der Technischen Universität München eingereicht und durch die Fakultät Wissenschaftszentrum Weihenstephan für Ernährung, Landnutzung und Umwelt am 12.06.2012 angenommen.

Diese Arbeit wurde im
Institut für Toxikologie am
Helmholtz Zentrum München angefertigt
und dort von Prof. Dr. J. G. Filser betreut.

Part of the thesis has been published

Li, Q., Csanády, G. A., Kessler, W., Klein, D., Pankratz, H., Pütz, C., Richter, N., and Filser, J.G. (2011). Kinetics of ethylene and ethylene oxide in subcellular fractions of lungs and livers of male B6C3F1 mice and male Fischer 344 rats and of human livers. *Toxicol. Sci.* **123,** 384–398.

Li, Q., Csanády, Gy. A., Klein, D., and Filser, J. G. (2009). Metabolism of ethylene oxide in microsomes and cytosol from livers and lungs of B6C3F1 mice, Fischer 344 rats, and humans. *Naunyn-Schmiedeberg's Arch. Pharmacol.* **379** (Suppl. 1)**,** 64.

Li, Q., Csanády, Gy. A., Artati, A., Khan, M. D., Riester, M. B., and Filser, J. G. (2008). Ethylene inhibits its own metabolism in liver and lung microsomes from male Fischer 344 rats and B6C3F1 mice. *Naunyn-Schmiedeberg's Arch. Pharmacol.* **377** (Suppl. 1)**,** 70.

Table of Contents

1 INTRODUCTION

1.1 Objective

The gaseous olefin ethylene (ET) is the largest-volume organic chemical produced worldwide. It is mainly used in the synthesis of polymers and industrial chemicals. ET is ubiquitously present in the environment, arising predominantly as a natural product from vegetation and from incomplete combustion of organic material. In mammals, ET is biotransformed to the reactive metabolite ethylene oxide (EO) which is mutagenic and carcinogenic. The International Agency for Research on Cancer (IARC, 2008) classifies EO as a “known human carcinogen”. In spite of the formation of its metabolite EO, ET was neither mutagenic *in vitro* nor *in vivo*. It was also not carcinogenic in an animal study, which was carried out in rats. IARC (1994a) evaluated ET as “not classifiable as to its carcinogenicity to humans”.

Validated physiological toxicokinetic models are required for estimating the risks of chemicals to human health. Although several working groups investigated the toxicokinetics and metabolism of ET and EO in laboratory animals, important toxicokinetic data on the ET metabolism mediated by cytochrome P450-dependent monooxygenase (CYP) and on the spontaneous and enzyme catalyzed elimination of EO are missing. Furthermore, no toxicokinetic data on EO in humans have been published. Therefore, in the present work CYP-mediated kinetics of ET and epoxide hydrolase (EH) as well as glutathione S-transferase (GST) catalyzed kinetics of EO were investigated using subcellular fractions prepared from livers of B6C3F1 mice, Fischer 344 rats or human donors or from lungs of mice or rats. The obtained kinetic parameters were verified on *in vivo* data and on data obtained additionally in homogenates of several rat tissues and of mouse liver.

1.2 Ethylene and ethylene oxide

1.2.1 Physicochemical properties

The olefin ET also known as ethene (CAS registry number 74-85-1; Figure 1.1) is a colorless flammable gas with a sweet odor (threshold 290 ppm; Amoore and Hautala, 1983). It is very slightly soluble in water (0.26% v/v), slightly soluble in ethanol, acetone and benzene, and soluble in diethyl ether (summarized in IARC, 1994a). Other physicochemical properties are listed in Table 1.1.

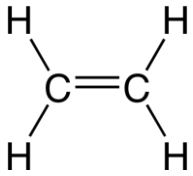

Figure 1.1 Molecular structure of ethylene

Table 1.1 Physicochemical properties of ethylene (IARC, 1994a)

Physicochemical property	Value
Molecular weight	28.05
Boiling point	-103.7°C
Melting point	-169°C
Vapor pressure	4270 kPa (0°C)
Relative vapor density	0.9686 (0°C; air = 1)
Lower explosive limit in air	2.75 vol%
Conversion factor	1 ppm = 1.15 mg/m^3 (25°C, 101.3 kPa)

EO (CAS registry number 75-21-8; Figure 1.2), also known as epoxyethane is a colorless flammable gas with a faintly sweet odor at room temperature and normal atmospheric pressure. EO is readily soluble in water and most organic solvents such as alcohol, diethyl ether, acetone and benzene (Lide, 2006). Under acidic condition, it hydrolyzes via ring opening. Other physicochemical properties are listed in Table 1.2.

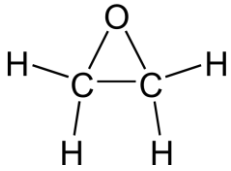

Figure 1.2 Molecular structure of ethylene oxide (EO)

Table 1.2 Physicochemical properties of ethylene oxide (IARC, 2008)

Physicochemical property	Value
Molecular weight	44.06
Boiling point	10.4-10.8°C (101.3 kPa)
Melting point	-111°C
Vapor pressure	145.6 kPa (20°C)
Relative vapor density	1.5 (20°C; air = 1)
Lower explosive limit in air	2.6-3.0 vol% in air
Conversion factor	1 ppm = 1.8 mg/m^3 (25°C, 101.3 kPa)

1.2.2 Production, use, exposure, and regulations

ET in the chemical industry is mainly produced by steam cracking of petroleum hydrocarbons, using a hydrocarbon feedstock (summarized in IARC, 1994a). The global production and consumption in 2010 was 123 million tons (IHS, 2011a). The gas is mainly used as feedstock in the production of polymers and industrial chemicals (Zimmermann and Walzl, 2007). Small amounts of ET are also used for control ripening of citrus fruits (summarized in IARC, 1994a).

ET is ubiquitously present in the environment and is released from both natural (~74%) and anthropogenic (~26%) sources (Sawada and Totsuka, 1986). Major natural sources are vegetation, volcanic emissions and natural gas (summarized in, e.g., IARC, 1994a). Major anthropogenic sources include biomass burning and combustion of fossil fuels (Sawada and Totsuka, 1986). Plants produce ET as a ripening hormone (reviewed in e.g., Bleecker and Kende, 2000). ET is also formed endogenously and is

exhaled by mice (Lawrence and Cohen, 1985; Artati, 2010), rats (Csanády et al., 2000; Frank et al., 1980; Sagai and Ichinose, 1980; Shen et al., 1989), and humans (Filser et al., 1992; Ram Chandra and Spencer, 1963; Shen et al., 1989). As main sources are discussed: lipid peroxidation (e.g. Kautiainen et al., 1991), enzyme- (Fu et al., 1979), copper- (Lieberman et al., 1965), or iron- (Kessler and Remmer, 1990) catalyzed oxidative destruction of methionine, oxidation of hemoglobin (Clemens et al., 1983) and the metabolism by intestinal bacteria (Törnqvist et al., 1989a); for review, see IARC (1994a). Ambient ET concentrations in rural environments of the USA, Canada, Japan and Northern Europe were published to be between 0.04 ppb and 13 ppb. In urban air, ET concentrations of between 3.5 ppb and 700 ppb were reported (Alberta Environment, 2003). ET concentrations in the ambient air surrounding a large ET producing facility in Canada were monitored between September 1999 and December 2001 (Alberta's Ethylene Crop Research Project, 2002). They were generally below 100 ppb but sometimes up to 300 ppb.

Exposure to high ET concentrations may occur at the work place. Fruit store workers were occupationally exposed to ET concentrations of between 0.02 and 3.35 ppm (Törnqvist et al., 1989b). In 2005, The American Conference of Governmental Industrial Hygienists established an average eight-hour (40 work hours per week) threshold exposure limit value (TLV) of 200 ppm (ACGIH, 2005), which still holds in 2011 (ACGIH, 2011). In a large Canadian ET production facility, workplace ET exposures were published to be below 15 ppm (NOVA Chemicals, 2007). From the German Commission for the Investigation of Health Hazards of Chemical Compounds in the Work Area of the Deutsche Forschungsgemeinschaft (DFG), no MAK value (8-hour average exposure threshold limit concentration at the workplace) was given because ET was considered to be carcinogenic to humans because due to its metabolism to EO (DFG, 1993). Also, no occupational exposure limit is given by the European Commission Employment, Social Affairs and Inclusion (ESAI).

EO is industrially produced by direct vapor-phase oxidation of ET with air or oxygen on a silver catalyst at 1 - 3 MPa at 200 - 300°C. In 2010, the worldwide production and consumption of EO was 21 million tons. The chemical is predominantly used in the manufacture of ethylene glycol (70%). Smaller amounts are used for the production of ethoxylates, polyethylene glycols, ethanolamines glycol ethers, and polyols (IHS, 2011b). In many countries, EO serves as a fumigant for food such as herbs, nuts,

cocoa beans, dried vegetables, and gums (IARC, 2008). In the European Union, this use is prohibited since 1991. According to Loaharanu (2003), the reason was the probable in-vivo chlorination of EO to ethylene-chlorohydrin (2-chloroethanol). 2-Chloroethanol is a highly toxic compound which had been considered as potentially carcinogenic because of its genotoxic properties *in vitro* (Fishbein, 1979). EO is also used worldwide as sterilization agent for hospital equipment, pharmaceutical products and medical devices (Mendes et al., 2007). EO is released into the environment predominantly from the EO producing and processing industry. In ambient air, the concentration of EO was reported to be 3.7 - 4.9 µg/m^3 (2.1 - 2.7 ppb) in Canada and 0.038 - 955.7 µg/m^3 (0.021 - 553.7 ppb) in Los Angeles, California, USA (WHO, 2003). Natural sources are considered as quantitatively irrelevant (WHO, 2003). Such sources are: generation as an ET metabolite in some plants, micro-organisms (Abeles and Dunn, 1985; De Bont and Albers, 1976), and humans (Filser et al., 1992), EO in cigarette smoke (Törnqvist et al., 1986) and skin-care products (Filser et al., 1994).

The TLV value for EO is 1 ppm (ACGIH, 2011), no MAK value is given for EO because it is considered to be a human carcinogen. In 2009, the Scientific Committee on Occupational Exposure Limits (SCOEL) of the ESAI has proposed an 8-hour time-weighted average (TWA) concentration of EO of 0.1 ppm in the atmosphere of workplaces (SCOEL, 2009). TWA values of EO are summarized in IARC (2008) for a series of countries to be between 0.1 and 5 ppm (with the exception of Brazil with 39 ppm). In the past, workplace exposures were rather high. Hospital sanitary workers involved in sterilization and degasification of medical devices were exposed to 8-h TWA EO concentrations of up to 10.7 ppm (Sarto et al., 1987) and up to 20 ppm (Sarto et al., 1984) in an Italian hospital. In a cohort study on the mortality of ethylene oxide-exposed industrial workers in USA, the historical average exposure concentration was estimated to be up to 77.2 ppm (Stayner et al., 1993).

1.2.3 Metabolism

Figure 1.3 shows schematically the initial steps of the ET metabolism in mammals according to Greim and Filser (1994).

In closed chambers containing ET exposed rats, the detection of exhaled EO was the first proof of the metabolism of ET to EO (Filser and Bolt, 1983). Shortly thereafter, the same working group demonstrated that liver microsomes of phenobarbital pretreated

rats transformed ET to EO when NADPH was present (Schmiedel et al., 1983). This process could be markedly inhibited by diethyldithiocarbamate. The authors concluded that ET was epoxidized by phenobarbital induced cytochrome P450 dependent monooxygenases (CYP; Schmiedel et al., 1983). Later, it was concluded from experiments in ET exposed rats that the ET metabolizing isoenzyme was most probably CYP2E1 (Fennell et al., 2004).

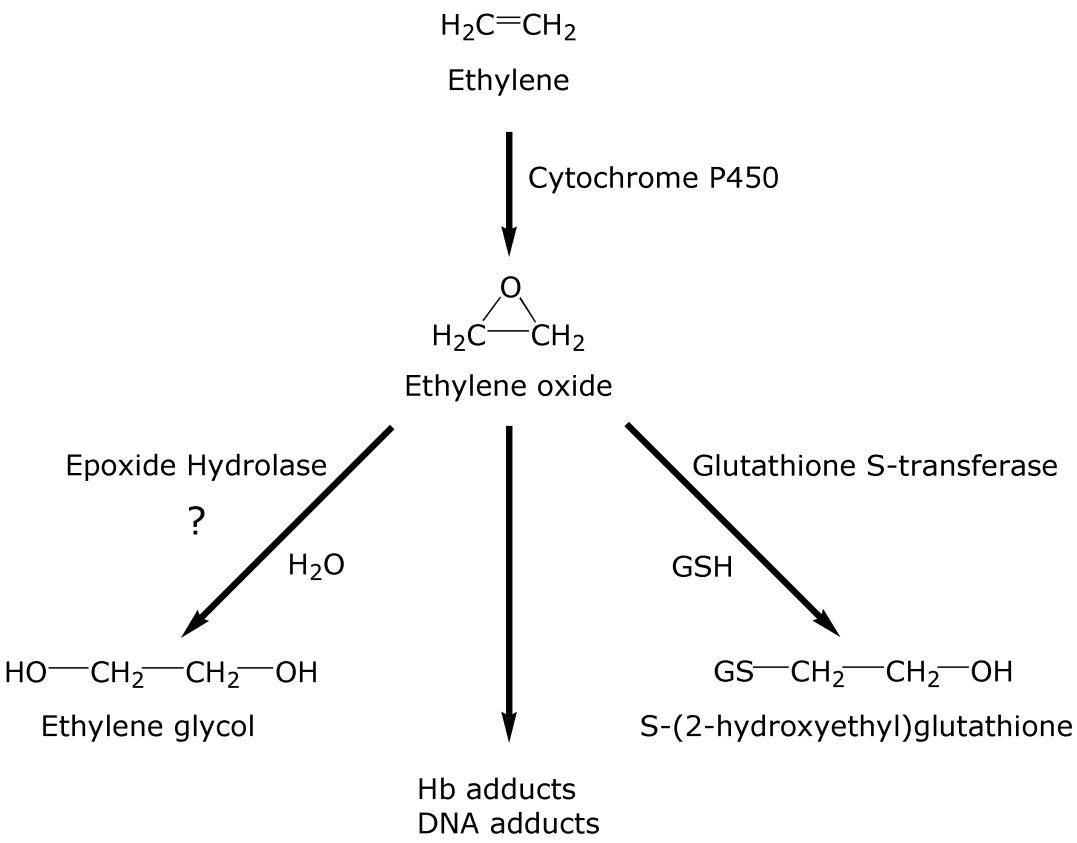

Figure 1.3 First metabolic steps of ethylene and ethylene oxide. The question mark signifies that the existence of this pathway has not been proven yet.

The electrophilic EO can hydroxyethylate nucleophilic groups in macromolecules (Fraenkel-Conrat, 1944). Because of this reaction, the formation of EO from ET was also shown indirectly by the hydroxyethylation of hemoglobin and DNA in ET exposed rats and mice and of hemoglobin in ET exposed humans (Ehrenberg et al., 1977; Eide et al., 1995; Segerbäck, 1983; Filser et al., 1992; Rusyn et al., 2005; Törnqvist et al., 1989b; Walker et al., 2000; Wu et al., 1999a).

In rodents (Jones and Wells, 1981; Tardif et al., 1987) and humans (Burgaz *et al.,* 1992; Haufroid et al., 2007; Popp et al., 1994), EO is metabolized by conjugation with glutathione (GSH) as was shown by the urinary excretion of thioethers like 2-hydroxyethyl mercapturic acid. In humans, the polymorphic GST-theta is the GST isozyme that catalyzes the GSH conjugation with EO (Föst et al., 1991, 1995). Ethylene glycol, the hydrolytic product of EO was reported to have been detected in urine of EO exposed animals (dog: Martis et al., 1982; mouse, rat, rabbit: Tardif et al., 1987). However, in both studies the method used for ethylene glycol analysis by direct injection of urine samples into a gas chromatograph with a packed column seems rather unspecific. GST mediated GSH conjugation of EO was the predominant elimination pathway of EO in subcellular fractions of livers and kidneys from mice and rats. Ethylene glycol formation, catalyzed by microsomal EH, was barley detectable, if there was any (Brown et al., 1996). Also, spontaneous EO hydrolysis was very slow. From the data given by Brown et al. (1996), its half-life can be calculated to be about 11.6 h. In part, EO may also enter the intermediary metabolism as can be concluded from findings of Jones and Wells (1981). After intraperitoneally administering a single dose of 2 mg [^{14}C]EO/kg body weight (b.w.) to rats, 1.5% of the dose was detected as $^{14}CO_2$ in the exhaled air.

1.2.4 Genotoxicity and carcinogenicity

Ethylene

Although N7-(2-hydoxyethyl)guanine was detected in DNA of ET exposed mice (Wu et al., 1999a) and rats (Eide et al., 1995), all other studies on genotoxicity of ET showed negative results. With or without a metabolic activation system, there was no indication of any mutagenic potency in one strain of *Salmonella typhimurium* exposed up to 7 h to an atmospheric ET concentration of 20% (Victorin and Ståhlberg, 1988). No induction of chromosomal aberration was detected in cultured Chinese hamster ovary cells exposed to ET (25% in air) for 3 h (Riley, 1996, cited in OECD, 1998). Following exposure of B6C3F1 mice and Fischer 344 rats for 4 weeks to ET concentrations of up to 3000 ppm, no increased incidence of micronuclei was detected in bone marrow cells (Vergnes and Pritts, 1994). ET was also not mutagenic in B6C3F1 mice and Fischer 344 rats that were exposed up to 4 weeks to ET concentrations of up to 3000 ppm

(Rusyn *et al.*, 2005; Walker et al., 2000). However, as mentioned above, adducts to hemoglobin and DNA increased dose dependently in both species.

ET was not carcinogenic and did not show signs of chronic toxicity in a two-year inhalation study in Fischer 344 rats exposed 6 h/d, 5 d/w to ET concentrations of up to 3000 ppm (Hamm et al., 1984). This outcome had been expected from toxicokinetic studies of ET and EO in rats as well as from binding and mutagenicity studies in mice and rats by predicting the EO formation to be too low to lead to tumors in a long-term carcinogenicity study with ET (Osterman-Golkar and Ehrenberg, 1982; Bolt and Filser, 1984, 1987; Törnqvist, 1994; Walker et al., 2000).

ET was categorized by IARC (1994a) as “not classifiable as to its carcinogenicity to humans” (Group 3) by taking into account the inadequate evidence in humans and experimental animals for the carcinogenicity of this chemical.

Ethylene oxide

EO hydroxyethylates nucleophilic groups of proteins and DNA as has been shown in various publications on EO exposed rodents and humans (Angerer et al., 1998; Boogaard et al., 1999; Ehrenberg et al., 1974; Duus et al., 1989; Farmer et al., 1996; Fennell et al., 2000; Osterman-Golkar et al., 1976, 1983; Potter et al., 1989; Ribeiro et al., 1994; Rusyn et al., 2005; Sarto et al., 1991; Schulte et al., 1995; Sega et al., 1991; Segerbäck, 1983; Tates et al., 1991; van Sittert et al., 1993, 2000; Walker et al., 1992a, b, 1993, 2000; Wu et al., 1999b; Yong et al., 2001, 2007). Protein and DNA alkylation by EO was first demonstrated by Ehrenberg and colleagues in mice exposed to radiolabeled EO (Ehrenberg et al., 1974). Osterman-Golkar et al. (1983) showed the hydroxyethylation of histidine residues of hemoglobin in EO exposed rats and, in the same species, the DNA alkylation at N7-guanine by radiolabeled EO. In mice and rats exposed up to 4 weeks to EO concentrations of up to 300 ppm, Walker et al. (1992a, b) investigated the formation and persistence of N-(2-hydroxyethyl)valine, the EO adduct with the N-terminal valine of hemoglobin, and of N7-(2-hydroxyethyl)guanine, the main EO adduct detected in DNA. Further DNA adducts were detected *in vitro* in EO treated calf thymus DNA (Segerbäck, 1983, 1990; Li et al., 1992; summarized in Wu et al., 2011). In EO exposed humans, only the formation N-(2-hydroxyethyl)valine could be quantified, so far (Angerer et al., 1998; Boogaard et al., 1999; Duus et al., 1989).

EO was a direct mutagen in microorganisms, in mammalian cells including human cells *in vitro*, and in Drosophila melanogaster. In almost all *in vitro* studies, mutagenicity was

absent after adding a metabolizing system. In EO exposed mammals including humans, sister chromatid exchange, chromosomal aberrations and micronuclei were increased. At high doses, EO induced dominant lethal mutations in mice and rats, and heritable translocations in mice. The genotoxic effects of EO are reviewed in Dellarco et al. (1990), IARC (1994b) and in Kolman et al. (2002).

Carcinogenicity of EO was first demonstrated in NMRI mice that had received subcutaneous injections of EO doses of up to 1.0 mg/animal/week for 95 weeks. Local tumors (mostly fibrosarcomas) were detected that increased dose dependently (Dunkelberg, 1981). The same author described the emergence of forestomach tumors (mainly squamous-cell carcinomas) in Sprague-Dawley rats that had been treated twice a week for up to nearly 3 years with intragastric EO doses of 7.5 and 30 mg/kg b.w. (Dunkelberg, 1982). In a long-term inhalation study with male and female B6C3F1 mice that were exposed to 0, 50, or 100 ppm EO (6 h/d, 5 d/w, up to 102 weeks), EO was carcinogenic inducing tumors in a dose dependent manner in lungs and the Harderian gland (both sexes). In females, lymphomas, uterine adenocarcinomas and mammary gland carcinomas were induced (NTP, 1987). Two long-term inhalation studies were conducted with Fischer 344 rats. In the first one, animals were exposed (6 h/d, 5 d/w) for two years to 0, 10, 33, or 100 ppm EO. The exposed animals showed several types of systemic tumors (peritoneal mesotheliomas in the testicular serosa and subcutaneous fibromas in males, mononuclear-cell leukemia and brain tumors in both genders) that increased dose dependently (Snellings et al., 1984; Garman et al., 1985). In the second study, male Fischer 344 rats were exposed to EO concentrations of 0, 50, or 100 ppm (7 h/d, 5 d/w, 2 y). Also in these animals, brain tumors and peritoneal mesotheliomas in the testicular region increased dose dependently. There was a significant increase in mononuclear-cell leukemia at the low but not at the high dose, possibly because of excessive mortality due to an outbreak of a mycoplasma pulmonis infection (Lynch et al., 1984).

In humans, a possible carcinogenic risk of EO was investigated in a series of epidemiological studies conducted in workers exposed either in EO producing chemical plants or in workplaces where EO was used for sterilization purposes. Högstedt et al. (1979) conducted the first epidemiological study in occupationally EO exposed humans. The authors reported increased incidences of leukemia and of cancers of the alimentary tract and urogenital system (estimated exposure concentrations:

5 - 25 ppm). In the following years, a series of epidemiological studies was published. In some of them, increased incidences of stomach (Högstedt et al., 1988), pancreatic (Hagmar et al., 1995; Norman et al., 1995), brain (Hagmar et al., 1995) and breast cancers (Norman et al., 1995) were described in addition to lymphohematopoietic cancers. A few studies were negative or doubtful (e.g. Kiesselbach et al., 1990; Kardos et al., 2003). A more recent follow-up study on the mortality (2852 cases) of a cohort of 18235 EO exposed workers, which was based on standardized mortality ratios, showed positive exposure-response trends for lymphoid cancer mortality in males and for breast cancer mortality in females. At the highest cumulative exposures and the longest latency, male (cumulative exposure >13500 ppm x day) and female workers (cumulative exposure >12322 ppm x day) had statistically significant excesses for these cancers (Steenland et al., 2004). There was no increased incidence for cancer in any other tissue except a small one for bone cancer (six cases versus three expected). In a much smaller follow up study on 2876 men and women with definite or potential exposure to EO, the analysis was based on 565 deaths. There was an excess mortality from non-Hodgkin's lymphoma and leukemia in the group of subjects with greatest potential for exposure to EO (Coggon et al., 2004). In both studies, the risk of human cancer from EO was concluded to be low.

EO has been classified by IARC (1994b, 2008) as carcinogenic to humans (Group 1). The classification was based on "sufficient evidence in experimental animals for the carcinogenicity of ethylene oxide" and the "supporting evidence" that "Ethylene oxide is a directly acting alkylating agent".

1.2.5 Toxicokinetics

Ethylene

The toxicokinetics of inhaled ET have been investigated in rats (Andersen et al., 1980; Bolt et al., 1984; Bolt and Filser, 1987), mice (Artati, 2010), and humans (Shen et al., 1989; Filser et al., 1992). Exposures were carried out using the "closed chamber technique" (for explanation, see Filser, 1992). In both animal species, ET metabolism was described by saturation kinetics according to Michaelis and Menten. In male Fischer 344 rats, the maximum rate of ET metabolism (V_{maxET}) was 8.6 µmol/h/kg b.w. and the apparent Michaelis-constant (K_{mapET}) was 218 ppm ET in air (Andersen et al.,

1980). Very similar results were obtained in male Sprague-Dawley rats: V_{maxET} was 8.5 µmol/h/kg b.w. and K_{mapET} was 204 ppm ET (Bolt and Filser, 1987). In the male B6C3F1 mouse, corresponding values were 15.5 µmol/h/kg b.w. and 105 ppm ET (Artati, 2010). In humans, the highest ET exposure concentration was 50 ppm. Therefore, only a "clearance of metabolism" of ET (related to the atmospheric ET concentration) of 9.3 l/h per 70 kg b.w. was obtained (Filser et al., 1992). It corresponds to the ratio V_{maxET}/K_{mapET} wich can be calculated to be 0.005 µmol/h/kg b.w./ppm (by dividing the clearance of ET metabolism by 24.45 l, the molar volume of an ideal gas at 25°C and 760 torr, and by a body weight of 70 kg). At ET concentrations below 10 ppm (mice; Artati, 2010) and 50 ppm (rats and humans; Shen et al., 1989), metabolic elimination of ET can be described by first-order kinetics. Under such exposure conditions, the alveolar retention of ET is very small: in humans, it was reported to be 2% (Filser et al., 1992). In rats, the same value of the alveolar retention is calculated by means of the kinetic constants for ET given in Bolt et al. (1984). In mice, an alveolar retention of 5.7% was obtained (Artati, 2010). This signifies that between 94.3% (mouse) and 98% (rat, human) of inhaled ET is exhaled unchanged; only small residual percentages are metabolized. In rats, the metabolic elimination of ET was quantitatively inhibited following pretreatment with diethyldithiocarbamate (Bolt et al., 1984). Because diethyldithiocarbamate is considered as a selective inhibitor of CYP2E1 (Guengerich et al., 1991), these results hinted to a CYP2E1-mediated metabolism of ET, as has been later confirmed by Fennell et al. (2004).

In spite of the evident straightforward saturation kinetics of ET in rodents, it was demonstrated in liver microsomes of phenobarbital pretreated rats that ET destroys its metabolizing CYP species by self-catalyzed N-2-hydroxyethylation of the pyrrole ring D of the prosthetic heme (Ortiz de Montellano and Correia, 1983; Ortiz de Montellano and Mico, 1980). The obvious inconsistency between the *in vivo* findings showing basic saturation kinetics of ET that can be described by V_{maxET} and K_{mapET} and the complex *in vitro* findings showing the suicide inhibition of CYP2E1 is still waiting to be explained.

Ethylene oxide

The toxicokinetics of inhaled EO has been investigated in different strains of rats (Filser and Bolt, 1984; Krishnan et al., 1992), in mice (Artati, 2010), and in humans (Shen et al., 1989; Filser et al., 1992) by means of the closed chamber technique. Also, after exposing mice for 3 h to constant atmospheric EO concentrations of 75 or 300 ppm in a

“semi-dynamic inhalation exposure chamber”, concentration-time courses of the EO elimination were monitored in the atmosphere of the chamber (Sega et al., 1991). In addition, toxicokinetic data of EO were obtained in blood, brain, muscles, and testes of mice and rats after exposing the animals up to 4 h to EO at constant concentrations of 100 or 330 ppm (Brown et al., 1996) and in blood of mice during 4-h exposures to EO concentrations of 50, 100, 200, 300 or 400 ppm (Brown et al., 1998). Brugnone et al. (1985, 1986) measured concentration-time courses of EO in blood and ratios of alveolar to atmospheric EO concentrations in EO exposed workers (exposure concentrations up to 12.5 ppm). In all three species, EO was rapidly eliminated according to first-order kinetics of at least up to 12.5 ppm and 300 ppm in humans (Brugnone et al., 1985; 1986) and rats (Brown et al., 1996), respectively, and of up to about 200 ppm in mice; at higher EO exposure concentrations, the elimination rate decreased due to depletion of GSH (Artati, 2010; Brown et al., 1996, 1998). Within the first-order range, alveolar retentions were reported to be 43% in a mouse of 25 g (Artati, 2010) and 75 - 80% in adult humans (Brugnone et al., 1985, 1986). In a 250 g rat, the alveolar retention of EO was 48% taking into account the toxicokinetic data given in Filser and Bolt (1984) and an alveolar ventilation of 117 ml/min (Arms and Travis, 1988). The difference in the alveolar retention between the rodent species and humans reflects the fact that relatively less of inhaled EO reaches the rodent lungs (about 60% of the alveolar ventilation) than the human lung (more than 90%) as discussed in Johanson and Filser (1992) and in Filser et al. (1993). Therefore, in the three species about 80% of EO that reaches the alveoli is metabolized. Most probably, the drastic difference in the first-order kinetics between ET and EO is less dependent on the different activities of the ET and EO metabolizing enzyme species but predominantly on the different bioavailability which is reflected by the blood-to-air partition coefficient ($p_{b:a}$). The $p_{b:a}$-value of ET was published to be 0.48 in rodents and 0.22 in humans (Csanády et al., 2000). For EO, a $p_{b:a}$-value of 61 was reported for the three species (Csanády et al., 2000). This signifies that at equal atmospheric concentrations of both compounds the accumulation of EO in lung blood is 2 orders of magnitude higher than that of ET.

Ethylene oxide as metabolite of ethylene

In rodents exposed to constant ET concentrations of ≥300 ppm, metabolically produced EO increased rapidly in blood and in the air of closed exposure chambers until reaching

an early peak. Thereafter, the EO concentrations decreased until a final plateau was reached. At lower ET exposure concentrations, there was no early peak present. Instead, EO increased continuously towards a plateau the level of which depended on the ET exposure concentration (mice: Artati, 2010; rats: Bolt et al., 1984; Fennell et al., 2004; Maples and Dahl, 1993; Erbach, 2010). The unusual kinetics of metabolically formed EO at high ET exposure concentrations was associated with a decrease of the whole hepatic CYP content down to 68% after 360 min of exposure to 600 ppm ET (Maples and Dahl, 1993) and of hepatic 4-nitrophenol hydroxylase activity (predominantly CYP2E1) to 50% after 4 h to 600 ppm (Fennell et al., 2004).

Taking into account the saturation kinetics of ET, it was suggested that exposure of rats to ET cannot result in a higher body burden by the carcinogenic EO than an exposure to a certain EO concentration. This so-called maximum equivalent EO concentration was estimated to be 2 ppm (Csanády et al., 2000), 5.6 ppm (Bolt and Filser, 1987), 6.2 ppm (Osterman-Golkar and Ehrenberg, 1982) or 10 ppm (Fennell et al., 2004). From studies on DNA adducts of ET or EO, Walker et al. (2000) obtained a maximum equivalent EO concentration of between 6.4 and 23.3 ppm. For mice, maximum equivalent EO concentrations of 4.0 ppm (hemoglobin adduct study; Segerbäck, 1983), 5.6 ppm (toxicokinetic study Artati 2010), or between 6.7 and 21.5 ppm (DNA adduct study; Walker et al., 2000), have been derived. Based on these data and on the results of carcinogenicity studies of EO in rats, it was predicted that ET would not give a positive response in a normal carcinogenicity study (Osterman-Golkar and Ehrenberg, 1982; Bolt and Filser, 1984, 1987; Walker et al., 2000; Artati, 2010).

Physiological toxicokinetic models

Physiological toxicokinetic models that describe uptake, distribution, metabolism and excretion of chemicals in various organs and tissues of the organism by means of mathematical equations are generally considered as excellent tools for estimating risks of chemicals to human health. To be considered as reliable for the purpose of risk estimation, such models require valid compound- and tissue-specific kinetic parameters (such as V_{max} and K_{map}) that can be obtained *in vitro* using subcellular tissue fractions of laboratory animals and of humans (WHO, 2010). Several physiological toxicokinetic models of ET together with EO (Csanády et al., 2000) or of EO solely (Fennell and Brown, 2001; Krishnan et al., 1992) have been developed. However, a model that contains the suicide inhibition of the ET-metabolizing CYP2E1 in mice, rats and

humans and that describes the EO burden not only in the rodent species but also in humans at low and high exposure concentrations of ET or EO is not available so far. Therefore, the goal of the present thesis was to acquire the toxicokinetic parameters that are necessary for the development of such a model. The liver is the organ that is most relevant for metabolism of xenobiotics and the lung is the entrance organ of inhaled xenobiotics; the latter was a target of EO induced tumors in the mouse. Consequently, the metabolism of ET and EO was investigated in subcellular fractions of livers and lungs of mice and rats and of livers of humans.

1.3 Aim of the work

The aim of the work was to determine toxicokinetically relevant parameters of ET and EO in subcellular fractions of livers and lungs of male B6C3F1 mice, male Fischer 344 rats, and of livers of humans.

Ethylene

- Pooled liver and lung microsomes should be prepared and the elimination of ET, the formation of EO, and the destruction of the ET metabolizing CYP-species should be studied in dependence of the ET exposure concentration. In order to test for the viability of mouse and rat liver microsomes, the elimination of styrene (ST) should be investigated, too. This olefin does not inhibit the activity of its metabolizing CYP-species.
- After genotyping in-house bred CYP2E1 knockout mice and verifying the knockout of this CYP-species, the relevance of CYP2E1 for the metabolism of ET should be studied by comparing the EO formation from ET in liver microsomes of the CYP2E1 knockout mice and of their wild-type counterpart.
- A new mathematical procedure should be developed in order to calculate from the measured data the toxicokinetic parameters which describe metabolic elimination of ET and its metabolism to EO as well as the suicide inactivation of the ET metabolizing CYP2E1.

Ethylene oxide

- Microsomal and cytosolic EH activities to EO as well as spontaneous EO hydrolysis should be determined as a function of the EO exposure concentration. As a positive control for the EH activity in rodent liver and lung microsomes, additional incubations should be carried out with propylene oxide (PO).
- The kinetics of spontaneous and of GST-catalyzed GSH conjugation with EO should be investigated in pooled cytosolic and in pooled microsomal incubations.
- Considering that the polymorphic GST-theta is the EO metabolizing GST isoenzyme in humans, the kinetics of the conjugation reaction should not only be studied in pooled human liver cytosol but also in hepatic cytosolic preparations of human individuals in order to become informed about the range of the EO elimination kinetics in humans.
- In a preliminary study, the quantitative relevance of kidney, lung, brain, or blood in the metabolism of EO should be compared with that of the liver by measuring the elimination of EO in homogenates of these organs.

2 MATERIALS AND METHODS

2.1 Materials

2.1.1 Chemicals and equipment

Chemicals

Acetaldehyde, 99%	Sigma-Aldrich, Steinheim
Chlorzoxazone	Sigma-Aldrich, Steinheim
DL-Isocitric acid trisodium salt hydrate (isocitrate), 97%	Sigma-Aldrich, Steinheim
Diethyl maleate (DEM), >97%	Fluka, Steinheim
DirectPCR® Lysis Reagent (Tail)	Peqlab, Erlangen
5,5'-Dithiobis(2-nitrobenzoic acid) (Ellman's Reagent)	Boehringer, Mannheim
Ethylene 3.5, >99.95%	Linde, Unterschleißheim
Ethylene oxide 3.0, >99.9%	Linde, Unterschleißheim
[$^{13}C_2$]Ethylene oxide, 99 Atom % ^{13}C	Sigma-Aldrich, Steinheim
Gel Loading Buffer (Bromophenol blue, 0.05% w/v; sucrose, 40% w/v; EDTA, 0.1 M, pH 8.0; SDS, 0.5% w/v).	Sigma-Aldrich, Steinheim
GeneRuler™ 100bp DNA Ladder	Fermentas, St. Leon-Rot
L-Glutathione reduced, ≥99%	Aldrich, Steinheim
Helium 5.0, >99.999%	Linde, Oberschleissheim
Hydrogen 5.0, >99.999%	Linde, Unterschleissheim
6-Hydroxychlorzoxazone, ≥98%	Sigma-Aldrich, Steinheim
Isocitrate dehyrogenase, purified from porcine heart, solution in 50% glycerol in EDTA buffer, pH=6.0 8.5 mg protein/ml (Biuret) and 15 units/mg protein 73 mg protein/ml (Biuret) and 13 units/mg protein	Sigma-Aldrich, Steinheim
Methane 4.5, >99.995%	Linde, Unterschleissheim
β-Nicotinamide adenine dinucleotide phosphate sodium salt ($NADP^+$), 97%	Sigma-Aldrich, Steinheim
ß-Nicotinamide adenine dinucleotide phosphate reduced tetrasodium salt (NADPH), 97%	Sigma-Aldrich, Steinheim
ß-Nicotinamide adenine dinucleotide, reduced form (NADH), 98%	Sigma-Aldrich, Steinheim

Nitrogen 5.0, >99.999%	Linde, Unterschleißheim
Oligonucleotide primer, Cyp2E1_mut-f, Cyp2E1_mut-r, Cyp2E1_wt-f, Cyp2E1_wt-r	Eurofins MWG Operon, Ebersberg
Oxygen 5.0, >99.999%	Linde, Unterschleißheim
PCR Buffer (10x, contains 15 mmol/l $MgCl_2$)	Qiagen, Hilden
Polyacrylamide gel, 4 - 20% TBE (Tris-Borate-EDTA) gels 1.0 mm x 15 well	Invitrogen, Karlsruhe
Potassium dihydrogen phosphate, ≥99.5%	Merck, Darmstadt
Potassium iodide, ≥99.5%	Merck, Darmstadt
Potassium sodium tartrate tetrahydrate, ≥99%	Merck, Darmstadt
Propylene oxide, >99.99%	ARCO, Rotterdam, The Netherlands
Protein standard set (bovine serum albumin, 20 - 60 mg protein/ml)	Sigma-Aldrich, Steinheim
Proteinase K, peqGOLD, RNase free	Peqlab, Erlangen
Sodium chloride, 0.9%	B. Braun Melsungen
Sucrose for biochemistry Reag. Ph Eur.	Merck, Darmstadt
SYBR® GREEN I (10000x, in DMSO)	Sigma-Aldrich, Steinheim
Synthetic Air, hydrocarbon content ≤0.1 ppm	Linde, Unterschleißheim
Taq DNA Polymerase, 250 units	Qiagen, Hilden
Titriplex® III (ethylenedinitrilotetraacetic acid disodium dihydrate; Na_2-EDTA x 2 H_2O), >99.0%	Merck, Darmstadt
Water, HPLC grade	Fisher, Loughborough, Leicestershire, UK

All other chemicals were obtained from Linde, Merck, or Sigma-Aldrich at the highest analytical grade available.

Equipment

Analytic balance, A210P	Sartorius, Göttingen
Centrifuge:	
Centrifuge Avanti, J-26XP with Rotor JA-25.50	Beckman, Palo Alto, USA
Centrifuge Sigma 1-15	Sigma, Osterode
Centrifuge Sorvall Superspeed RC2-B with rotor Sorvall-SS34	DuPont, Bad Homburg
Centrifuge tubes, glass, round bottom, 12 x 100 mm (diameter x height), capacity 6 ml	Schott, Mainz

Centrifuge tubes: Nalgene UltraPlus, 26.3 ml, PC/PPO	Nalge, Rochester, USA
Centrifuge tubes: Sorvall tubes 50 ml, Polypropylene	DuPont, Wilmington, USA
Columns:	
Capillary column PoraPlot U, 25 m × 0.32 mm I.D., 10 µm film thickness	Chrompack, Frankfurt
Cold trap column CP Sil 8 CB, 30 cm × 0.53 mm I.D., 5.0 µm film thickness	Chrompack, Frankfurt
Stainless steel column packed with Tenax TA 60-80 mesh, 1.5 m x 1/8” (2 mm I.D.)	Chrompack, Frankfurt
Stainless steel column packed with Tenax TA 80-100 mesh, 3.5 m x 1/8” (2 mm I.D.)	Chrompack, Frankfurt
Column: Luna C18(2), 150 mm × 2 mm I.D., particle size 5 µm	Phenomenex, Aschaffenburg
Precolumn, deactivated fused silica 5 m × 0.53 mm I.D.	Agilent, Waldbronn
dNTP mix (Deoxynucleoside triphosphates) 10 mmol/l in aqueous solutions titrated, pH 7.0, >99% (each component)	Fermentas, St. Leon-Rot
Disposable cuvettes, 1.5 ml semi-micro	Brand, Wertheim
Eppendorf cups 1.5, 2.0 ml	Eppendorf, Hamburg
Eppendorf GELoader® Tips	Eppendorf, Hamburg
Eppendorf PCR 8 strip tubes 0.2 ml	Eppendorf, Hamburg
Gas chromatography system:	Shimadzu, Duisburg
-GC-8A	
-Flame ionization detector	
-Integrator: CR-6A Chromatopac	
Gas chromatography system:	
-GC HP-6890A	Agilent, Waldbronn
-Chrompack CP4010 PTI/TCT thermal desorption cold trap injector	Chrompack, Frankfurt
-Chrompack CP4010/4020 Controller	Chrompack, Frankfurt
-Mass Selective Detector HP 5973	Agilent, Waldbronn
-Kayak XM 6000 PC workstation	
-Software: ChemStation B.03.00.611	Agilent, Waldbronn Hewlett Packard, Waldbronn

Gel-electrophoresis chamber, XCell SureLock™ Mini-Cell, vertical	Invitrogen, Karlsruhe
GeneAMP PCR system 9700	Applied Biosystems, Darmstadt
Glass desiccators, different volumes, 770-2810 ml	Glaswek Wertheim, Wertheim
Homogenizer system:	B. Braun, Melsungen
-Homogenizer Potter S	
-Homogenizer vials (2, 15, 50 ml)	
-Glass with Teflon plunger	
IVC top-flow system	Tecniplast , Buguggiate, Italy
LC/MS/MS System	
-Liquid Chromatograph HP1100 series	Agilent, Waldbronn
-Binary HPLC pump HP 1100	
-Auto sampler HP 1100 equipped with a 100-well plate holder	
-Column Oven HP 1100	
-Triple quadrupole mass spectrometer API 4000 with turbo ion spray interface	Applied Biosystems, Darmstadt
-Software: Analyst 1.4.2	
Micro inserts for auto sampler vials, glass, 6 mm, 0.1 ml, 15 mm tip	K&K Laborbedarf, Muenchen
HSE-Operation table size 5 (for rodents)	Hugo Sachs Elektronik-Harvard Apparatus, March-Hugstetten
pH Electrode Inlab® Micro	Mettler Toledo, Urdorf, Switzerland
pH meter, Knick 646	Knick, Berlin
Polaroid MP4 land camera	Polaroid, Offenbach
Polaroid Type 667 black and white print film	Polaroid, Offenbach
Septa, PTFE-coated silicone, 12.5 mm diameter	SGE, Weiterstadt
Standard diet 1324 for animals	Altromin, Lage
Surgical instruments (scissors, forceps)	Aesculap, Tuttlingen
SYBR® Green gel stain photographic filter	BMA, Bio Whittaker Molecular Applications, Rockland, USA

Syringes	
Gastight glass syringes 10, 20 ml	Hamilton, Bonaduz, Swizerland
Microliter syringes 5, 10, 50, 100 µl	Hamilton, Bonaduz, Swizerland
Sterile non pyrogenic syringes and painless needle combination	NOVICO, Ascoli Piceno, Italy
Unimetric syringes 50, 100, 500 µl	Unimetrics, Illinois, USA
Syringe filter Minisart, pore size 0.45 µm	Sartirius, Göttingen
Tedlar gas sampling bag 0.6 L with JACO septum port	Alltech, Rottenburg-Hailfingen
Ultracentrifuge Beckman L8-M with Rotor 50.2 Ti	Beckman, Palo Alto, USA
Ultraviolet/Visible Spectrophotometer Lambda 16 equipped with	Perkin Elmer, Überlingen
-Thermostat MS equipped with cooler M3	Lauda, Königshofen
-Software UVCSS 4.0	Perkin Elmer, Überlingen
Vials	
Autosampler vial glass 2 ml, white, with crimp caps (aluminum) 11 mm with telflon/silicon septa	Wicom, Heppenheim
Headspace vials, glass, 8, 15 ml, with rim for clamp caps, butyl/PTFE septum	K&K Laborbedarf, München
Headspace vials, glass, about 38 ml, with screw caps, silicon/PTFE septum	Kuglstatter, Garching
Vortex Minishaker MS2	IKA works, Wilmington, NC, USA
Water bath GFL 1083	GFL, Burgwedel

2.1.2 Animals and livers or hepatic subcellular fractions from human donors

Male Fischer 344 rats (about 250 g b.w., animal number n= 209), male B6C3F1 mice (about 25 g b.w., n=480) and male 129S1/SvImJ mice (about 22 g b.w., n=75) were obtained from Charles River, Sulzfeld. In the following, the Fischer 344 rats are called “rats” and the B6C3F1 mice are called “mice”. The 129S1/SvImJ (CYP2E1+/+, stock number 002448) mice are called “wild-type mice” because they represent the wild-type counterparts of the CYP2E1 knocked out mice 129/Sv-Cyp2e1^{tm1Gonz}/J (CYP2E1-/-,

stock number 002910) that are here called “CYP2E1 knockout mice”. Four to five week old revitalized CYP2E1 knockout mice (5 males, 7 females), were obtained from The Jackson Laboratory, Bar Habor, ME, USA and delivered by Charles River, Sulzfeld. These animals were bred quarantined in the animal facility of the Department of Comparative Medicine of the Helmholtz Center Munich. Of the offspring, male mice were chosen (about 22 g b.w., n=171). Before use, all animals were housed in macrolon type III cages in the IVC top-flow system, which provided the animals with filtered room air. A light and dark of 12 hours cycle was maintained in the room. The animals were kept at constant room temperature (23°C) and fed with standard diet 1324 (Altromin, Lage) and tap water.

Pooled human liver microsomes and cytosol were from BD Biosciences, San José, CA, USA and delivered from Becton Dickinson, Heidelberg. Microsomes had been prepared from livers of 25 male and female individuals, 21 - 64 years old (Table 2.1) and cytosol from livers of 11 male and female donors, 1.9 - 70 years old (Table 2.2). Microsomal protein concentration in 250 mmol/l sucrose was 20 mg/ml. Cytosolic protein concentration was 20 mg/ml in a solution consisting of 150 mmol/l KCl, 50 mmol/l Tris, pH 7.5 and 2 mmol/l EDTA.

A liver sample of a 75-year-old woman was obtained from the University Hospital Rechts der Isar of the Technische Universität München, Munich. The donor suffered from metastasis of rectum cancer and was not treated with oncological drugs when a section of the liver was taken on the occasion of a liver transplantation. A liver sample of a male adult (22 years old) was obtained from the Institut für Rechtsmedizin of the Ludwig-Maximilians-Universität München, Munich. The liver section was obtained during autopsy, about 6 hours 30 minutes after death. Immediately after the explantations, liver samples were put on ice and transported to the Institute of Toxicology of the Helmholtz Center Munich and stored at - 80°C until preparation of microsomes and cytosol, separately for each liver, as described below (2.2.2).

Table 2.1 Donor information of pooled liver microsomes (BD Biosciences, Catalog Number 452161, Lot Number 99268)

Code	Sex	Age (y)	Race	Tobacco	Alcohol	Cause of death
HH628	m	48	cc	n	s	Cerebrovascular accident
HH629	m	47	cc	n	u	Anoxia cardiovascular after pneumonia
HH666	f	58	hp	n	s	Intracranial hemorrhage
HH667	f	58	cc	n	s	Subarachnoid hemorrhage
HH705	f	42	cc	n	n	Intracranial hemorrhage
HH568	m	32	hp	n	u	Anoxia, cardiopulmonary arrest
HH576	m	48	cc	u	s	Intracranial bleed
HH579	m	54	cc	u	u	Intracranial bleed
HH584	m	56	hp	n	u	Intracranial bleed
HH589	f	48	cc	n	u	Aneurysm
HH184	m	21	cc	n	u	Respiratory failure
HH196	m	49	hp	u	n	Heed trauma
HH501	f	36	cc	n	u	Gun shot wound to head
HH544	m	46	cc	n	u	Anoxic injury
HH557	m	36	hp	n	u	Intracranial hemorrhage after motor cycle accident
HH13	m	55	cc	u	n	Aneurysm
HH113	m	64	cc	u	s	Anoxia
HH166	m	49	cc	u	n	Head trauma
HH181	m	50	cc	n	n	Head trauma
HH182	m	37	cc	u	u	Head trauma
HH183	m	44	hp	n.a.	n.a.	Head trauma
HH724	m	49	cc	n	n	Cerebrovascular accident after aortic dissection
HH759	f	60	cc	n	u	Cerebrovascular accident intracranial hemmorage
HH824	f	40	hp	n	s	Subarachnoid hemorrhage after motor vehicle accident
HH852	m	55	cc	n	n	Anoxia, seizure

m = male, f = female, cc = caucasian, hp = hispanic, n = nonuser, s = social user, u = user by habit, n.a. = not available. All human specimen had been negatively tested for the human immunodeficiency virus, the human T-lymphotropic virus, and hepatitis.

Table 2.2 Donor information of pooled liver cytosol (BD Biosciences, Catalog Number 452861, Lot Number 85946)

Code	Sex	Age (y)	Race	Tobacco	Alcohol	Cause of death
HH1	f	31	cc	u	n	Motor vehicle accident
HH3	m	38	cc	u	n	Head injury
HH6	f	62	cc	n.a.	n.a.	Cerebrovascular disease
HH7	m	1.9	hp	n.a.	n.a.	Cerebral infarction
HH13	m	55	as	u	n	Aneurysm
HH12	f	40	cc	u	u	Anoxia
HH23	m	4	cc	n.a.	n.a.	Drowning
HH31	f	51	cc	u	u	Stroke
HH36	f	70	cc	n.a.	n.a.	Cerebrovascular disease
HH51	f	41	aa	u	n	Anoxia
HH69	m	60	cc	n	n	Head Trauma

m = male, f = female, aa = african American, as = asian, cc = caucasian, hp = hispanic, n = nonuser, u = user by habit, n.a. = not available. All human specimen had been negatively tested for the human immunodeficiency virus, the human T-lymphotropic virus, and hepatitis.

2.2 Methods

2.2.1 Genotyping CYP2E1 in wild-type and CYP2E1 knockout mice

Background information

In order to prove de facto the absence of CYP2E1 in the CYP2E1 knockout mice, each individual was genotyped. Genotyping was based on testing the availability of specific DNA sequences in the mouse genome coding for CYP2E1. For this purpose, the polymerase chain reaction (PCR) technique (Mullis et al., 1986) was used. The PCR is a technique to amplify a single or few copies of a specific region of DNA. It consists of a series of 20 - 40 repeated temperature cycles, in which the DNA template is amplified by several orders of magnitude. After addition of the thermostable Taq polymerase, deoxynucleoside triphosphates (dNTP) and primers were added to the samples containing a tail lysate. The PCR is initialized by heating the samples to a temperature of 94 - 98°C to activate the Taq DNA polymerase. In the denaturation step, short

heating (94 - 98°C, 20 - 30 second) causes DNA melting by disrupting the hydrogen bonds between complementary bases, yielding single strands of DNA. In the annealing step, the temperature is lowered to 50 - 65°C for 20 - 40 seconds allowing annealing of the primers to single-stranded DNA. Then, the polymerase binds to the primer-template hybrid. In the elongation step, the temperature is raised to 75 - 80°C, the optimum condition for the Taq polymerase, which synthesizes a new DNA strand fragment complementary to the DNA template strand. By multiple repetitions of denaturation, annealing and elongation steps, the specific DNA fragments are exponentially amplified (Figure 2.1). In order to analyze the PCR products, gel electrophoresis was performed. Gel electrophoresis is used for the separation of DNA by means of an electric field applied to a gel matrix. The gel consists of polyacrylamide of different concentrations forming a porous matrix with different sized meshes. DNA fragments are negatively charged by their sugar-phosphate backbone. By applying an electric field, the fragments and the additionally injected mixture of molecular weight markers (discrete DNA fragments ranging in size from about 80 to about 1050 base pairs) migrate from their loading slots through the meshes of the gel with rates that depend primarily on their fragment size (the larger the fragment the slower the migration rate). After ending the electrophoresis and staining the gel with a specific DNA stain, the positions of the migrated DNA fragments are visualized by UV light. The fragments are then analyzed from their size by comparing with the DNA ladder from the molecular weight markers.

Lysis of mouse tails

According to the procedure described by Peqlab (2009), about 0.2 - 0.3 cm were cut off from the tail of a wild-type or a CYP2E1 knockout mouse and given into an Eppendorf cup (1.5 ml). Then, 200 - 250 µl DirectPCR® Lysis Reagent (Tail) was added together with freshly prepared 0.2 - 0.3 mg/ml proteinase K and the mixture was incubated overnight at 56°C. Thereafter, the obtained crude lysate was incubated at 95°C for 45 minutes in a heating block. Of the lysate, 2 µl was used for the PCR reaction.

Polymerase chain reaction (PCR)

The PCR procedure and the nucleotide sequence of the primers (Table 2.3) were adapted from the information of The Jackson Laboratory (2009). The primer for wild-type CYP2E1 detects the normal alleles of this gene. The primer used for the samples

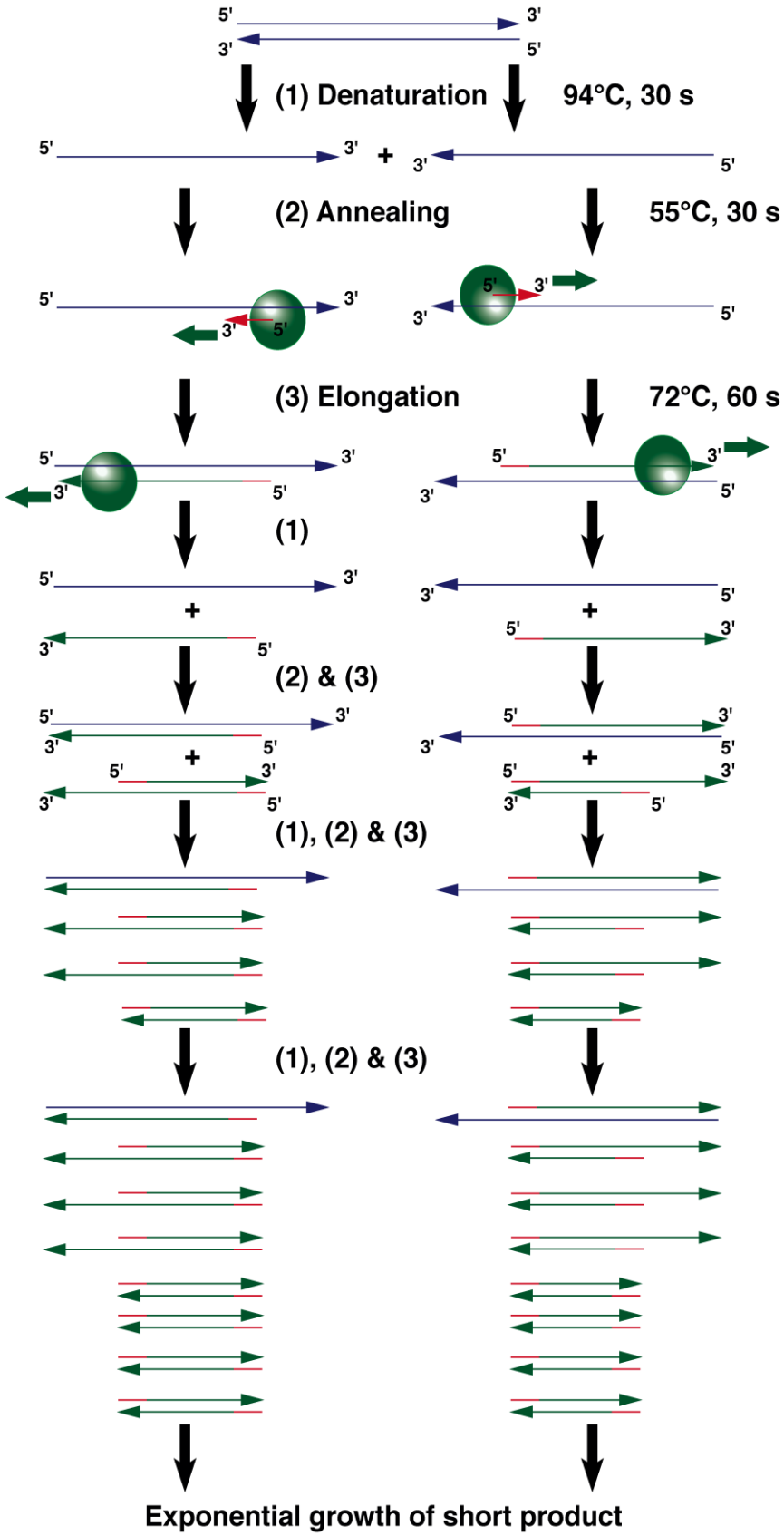

Figure 2.1 Schematic drawing of the polymerase chain reaction (adapted from Mullis et al., 1986 and from M. P. Ball, http://mad.printf.net)

from the CYP2E1 knockout mice detects the gene response for the neomycin resistance. The primers were used to prepare “PCR mixes” in Eppendorf PCR 8 strip tubes containing also Taq polymerase, nucleotides (dNTP) and PCR buffer (see Table 2.4). To each tube, a tail lysate sample was given which was obtained from each individual mouse. All in all, PCR mixes were prepared from 79 CYP2E1 knockout mice and from one wild-type mouse.

After tightly closing the Eppendorf PCR 8 strip tubes by means of Eppendorf cap strips, the PCR was carried out using the GeneAMP PCR system 9700. The PCR cycling conditions are listed in Table 2.5.

Table 2.3 Primers used for PCR[1] for genotyping CYP2E1 knockout and wild-type mice

Primer	Sequence 5' --> 3'	Primer Type
Cyp2E1_wt-f	AGT GTT CAC ACT GCA CCT GG	Wild-type, forward
Cyp2E1_wt-r	CCT GGA ACA CAG GAA TGT CC	Wild-type, reverse
Cyp2E1_mut-f	CTT GGG TGG AGA GGC TAT TC	CYP2E1 knockout, forward
Cyp2E1_mut-r	AGG TGA GAT GAC AGG AGA TC	CYP2E1 knockout, reverse

[1]: All primers were dissolved in double-processed tissue culture water before use.

Table 2.4 “PCR mix” components

Reaction component	Volume in PCR tube [µl]	Concentration in PCR tube
Double-processed tissue culture water	17.88	-
PCR Buffer, 10x	2.5	1.00x
dNTP, 10 mmol/l	0.5	0.20 mmol/l
Primers Cyp2E1_wt-f and Cyp2E1_wt-r, 12.5 µmol/l each in water	1.0	0.50 µmol/l (each primer)
Primers Cyp2E1_mut-f and Cyp2E1_mut-r, 12.5 µmol/l each in water	1.0	0.50 µmol/l (each primer)
Taq DNA Polymerase, 5 U/µl	0.12	0.024 U/µl
Lysate	2.0	-
Total	25	-

Table 2.5 PCR cycling conditions

Step	Temperature [°C]	Time	Note
1	95	5 min	-
2	94	30 sec	-
3	55	30 sec	-
4	72	60 sec	Repeat steps 2-4 for 30 cycles
5	72	10 min	-
6	4	-	Hold

Electrophoresis

The PCR products were analyzed by vertical Electrophoresis at 200 V using an XCell SureLock™ Mini-Cell gel electrophoresis chamber with a ready-to-use polyacrylamide gel (4-20% gel in 1xTBE buffer consisting of 89 mmol/l Tris, 89 mmol/l boric acid, and 1 mmol/l EDTA, pH 8.0).

To 10 µl of each PCR reaction product, 5 µl Gel Loading Buffer was added. After vortexing, 10 µl of each sample was added by means of Eppendorf GELoader® Tips into a well of the polyacrylamide gel. In order to estimate the size of the amplification product, 10 µl of the GeneRulerTM 100 bp DNA ladder was added into one well of the gel. The electrophoresis was performed for 70 minutes. Thereafter, the gel was placed in a staining dish and stained in a time frame between 20 - 40 minutes with SYBR® GREEN I (1x in 1xTBE buffer). The stained gel was illuminated at 302 nm using the Transilluminator IL-200M. Photographs were taken with a Polaroid camera loaded with a Polaroid Type 677 black and white print film using the SYBR® Green gel stain photographic filter. The fragments of DNA were identified with the help of the DNA ladder.

2.2.2 Preparation of microsomes, cytosol, and homogenates from diverse tissues

Liver microsomes and cytosol

Microsomes and cytosol were prepared according to Kreuzer et al. (1991) from male Fischer 344 rats, male B6C3F1 mice, male wild-type mice, male CYP2E1 knockout

mice, and from male and female human donors. After sacrificing the animal using carbon dioxide, it was fixed at the four paws on an animal-operating table with the ventral side up. The abdominal and the thoracic wall were opened using scissors and forceps. The intestine was pulled out and the animal was bleed by cutting the vena cava below the liver. Then, the gall bladder was removed from the liver (mouse). Thereafter, the liver was isolated and the blood dabbed off with a fuzz-free paper. Before proceeding, the liver was placed on an aluminum foil and put on ice for a short while until livers of 10 rats or 50 mice were harvested.

Thawed liver pieces from human individuals (up to 70 g) or the pooled organs from rats or mice were brought into a cold room (temperature was below 4°C), cut with scissors into small pieces, and divided into portions of approximately 13 g. Each portion was transferred into a Teflon-glass homogenizer that contained 52 ml of 0.25 mol/l sucrose. The organs were homogenized (1500 rpm) by 10 times moving slowly up and down the Teflon plunger under ice cooling. The plunger and homogenizer vial were flushed with deionized water after each homogenization.

The obtained homogenates were transferred into centrifuge tubes (Sorvall, 50 ml) and centrifuged for 30 minutes at 0°C and 10000 x g (13000 rpm) using a Sorvall Superspeed RC2-B centrifuge equipped with a Sorvall-SS34 rotor. Thereafter the upper (lipid) layer of the supernatant was carefully removed using Pasteur pipettes. The remaining supernatant was transferred into centrifuge tubes (Nalgene UltraPlus, 26.3 ml) which were tarred very accurately before centrifuging at 0°C and 100000 x g (30000 rpm) for 70 minutes by means of a Beckman L8-M ultracentrifuge equipped with a 50.2 Ti rotor. After centrifugation, the lipid layer was removed again as described above. The supernatant (cytosolic fraction) was decanted into a beaker. It was filtered by using a disposable syringe (10 ml) equipped with a Minisart syringe filter (pore size 0.45 µm), transferred into Eppendorf cups (2 ml), frozen in liquid nitrogen, and then stored in a deep freezer at -80°C until use.

The pellets remaining in the centrifugation tubes were re-suspended in 4 ml of 0.15 mol/l potassium chloride and homogenized again. The obtained suspension was centrifuged again for 70 minutes at 0°C and 100000 x g. The supernatants were discarded and one ml of a KH_2PO_4 buffer (0.15 mol/l) was added. The microsomal fraction of the pellets was carefully separated from the caramel-like, transparent glycogen fraction by slightly shaking the centrifuge tube. The obtained microsomes

were again homogenized, transferred into Eppendorf cups (1.5 ml), frozen in liquid nitrogen, and stored in a deep freezer at -80°C until use.

Lung microsomes and cytosol

After sacrificing the animals (male Fischer 344 or male B6C3F1 mice) by CO_2 asphyxiation, pulmonary microsomes and cytosol were prepared by basically the same procedure as described above for livers. The only differences were that lungs had to be cut into very small pieces and that the homogenization step was distinctly more time-consuming. The finally prepared subcellular fractions were transferred into Eppendorf cups and stored at -80°C until use.

Preparation of blood and of homogenates from liver, kidney, lung, or brain

All animals were deeply anesthetized by CO_2 asphyxiation (verified by complete loss of reaction to a painful stimulus). The abdominal cavity was opened and the diaphragm as well as the vena cava inferior was cut through.

Blood (about 5 ml) was collected from the vena cava inferior of male Fischer 344 rats using a sterile non-pyrogenic syringe equipped with a “painless needle”. After heparinizing, samples were transferred into Eppendorf cups (2 ml) and stored at -80°C until use.

Homogenates of liver, kidney, lung and brain were prepared from male Fischer 344 rats. From male B6C3F1 mice, only liver homogenates were prepared. The organs were removed after exsanguination of the animals. In order to exsanguinate the liver completely, it was additionally perfused via the right atrium with about 20 ml of physiological NaCl solution (0.9%) before removing it. Thereafter, all organs were rinsed with physiological NaCl solution and then dabbed off with laboratory fuzz-free paper. After weighing, each organ was placed on an ice-cooled aluminum foil before cutting it into small pieces in a walk-in refrigerator (about 3°C) and transferring it into a Teflon-glass homogenizer (15 ml) containing phosphate buffer (150 mmol/l; 3-fold organ volume). All organs were homogenized under ice cooling. Thereafter, the homogenates were transferred into Eppendorf cups (2 ml) which were situated in ice for the immediate measurement, or stored at - 80°C until use.

2.2.3 Analytical procedure

2.2.3.1 Determination of ethylene, ethylene oxide, propylene oxide, acetaldehyde, and styrene by gas chromatography with flame ionization detection

Atmospheric concentrations of ET, EO, PO, acetaldehyde (AA), and ST were determined using GC-8A gas chromatographs (GCs) equipped with flame ionization detectors (FIDs). A gas sample, collected by means of a gas-tight glass syringe either from the gas phase of a desiccator or of a headspace vial, was injected into the GC. Separation was carried out on 1/8" stainless-steal columns filled with Tenax TA (60-80 mesh for ET and 80-100 mesh for EO, PO, AA, and ST); the column used for the ET determination was 1.5 m x 1/8" (2 mm I.D.), that for EO, PO, AA, and ST was 3.5 m x 1/8" (2 mm I.D.). The concentration of each compound was calculated using an external calibration curve. The precisions of the measurements were below 1%.

The GC settings and the compound-specific parameters retention time and detection limit are summarized in Tables 2.6 and 2.7. Characteristic chromatograms of ET, EO, PO, AA, and ST (obtained from calibration experiments) are shown in Figure 2.2.

Table 2.6 GC settings for the determination of ethylene (ET), ethylene oxide (EO), propylene oxide (PO), acetaldehyde (AA), and styrene (ST)

GC settings	Compound				
	ET	EO	PO	AA	ST
Injector temperature [°C]	130	200	230	200	300
Detector temperature [°C]	130	200	230	200	300
Oven temperature [°C]	60	150 (130*)	180	150	220
N_2 pressure [kPa]	200	250	200	250	250
H_2 pressure [kPa]	60	60	60	60	60
Air pressure [kPa]	60	60	60	60	60
Injection volume [µl]	50	50 (500**)	50	500	50

*: In some measurements, a lower temperature of 130°C was used in order to carry out a better separation of peaks. **: The injection volume was 500 µl, when very low concentrations (< 10 ppm) of ethylene oxide were measured.

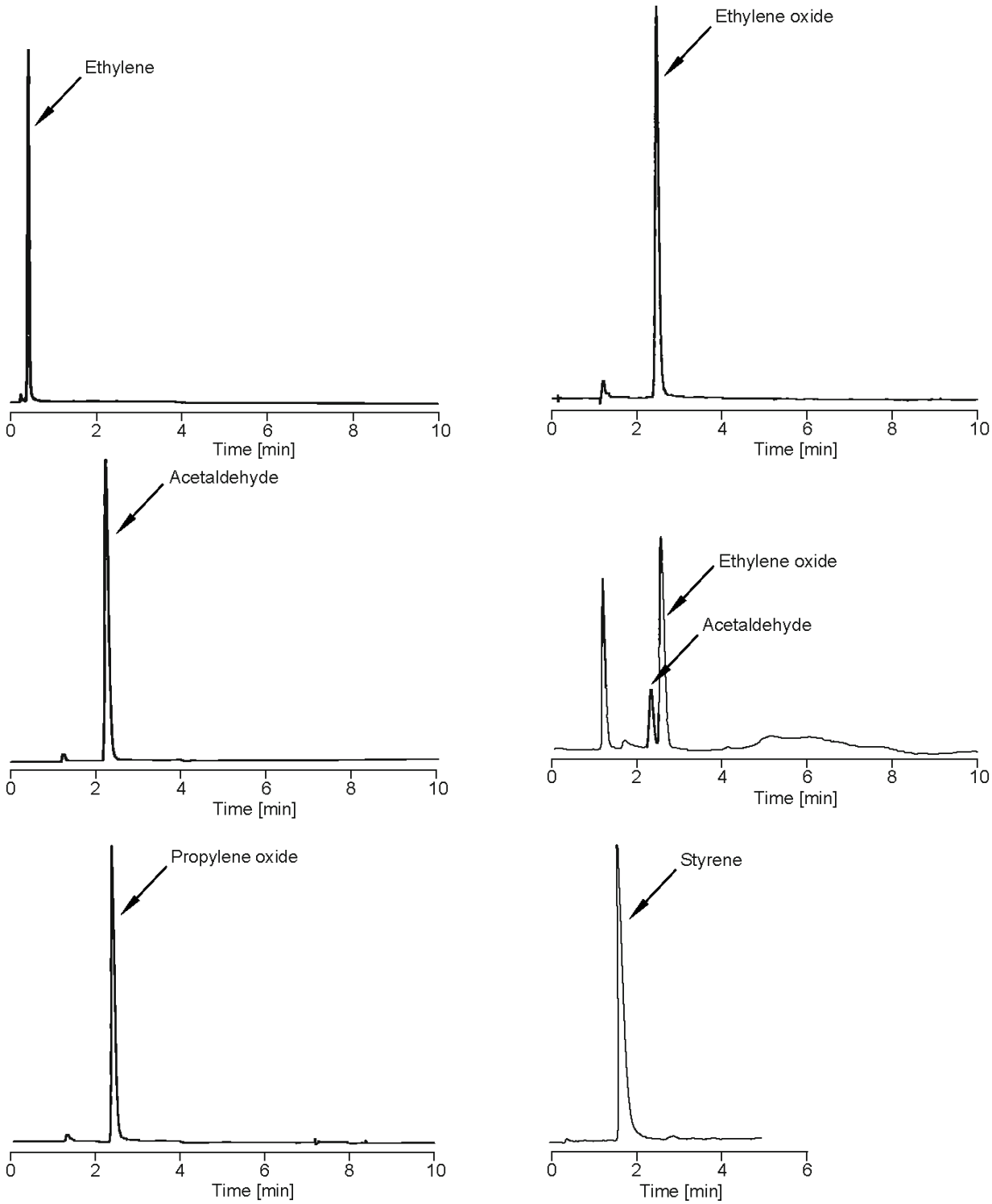

Figure 2.2 GC/FID chromatograms of ethylene, ethylene oxide, acetaldehyde, propylene oxide, (100 ppm each), styrene (300 ppm), and a mixture of acetaldehyde (1 ppm) and ethylene oxide (5 ppm). The GC settings are given in Table 2.6

Table 2.7 Retention times and detection limits of ethylene (ET), ethylene oxide (EO), propylene oxide (PO), acetaldehyde (AA), and styrene (ST)

Compound	Retention time [min]	Detection limit* [ppm]
ET	0.5	0.1
EO	2.6 (3.2**)	0.5 (0.1***)
PO	2.4	0.3
AA	2.3	0.1
ST	1.7	0.1

*: Three times the background noise; **: oven temperature: 130°C (see Table 2.6); ***: injection volume: 500 µl (see Table 2.6).

Calibrations of the GC methods

In glass desiccators (770 - 2810 ml), various stock concentrations of the analytes (ET, EO, PO, AA, and ST) were prepared. Of the gaseous analytes ET and EO, defined amounts were collected directly from the gas cylinder using sterile disposable EO-free syringes and injected immediately into a desiccator via a PTFE-coated silicone septum attached by a screw cap to the ground glass joint of the desiccator. For the highly volatile liquids PO, AA, and ST, defined amounts of each liquid were taken from its storage bottle by means of a Hamilton microliter syringe and injected into the desiccator. Injection volumes for stock concentrations were calculated using Equation 2.1a (for ET or EO) or Equation 2.1b (for PO, AA, or ST):

$$V_{inj} = \frac{c_{stock} \cdot V_{des}}{10^6} \qquad 2.1a$$

V_{inj} Injection volume of ET or EO [ml]

c_{stock} Desired gas concentration of ET or EO [ppm] in the stock desiccator

V_{des} Volume of the desiccator [ml]

$$V_{inj} = \frac{c_{stock} \cdot V_{des} \cdot MW}{d \cdot MV \cdot 10^3} \qquad 2.1b$$

V_{inj} Injection volume of liquid PO, AA, or ST [µl]

c_{stock} Desired gas concentration of PO, AA, or ST [ppm] in the stock desiccator

V_{des} Volume of the desiccator [ml]

MW Molecular weight [g/mol] of the analyte (PO: 58.08, AA: 44.05, ST: 104.15)

d Density of the analyte [g/ml] at 20°C (PO: 0.830, AA: 0.784, ST: 0.909)

MV Molar volume of gas at 25°C and an atmospheric pressure of 740 torr: 25130 ml/mol

In order to produce lower concentrations than those in a stock desiccator, calculated gas volumes were taken from the stock desiccator and injected into other desiccators the volumes of which had been determined before. For this purpose disposable syringes were used. The volumes of gas samples were calculated using Equation 2.2:

$$V_{col} = \frac{c_{req} \cdot V_{des}}{c_{stock}} \qquad 2.2$$

V_{col} Gas volume [ml] collected from the stock desiccator

c_{req} Requested gas concentration of the analyte [ppm]

V_{des} Volume of the desiccator [ml]

c_{stock} Gas concentration of the analyte [ppm] in the stock desiccator

The atmospheres of the desiccators were swirled at least for 10 minutes using magnetic stirrers and magnetic stirring bars. Thereafter, three gas samples were taken by a microliter syringe and injected into the GC. Calibration curves were constructed by plotting the peak heights against the corresponding concentrations that were in the ranges required for the experimental studies (Figure 2.3). At each exposure experiment, a one-point calibration was performed for each investigated compound being within the range of its actual concentration.

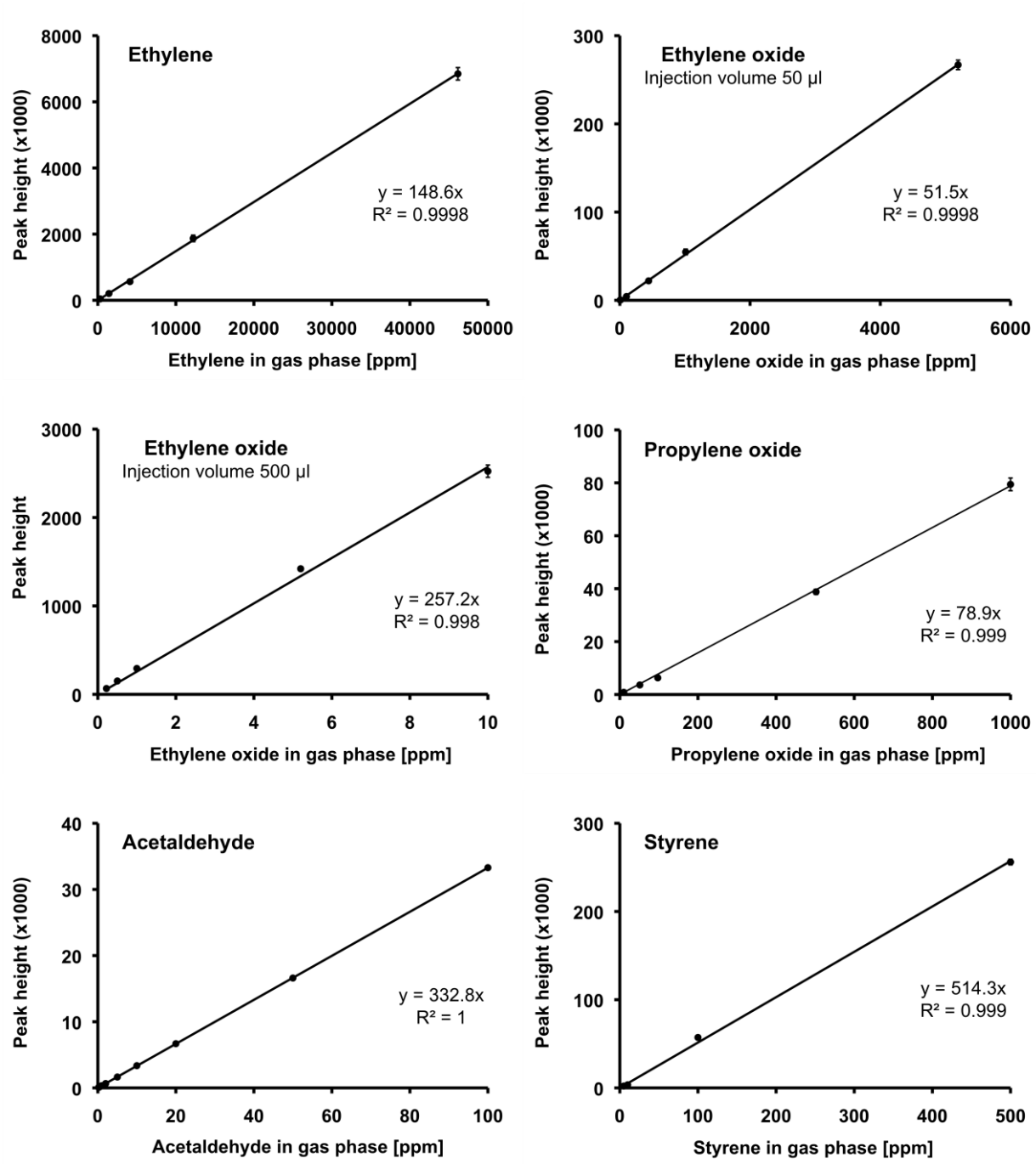

Figure 2.3 Calibration curves for the determination of ethylene (300 - 46200 ppm: injection volume 50 µl), ethylene oxide (5 - 5000 ppm: injection volume 50 µl and 0.22 - 10 ppm: injection volume 500 µl), propylene oxide (10 - 1000 ppm: injection volume 50 µl), acetaldehyde (0.2 - 100 ppm: injection volume 500 µl), and styrene (5 - 500 ppm: injection volume 50 µl) by GC/FID. Symbols, error bars: mean ± SD (n=3). If no error bas are visible, they are smaller than the symbol size. Lines were obtained by linear regression analysis. Peak heights are given in arbitrary units.

2.2.3.2 Determination of ethylene oxide using gas chromatography with mass-selective detection

From a headspace vial (38 ml) a gas sample of 10 ml was taken using a gastight glass syringe and injected immediately through a septum into a gas sampling bag (Tedlar, 0.6 l) the gas phase of which had been pumped out before by means of a gastight glass syringe. Then, 10 ml of the internal standard [$^{13}C_2$]ethylene oxide ($^{13}C_2$-EO) was collected from a stock desiccator ($^{13}C_2$-EO concentration about 8 ppm) and injected into the gas sampling bag. The concentration of the internal standard in the gas sampling bag was about 4 ppm. Water vapor was freezed out by putting the gas sampling bag into an ultra low temperature freezer (-80°C) for 20 minutes. Thereafter, a gas sample of 5 ml was taken from the bag using a gastight glass syringe and its EO concentration was determined by GC equipped with a mass-selective detector (MSD). The gas probe was slowly (within 5 minutes) injected into the thermal desorption cold trap injector containing a column CPSil 5 CB 30 cm x 0.53 mm which was precooled to -150°C. Immediately after injection, the cold trap was heated to 200°C and maintained at this temperature for 5 minutes. The analytes were separated on a capillary column Poraplot U (25 m $\times$ 0.32 mm ID, film thickness 0.25 µm), using helium as carrier gas with a flow of 1.9 ml/min. The temperature program of the column oven was started in parallel with the heating of the trap. The initial temperature of 70°C was held for 1 minutes. Then, it increased with a rate of 8°C/min to 140°C and remained constant for 1 minutes. Afterwards, it increased with a rate of 20°C/min to 170°C where it remained constant for 15 minutes. Finally, the temperature decreased to 70°C. The temperature of the transfer line to the MSD was kept constant at 280°C. For ionization, the MSD was used in the positive chemical ionization (CI) mode with methane as reactant gas. The temperatures of the ion source and of the quadrupol were 250°C and 150°C, respectively. EO and $^{13}C_2$-EO were quantified in the single ion monitoring (SIM) mode using the M-H$^+$ ions m/z=45 (EO) and m/z=47 ($^{13}C_2$-EO), respectively. Chromatograms were manually integrated by using the HP Chemstation software. The retention times of both EO and $^{13}C_2$-EO were about 7 minutes (Figure 2.4).

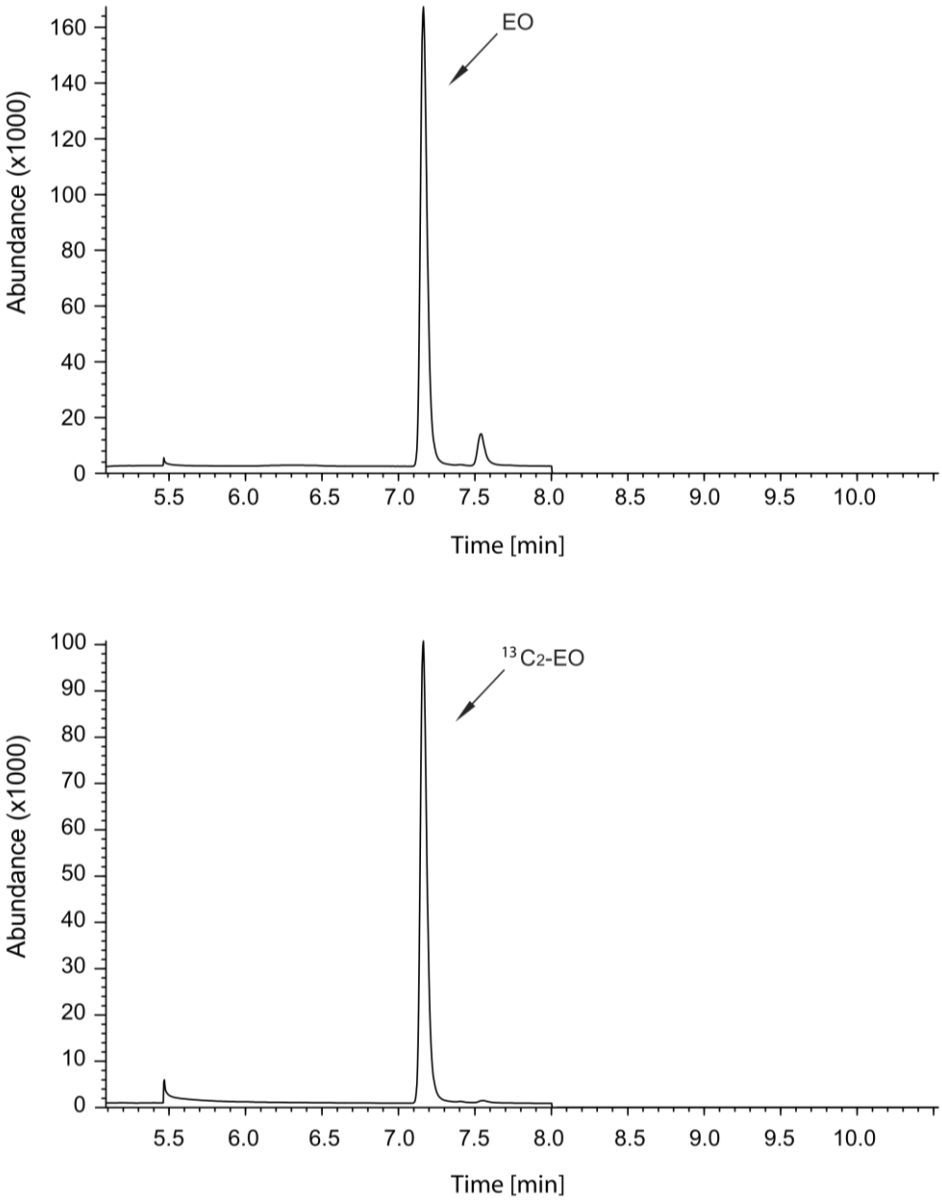

Figure 2.4 GC/MSD chromatograms of ethylene oxide (EO; 6.6 ppm) and [$^{13}C_2$]ethylene oxide ($^{13}C_2$-EO; 4.3 ppm). The GC/MSD setting are given in the text.

The calibration samples were prepared using heat-inactivated microsomes suspended in potassium phosphate buffer (150 mmol/l, pH 7.4). For this purpose, different EO concentrations were injected into headspace vials (38 ml) containing heat-inactivated microsomes and incubated at 37°C for 15 minutes. Gas samples of 10 ml were mixed with the internal standard and analyzed as described above. A calibration curve was obtained by plotting the peak height ratio of EO to the internal standard $^{13}C_2$-EO (about 4 ppm; the exact concentration was calculated using the volume of the air sample bag)

against the corresponding EO concentration (Figure 2.5). The detection limit was 1 ppb (3 times the background noise).

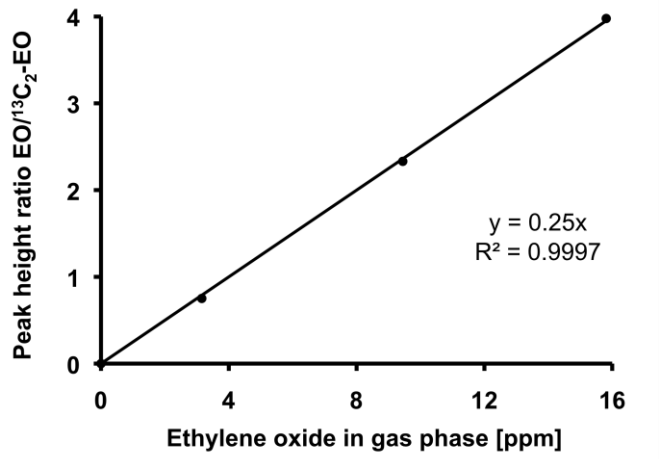

Figure 2.5 Calibration curve of ethylene oxide (EO; 3 - 16 ppm; m/z 45) determined by GC/MSD with [$^{13}C_2$]ethylene oxide ($^{13}C_2$-EO; 4 ppm; m/z 47) as internal standard. Symbols: single values; line: fit by linear regression analysis.

2.2.3.3 Determination of CYP2E1 activity

The activity of CYP2E1 in microsomes was determined using chlorzoxazone as specific substrate, which is metabolized to 6-hydroxychlorzoxazone (Figure 2.6; Chittur and Tracy, 1997; Peter et al., 1990). After incubating chlorzoxazone for 10 minutes in microsomal suspensions, the metabolite 6-hydroxychlorzoxazone was measured using high performance liquid chromatography coupled to tandem mass spectrometry (LC/MS/MS) (own method based on that of Walsky and Obach, 2004).

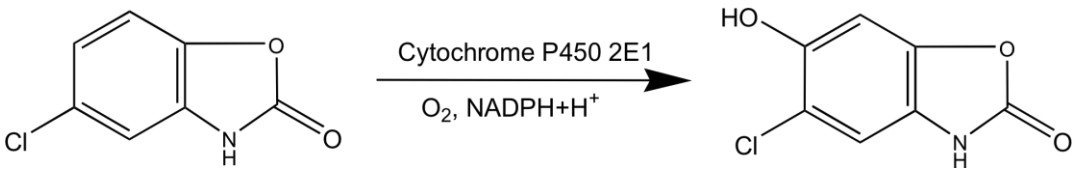

Figure 2.6 Cytochrome P450 2E1 mediated metabolism of chlorzoxazone.

Microsomal incubation with chlorzoxazone

In a centrifuge tube (6 ml) equipped with a screw cap, the following aqueous solutions were added: 1370 µl potassium phosphate buffer (100 mmol/l, pH=7.4), 100 µl $MgCl_2$ (100 mmol/l), 100 µl NADPH (10 mmol/l), and 100 µl NADH (10 mmol/l); the substances were dissolved in potassium phosphate buffer (100 mmol/l, pH=7.4). The tube was vortexed for 20 seconds and put on ice. Thereafter, 100 µl of microsomal suspension (4 mg protein/ml) was added. The tube was incubated for 3 minutes in a water bath at 37°C. The reaction was started by adding 60 µl of a methanolic chlorzoxazone solution (5.2 mg/ml). After an incubation period of exactly 10 minutes at 37°C, the reaction was stopped by adding 2 ml of ice-cold acetonitrile resulting in the precipitation of microsomal proteins. After cooling the centrifuge tube on ice for 15 minutes, the sample was centrifuged in a Sigma centrifuge for 10 minutes at 4000 x g. To 50 µl of the supernatant, 950 µl ammonium acetate (NH_4OAC) buffer (5 mmol/l aqueous NH_4OAC, 50/50 v/v in methanol) was added, and 5 µl of the solution was analyzed for 6-hydroxychlorzoxazone by LC/MS/MS.

Determination of 6-hydroxychlorzoxazone by LC/MS/MS

Separation was done isocratically on a column Luna C18(2), 150 × 2 mm I.D. 5 µm with 50% MeOH and 50% 5 mmol/l NH_4OAC as mobile phase at a flow rate of 300 µl/min. The column, thermostated at 24°C, was coupled to a triple stage quadrupole mass spectrometer API 4000 with a TurboIonSpray source, which was used in the negative ionization mode. The TurboIonSpray parameters were: head temperature 700°C, TurboIonspray voltage - 3700 V, nitrogen as curtain gas (10 psi), nebulizer (GAS1 = 20 psi), turbo gas (GAS2 = 40 psi), and collision gas (CAD = 11 psi). The entrance potential (EP = - 10 V) and declustering potential (DP = - 46 V) were the same for all the ions. The compound specific parameters for the multiple reaction monitoring mode (MRM) are given in Table 2.8.

Chromatograms were recorded and integrated by using the software Analyst. Figure 2.7 shows a typical LC/MS/MS chromatogram of 6-hydroxychlorzoxazone with the peak corresponding to the transitions *m*/*z* 184 → 120 which was used as quantifier.

Table 2.8 Compound specific parameters for the determination of 6-hydroxychlorzoxazone by LC/MS/MS

Q1 Mass [amu]	Q3 Mass [amu]	Dwell [msec]	CE [V]	CXP [V]
184.00	120.00	100.00	- 27	- 8
184.00	148.00	100.00	- 22	- 5

Q1: Quadruple 1, Q3: Quadruple 3, CE: collision energy, CXP: cell exit potential

Calibration samples

For calibration, microsomal incubations were prepared as described above with the exception that different concentrations of 6-hydroxychlorzoxazone (from 0.0 to 2.8 mg/ml in methanol) were added to the microsomal incubation instead of chlorzoxazone. The incubation step was omitted. The solution prepared after protein precipitation was then subjected to analysis by LC/MS/MS. A calibration curve, obtained by plotting the peak area of the transition m/z 184 → 120 against the 6-hydroxychlorzoxazone concentration, is shown in Figure 2.8. The detection limit (3 times the background noise) was 0.8 µmol/l microsomal incubation.

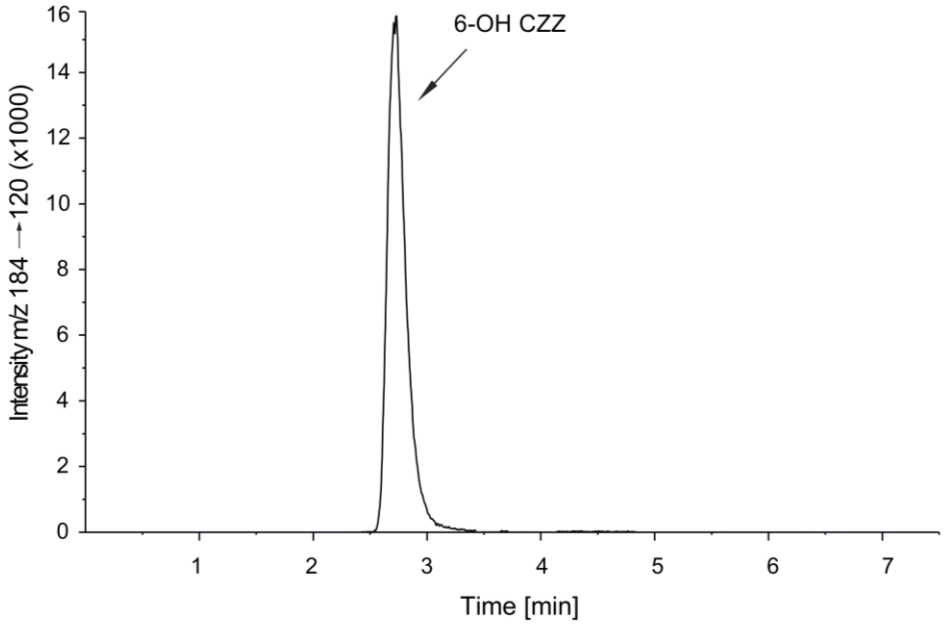

Figure 2.7 LC/MS/MS-chromatogram of 6-hydroxychlorzoxazone (6-OH CZZ; 0.12 mmol/l in methanol). Intensity is given in arbitrary units.

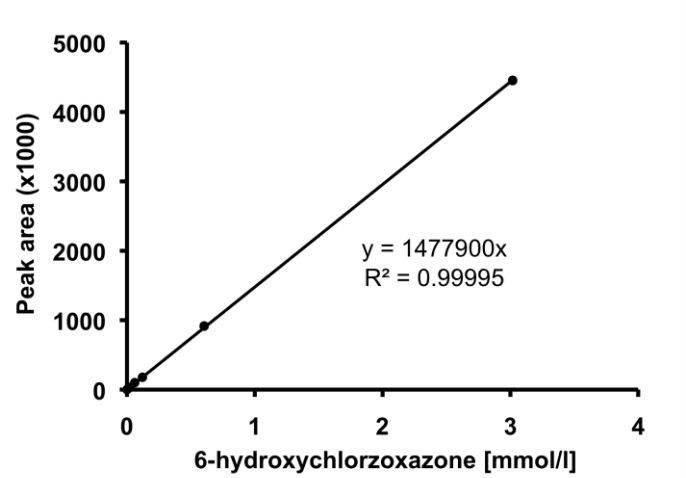

Figure 2.8 Calibration curve of 6-hydrochlorozoxazone (0.006 - 3.017 mmol/l) determined by LC/MS/MS (m/z 184 → 120). Symbols: single values (each concentration was determined twice); line: fit by linear regression analysis. Peak areas are given in arbitrary units.

The CYP2E1 activity was calculated using Equation 2.3.

$$v_{CYP} = \frac{c_{6OHCZZ}}{t \cdot P_{in}} \qquad 2.3$$

v_{CYP}: CYP2E1 activity [nmol/min·mg protein]

c_{6OHCZZ}: Concentration of 6-hydroxychlorzoxazone [nmol/ml] in the incubation medium

t: Incubation time [min]

P_{in}: Protein concentration [mg protein/ml] in the incubation medium

2.2.3.4 Quantification of glutathione

The GSH concentrations in liver homogenates were determined according to Eyer and Podhradsky (1986) using Ellman's reagent (5,5'-dithiobis-(2-nitrobenzoic acid); DTNB). When DTNB reacts with thiols, the disulfide bond of DTNB is cleaved yielding a disulfide with the reactant thiol and the yellowish 2-nitro-5-thiobenzoate which is determined by spectrophotometry at a wavelength of 412 nm. Principally, the reaction of DTNB with thiols is not specific for GSH. However, after precipitation of liver proteins

using metaphosphoric acid, the remaining water-soluble thiols consist to more than 95% of GSH (Summer and Greim, 1980).

A 200 µl sample of the liver homogenate (see 2.2.2) was diluted with 1800 µl potassium phosphate buffer (10 mmol/l, pH 7.4). Of this solution, 450 µl were given into a 2 ml Eppendorf cup and 700 µl of the aqueous precipitation solution (metaphosphoric acid 1.67%, Titriplex III 0.02%, and sodium chloride 30.0%) were added. After vortexing and incubation for 5 minutes at room temperature, proteins were sedimented by centrifugation (Sigma 1-15) at 16000 x g for 5 minutes at 0°C. Of the supernatant, 500 µl were given in an Eppendorf cup and 40 µl NaOH (1 mol/l) was added in order to reach a pH value of between 6.0 and 6.3. After addition of 250 µl DTNB solution (1 mol/l in 1% NaCl), the solution was vortexed and then incubated in dark at room temperature for 15 minutes. Thereafter, the sample was transferred into a glass cuvette and measured at room temperature against air at 412 nm using a UV/VIS spectrophotometer.

Calibration samples were prepared by adding 700 µl of the above mentioned precipitation solution into 2 ml Eppendorf cups that contained 450 µl freshly prepared ice-cold GSH standard solutions (0.0 - 0.3 mmol/l, dissolved in 0.01 mol/l potassium phosphate buffer, pH 7.4). Further treatment of the solutions was exactly as described above. A calibration curve was constructed by plotting the GSH concentrations against the absorbances that have been corrected by the blank sample (Figure 2.9). The curve was linear in the GSH concentration range of between 0.005 and 0.3 mmol/l diluted liver homogenate.

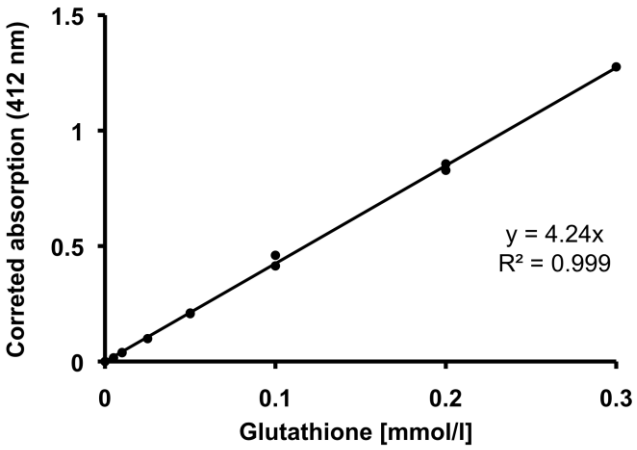

Figure 2.9 Calibration curve of glutathione determined as 2-nitro-5-thiobenzoate. Symbols: single values (each concentration was determined twice); line: fit by linear regression analysis.

2.2.3.5 Protein determination

The protein concentration was determined using a modified Biuret method (Faller, 1998). The Biuret reaction includes a reagent containing copper (II) ions in alkaline solution. Molecules which contain two or more peptide bonds associate with the copper ions to form a coordination complex of blue or violet color which is determined by spectrophotometry at a wavelength of 546 nm. The background absorption is determined after decolorization by adding KCN that forms a stronger complex with the copper ions.

Samples from homogenate, microsomes and cytosol

Homogenates (~1 ml) were suspended for 10 minutes at room temperature in equal volumes of aqueous NaOH (0.1 mol/l) solution. Microsomal and cytosolic sample were used directly. Of each sample, 20 µl were given into a 2 ml Eppendorf cup, which contained 1000 µl of the Biuret reagent (0.1 mol/l sodium hydroxide, 16 mmol/l Ka-Na tartarate, 15 mmol/l potassium iodide, 6 mmol/l copper (II) sulfate). A blank sample consisting of the Biuret reagent and deionized water only was also prepared. The samples were vortexed and incubated in the dark for 30 minutes at room temperature. Thereafter, they were transferred into plastic cuvettes and measured using a UV/VIS spectrometer at 546 nm against air. After adding KCN, each sample served as its own blank. The samples were transferred into Eppendorf cups again. To each cup, 50 µl of a KCN solution (6 mol/l) was added. After vortexing and incubation for 5 minutes at room temperature, the absorption of the samples was measured at 546 nm against air.
The absorption related to the protein content of each sample was calculated from the difference between the absorptions before and after the addition of KCN. Then the absorption resulting from the blank sample with Biuret reagent and water only was subtracted.

Calibration samples

Calibration samples were prepared using 2 ml Eppendorf cups into which 1000 µl of the Biuret reagent and 20 µl of standard protein solutions (bovine serum albumin) were added. The solutions were vortexed and treated further exactly as the biological samples. The calibration curve was obtained by plotting the protein concentrations against the absorptions obtained as described above (Figure 2.10).

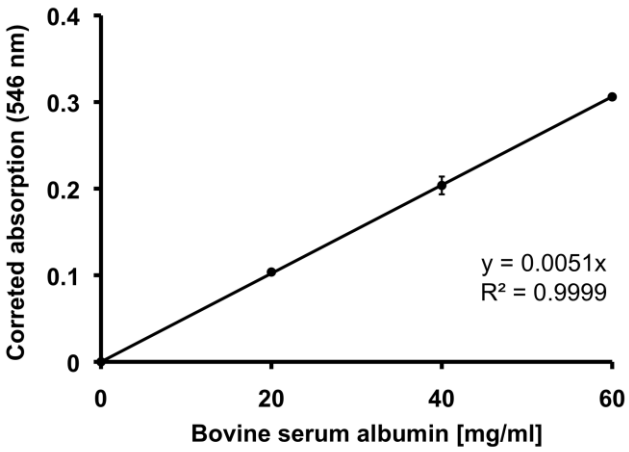

Figure 2.10 Calibration curve of protein determination by the Biuret method using bovine serum albumin as standard. Symbols, error bars: mean ± SD (n=3). If no error bars are visible, they are smaller than the symbol size. The lines were obtained by linear regression analysis.

2.2.4 Exposure experiments *in vitro* with ethylene, ethylene oxide, propylene oxide, or styrene

2.2.4.1 General procedure

A subcellular fraction or a tissue homogenate was incubated together with the required coenzymes in a closed headspace vial (~38 ml) which was placed in a heavily shaking water bath at 37°C (Figure 2.11). After an incubation period of 5-10 minutes, gaseous ET, EO, PO, or ST was collected via a Teflon-coated rubber septum from the corresponding storage desiccator using a calibrated disposable syringe and

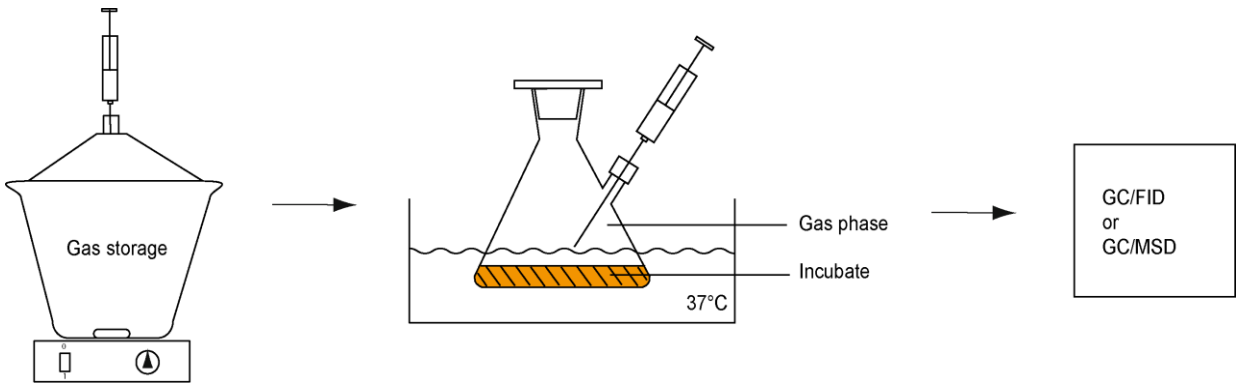

Figure 2.11 Scheme of incubation procedure for studying the in-vitro metabolism of ethylene, ethylene oxide, propylene oxide, or styrene.

immediately injected via a septum into the atmosphere of the headspace vial in order to achieve a defined initial gas concentration in the range of 10 - 10000 ppm. Thereafter, gas samples (maximum total volume: 3 ml per incubation) were taken periodically from the headspace and analyzed by GC/FID or by GC/MSD.

2.2.4.2 Microsomal inbubations

Ethylene and styrene

A headspace vial containing microsomes, $MgCl_2$ (5 mmol/l in the final incubation medium) and phosphate buffer (0.15 mol/l, pH 7.4) was situated in a heavily shaking water bath at 37°C. Volumes and protein concentrations of the microsomal solutions were 4 ml and 5 mg/ml (rodent livers) and 2 ml and 10 mg/ml (rat lungs and human livers), respectively. The gas phase in the vial was totally exchanged by pumping 100 ml of a gas sample containing the specified ET concentration through the vial using a 100 ml syringe equipped with a canula and a second canula both of which pierced the septum. A NADPH-regenerating system ($NADP^+$ 3.13 mmol/l, isocitrate 25 mmol/l, isocitrate dehydrogenase 0.63 U/l), dissolved in phosphate buffer, was prepared in a 2 ml Eppendorf cup. Both the headspace vial and the Eppendorf cup with the NADPH-regenerating system were kept in the water bath for 5 minutes. Then, the incubation was started by injecting 0.64 ml (for the 2-ml suspension) or 1.28 ml (for the 4-ml suspension) of the NADPH-regenerating system through the septum into the headspace vial. The final concentration of the NADPH-regenerating system in the incubation medium consisted of $NADP^+$ 1 mmol/l, isocitrate 8 mmol, and isocitrate dehydrogenase 0.2 U/l. Gas samples (50 or 500 µl) were collected at selected time points and were monitored by GC/FID for ET and/or the metabolically formed EO. Control experiments were done with heat-inactivated microsomes. The measured atmospheric EO concentrations were used to calculate the initial formation rate of EO (see 2.2.5).

In order to test whether the EO formation could be increased when using the coenzyme NADPH directly instead of the NADPH regenerating system, some microsomal incubations were started by injection of 0.2 ml of 10 mmol/l NADPH into the phosphate buffer resulting in a NADPH concentration of 0.5 mmol/l in the incubation medium.

The metabolic elimination of ET was quantified using a microsomal incubation medium (10 ml) with a high protein concentration of 10 mg/ml.

In order to confirm the CYP activities in hepatic microsomes of mice and rats, incubations were also carried out with vaporous ST. Volumes and protein concentrations of the incubation media were 1 ml and 2 mg/ml, respectively. Gas samples (50 µl) were monitored by GC/FID for ST.

Ethylene oxide and propylene oxide

A headspace vial containing microsomes (5 mg protein/ml in the final incubation medium), $MgCl_2$ (5 mmol/l) and phosphate buffer (0.15 mol/l, pH 7.4) was placed in a heavily shaking water bath at 37°C. The overall volume of the incubation medium was 1 ml. After incubating the vial in the water bath for 10 minutes, 0.7 - 4 ml air was removed by a gastight glass syringe. Then, the same volume of EO or PO of a defined concentration was injected into the vial. The volumes were calculated by means of Equation 2.4 and depended on the desired initial EO or PO concentration in the gas phase (10 to 10000 ppm). Gas samples (50 µl) were collected at selected time points and were analyzed for EO or PO by GC/FID. Control experiments were done with heat-inactivated microsomes.

$$V_{inj} = \frac{c_{in} \cdot (V_g + K_{eqEO} \cdot V_l)}{c_{desi}} \qquad 2.4$$

V_{inj}: Volume of gaseous EO [ml] injected into the headspace vial

c_{in}: Desired initial concentration of EO [ppm] in the gas phase of the heaspace vial (before start of the experiment)

V_g: Volume of the gas phase [ml] of the headspace vial

K_{eqEO}: Distribution coefficient incubation medium-to-air

V_l: Volume of the liquid phase [ml]

c_{desi}: Concentration of EO [ppm] in the desiccator

2.2.4.3 Cytosolic incubations

Cytosolic incubations were carried out solely with EO. A headspace vial (~38 ml) containing cytosol (3 mg protein/ml in the final incubation medium), $MgCl_2$ (5 mmol/l), GSH (15 mmol/l) and phosphate buffer (0.15 mol/l, pH 7.4) was placed in a heavily shaking water bath at 37°C. The final volume of the incubation medium was 1 ml. After

keeping the vial in the water bath for 10 minutes, a given volume of air was removed by a gastight glass syringe. The incubation was started by injecting the identical volume of pure gaseous EO or of an EO/air mixture of a defined EO concentration. The volume of air to be replaced by EO was calculated by means of Equation 2.4. It depended on the desired initial EO concentration in the gas phase of between 10 and 3000 ppm. Gas samples (50 µl) were collected at selected time points and were monitored by GC/FID for EO. Control experiments were done with heat-inactivated cytosol in the presence of DEM instead of GSH. DEM was given to deplete residual GSH (Boyland and Chasseaud, 1970). In order to determine the nonenzymatic conjugation of EO with GSH, incubations were done with heat-inactivated cytosol and GSH (15 mmol/l in incubation medium). In order to determine the extent of the nonenzymatic hydrolysis of EO, incubations were done with native cytosol and DEM (3 mmol/l in incubation medium).

2.2.4.4 Determination of distribution coefficients and distribution factors of ethylene and ethylene oxide

The distribution coefficient (K_{eq}) is the thermodynamic concentration ratio of a compound between two phases at a given temperature.

In order to determine the K_{eq} incubation medium-to-air of EO (K_{eqEO}), a headspace vial (vial F, Figure 2.12) containing heat-inactivated microsomes (5 mg protein/ml) or cytosol (3 mg protein/ml) and a empty headspace vial (vial E, Figure 2.12) were placed in a heavily shaking water bath at 37°C for 10 minutes. Then, the incubations were started by injecting into both vials the same amount of EO using the same syringe. Gas

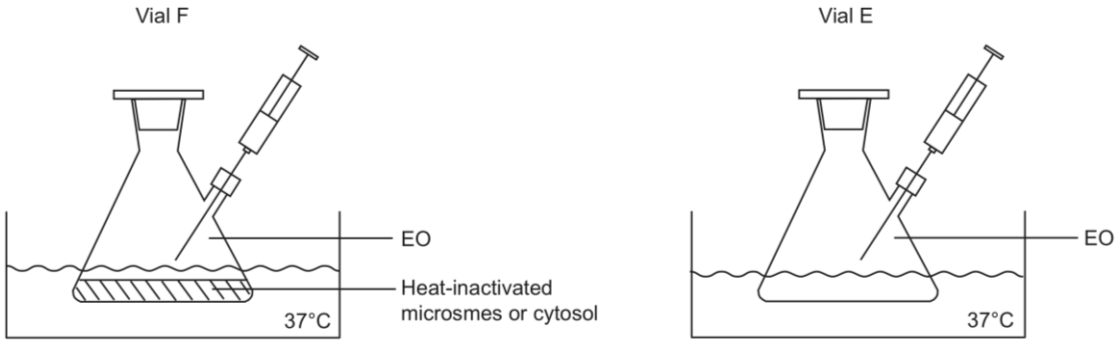

Figure 2.12 Experimental system to measure the distribution coefficient incubation medium-to-air of ethylene oxide (EO).

samples (50 µl) were collected at selected time points and were monitored by GC/FID for EO during the incubation period of 40 minutes. Using the average concentrations calculated from the resulting concentration-time courses, K_{eqEO} was obtained by means of Equation 2.5.

$$K_{eqEO} = \frac{c_E \cdot V_E - c_F \cdot V_{Fg}}{c_F \cdot V_{Fl}} \qquad 2.5$$

K_{eqEO}: Distribution coefficient incubation medium-to-air of EO
c_E: Concentration of EO [ppm] in headspace vial E
V_E: Volume [ml] of the vial E
c_F: Concentration of EO [ppm] in the gas phase of headspace vial F
V_{Fg}: Volume of the gas phase [ml] in the headspace vial F
V_{Fl}: Volume of the liquid phase [ml] in the headspace vial F

For the determination of K_{eq} of ET (K_{eqET}), only the headspace vial containing heat-inactivated microsomes (5 mg protein/ml) was placed in a non-shaken water bath at 37°C for 10 minutes. The incubation was started by injecting a defined amount of ET into the vial. Gas samples (50 µl) were collected at selected time points for up to 40 minutes and were analyzed for ET by GC/FID. An e-function (Equation 2.6a) was fitted through the concentration-time course of atmospheric ET. The obtained curve shows the loss of ET from the gas phase until the thermodynamic equilibrium is reached. K_{eqET} was calculated from the C_A and C_B values using Equation 2.6b.

$$c_{ET(t)} = C_A \cdot e^{-kt} + C_B \qquad 2.6a$$

$c_{ET(t)}$: Concentration of ET in the gas phase [ppm] at time point t
C_A: Difference between the initial ET concentration in air [ppm] and the final one when equilibrium is reached
k: Rate constant [1/h]
C_B: Final ET concentration in air [ppm] at equilibrium

$$K_{eqET} = \frac{C_A \cdot V_g}{C_B \cdot V_L} \qquad 2.6b$$

K_{eqET}: Distribution coefficient incubation medium-to-air of ET

C_A, C_B: See Equation 2.6a

V_g: Volume of the gas phase [ml] of the headspace vial containing the heat-inactivated subcellular fraction

V_l: Volume of the liquid phase [ml] of the headspace vial

The distribution factor (K_{st}) of a gaseous compound gives the steady-state concentration ratio between a liquid and a gas phase when metabolism takes place. In the low concentration range in which the rate of metabolism follows first-order kinetics, K_{st} is constant. Its value depends on K_{eq}, on the mass exchange rates between the two phases, and on the rate of the metabolic elimination. In case of saturation kinetics, K_{st} becomes also dependent on the compound concentration. At high concentrations, when the maximum rate of metabolism is reached (zero-order kinetics), K_{st} approaches K_{eq} (Filser, 1992).

In order to determine K_{st} of EO at concentrations of 80, 150, and 520 ppm EO, two headspace vials were used (Figure 2.13). Five ml of the incubation medium consisting of cytosol (3 mg protein/ml), $MgCl_2$ (5 mmol/l), GSH (15 mmol/l) and phosphate buffer (0.15 mol/l, pH 7.4) were given into vial H (~38 ml). Vial G (~38 ml) contained 2 ml of a saturated urea solution in phosphate buffer (about 1.7 g urea per ml buffer). The urea

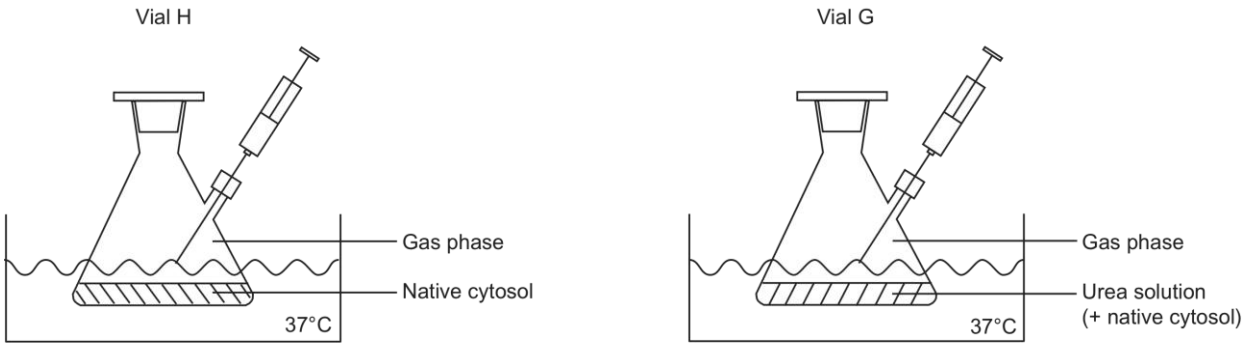

Figure 2.13 Experimental system to measure the distribution factor (K_{st}) of ethylene oxide between native cytosol and air. K_{st} was calculated from the ratio of the EO concentration in the liquid phase and in the gas phase of vial H (Equation 2.7a). The EO concentration in the liquid phase of vial H was calculated from the EO concentration in the gas phase of vial G after adding an aliquot of the liquid phase in vial H (Equation 2.7b).

was used to inactivate GST. Both vials were incubated for 10 minutes at 37°C in a heavily shaking water bath. Thereafter, the incubation was started by replacing 0.3 ml of air by the identical volume of pure EO. At the end of the incubation, the EO concentration in the gas phase was determined by GC/FID. At the same time, 1 ml of the cytosolic incubation medium was collected by a disposable syringe and immediately injected into vial G, from which 1 ml of its gaseous atmosphere had been removed before. After a further incubation for 5 minutes, 50 µl of the gas phase of vial G was collected and the EO concentration was determined. The calculation of K_{st} was calculated using Equation 2.7.

$$K_{st} = \frac{c_{lH}}{c_{gH}} \qquad 2.7a$$

$$c_{lH} = \frac{K_{eqG} \cdot c_{gG} \cdot V_{lG} + c_{gG} \cdot V_{gG}}{V_{in}} \qquad 2.7b$$

K_{st}: Distribution factor incubation medium-to-air of EO in vial H

c_{lH}: Concentration of EO [ppm] in the liquid phase of vial H at the end of incubation

c_{gH}: Concentration of EO [ppm] in the gas phase of vial H at the end of incubation

K_{eqG}: Distribution coefficient of EO between the saturated urea solution and the gas phase

c_{gG}: Concentration of EO [ppm] in the gas phase of vial G after injection of incubation medium from vial H

V_{lG}: Volume of liquid phase [ml] of vial G after injection of incubation medium from vial H

V_{gG}: Volume of gas phase [ml] of vial G after injection of incubation medium from vial H

V_{in}: Volume of incubation medium [ml] collected from vial H

2.2.4.5 Incubations of tissue homogenates

A headspace vial (~38 ml) containing 1 ml of tissue homogenate was placed in a heavily shaking water bath at 37°C. The protein concentration of the homogenate was

between 6.0 and 38 mg/ml, depending on the preparation of the tissue (2.2.2). After keeping the vial in the water bath for 5 minutes, approximately 3.8 ml air was removed by a gastight glass syringe, and the incubation was started by injecting the same volume of EO with a concentration of ~2900 ppm into the vial. Gas samples (50 µl) were collected at selected time points and analyzed for EO by GC/FID.
In order to maintain a sufficient level of GSH for the metabolism of EO over the incubation periods with native homogenates, 0.05 ml of GSH (300 mmol/l buffer) was added, resulting in an initial GSH concentration in the incubation medium of at least 15 mmol/l.
For determining the extent of the nonenzymatic hydrolysis of EO, experiments were done with native homogenates in the presence of DEM (150 mmol/l buffer; 0.02 ml) instead of GSH.

2.2.5 Toxicokinetic analysis

General information

Atmospheric concentrations given in ppm at 37°C can be transformed to mol/l by division with the molecular volume of an ideal gas at 37°C (25.43 l). Actual amounts $N_{(t)}$ of compounds in the vial are given by multiplication of the actual concentration in air $c_{a(t)}$ with the compound specific volume of distribution V_d:

$$N_{(t)} = c_{a(t)} \cdot V_d \qquad 2.8$$

Because the vials were always vigorously shaken, V_d was always the sum of the air volume V_g in the vial with the product of the liquid volume V_l in the vial with the compound- and medium- (cytosolic or microsomal incubation) specific K_{eq} incubation medium-to-air (Equation 2.9).

$$V_d = V_g + V_l \cdot K_{eq} \qquad 2.9$$

ET or EO gas uptake studies

In the ET or EO gas uptake studies, the atmospheric concentration-time courses of ET or EO were fitted using an e-function (Equation 2.10). or a differential equation

describing saturation kinetics according to Michaelis and Menten (Equation 2.11). In the case of first-order kinetics, the fitting program calculated the first-order rate constant k_{me} or k_{ce}. The elimination half-life is then given by $\ln 2/k_{me}$ or $\ln 2/k_{ce}$.

$$c_a = c_{a(0)} \cdot e^{-k \cdot t} + A \qquad 2.10$$

The concentration in the air phase of the vial is represented by c_a and the elimination rate constant by k. "A" means a constant concentration of $A \geq 0$.

$$dc_a/dt = \frac{-V^*_{max} \cdot c_a}{K^*_{map} + c_a} \qquad 2.11$$

dc_a/dt: Rate of an enzyme-mediated substance conversion
V^*_{max}: Maximum concentration change in the atmosphere of the headspace vial
K^*_{map}: Apparent Michaelis constant related to the atmospheric concentration

With the amount of protein (Pr) in the experimental onset, the expression $V^*_{max} \cdot V_d/Pr$ gives the maximum elimination rate V_{max} (amount of compound per time unit per mg protein) in the corresponding experiment:

$$V_{max} = V^*_{max} \cdot V_d/Pr \qquad 2.12$$

The compound- and species-specific value of K_{map} (the apparent Michaelis constant related to the incubation medium) is given by the product of K^*_{map} with K_{eq} (for definition of K_{eq}, see above):

$$K_{map} = K^*_{map} \cdot K_{eq} \qquad 2.13$$

Experiments with constant ET exposure concentrations

In ET incubation experiments with quasi-constant ET concentrations, metabolically formed EO was detected in the air phase of the exposure systems. Considering that the EO formation took place only in the liquid phase, each measured air-phase

concentration of EO (c_{EOa}) was used to calculate the corresponding amount of EO in the whole system and relating it to the liquid phase, solely (Equation 2.14).

$$c_{EOl} = \frac{c_{EOa} \cdot (V_g + K_{eqEO} \cdot V_l)}{V_l} \qquad 2.14$$

Here, c_{EOl} is the "theoretical" EO concentration in the liquid phase. K_{eqEO} is the thermodynamic distribution coefficient of EO in microsomal incubations.

The following function was fitted to the time-dependent, experimentally obtained c_{EOl} data. This function was derived from theoretical considerations (see 3.2.1.2):

$$c_{EOl} = C_1 \cdot (1 - e^{-k \cdot t}) \qquad 2.15$$

C_1 is the fitted EO concentration for t->∞ and k is a rate constant.

Initial formation rates of EO (v_{init}), normalized to a protein content of 1 mg, were calculated from the derivative of Equation 2.15 at t=0 by taking into account V_l and Pr (see 3.2.1.2):

$$v_{init} = \frac{k \cdot C_1 \cdot V_l}{Pr} \qquad 2.16$$

Further toxicokinetic procedures

The elimination of ethylene oxide determined in microsomal incubations consists of two parts: one reflects the EH-mediated and one the non-enzymatic, spontaneous hydrolysis. The rate constants of both elimination processes are given in Equation 2.17. The three rate constants were obtained from the incubation experiments by modifying the incubation media.

$$k_{me} = k_{meEH} + k_{eHyd} \qquad 2.17$$

k_{me}: Rate constant of overall elimination [1/min] in microsomal incubations

k_{meEH}: Rate constant of elimination catalyzed by EH [1/min]

k_{eHyd}: Rate constant of nonenzymatic spontaneous hydrolysis [1/min]

The elimination of EO determined in cytosolic incubations consists of three processes: enzymatic elimination catalyzed by GST, non-enzymatic GSH conjugation, and non-enzymatic spontaneous hydrolysis. The rate constants of these elimination processes are given in Equation 2.18. The three rate constants were obtained from the incubation experiments by modifying the incubation media.

$$k_{ceGST} = k_{ce} - k_{ceGSH} - k_{eHyd} \qquad 2.18$$

k_{ceGST}: Rate constant of elimination catalyzed by GST [1/min]

k_{ce}: Rate constant of overall elimination [1/min] in cytosolic incubations

k_{ceGSH}: Rate constant of non-enzymatic GSH conjugation [1/min]

k_{eHyd}: Rate constant of non-enzymatic spontaneous hydrolysis [1/min]

The clearance of the GST-mediated EO elimination [µl/min/mg protein] is the ratio of V_{maxGST} to K_{mapGST} and is given by:

$$\frac{V_{maxGST}}{K_{mapGST}} = \frac{k_{ceGST} \cdot V_d \cdot 1000}{K_{eq} \cdot Pr} \qquad 2.19$$

$\frac{V_{maxGST}}{K_{mapGST}}$: Clearance of GST-mediated EO elimination in cytosol [µl/min/mg protein]

V_{maxGST}: Maximum rate of GST-mediated EO elimination [nmol EO/min/mg protein]

K_{mapGST}: Apparent Michaelis constant [mmol/l] of GST-mediated EO elimination

V_d: Volume of distribution [ml], see above Equation 2.9

Pr: Amount of protein [mg]

Programs used for the toxicokinetic analysis

The program Prism 5 for Macintosh (GraphPad Software, California, USA) was used to fit e-functions to the gas uptake data. The program Berkeley Madonna 8.3.18

(University of California, Berkeley, USA) was used to fit Michaelis-Menten-type kinetics to the human microsomal EO concentration-time data. Prism 5 for Macintosh was again used to fit Michaelis-Menten-type kinetics to the data representing various v_{init} values of EO against the corresponding ET substrate concentrations in ET incubation experiments with quasi-constantly remaining ET concentrations. All other calculations were done with Microsoft Excel 2008 for Mac (Microsoft Corporation).

2.2.6 Statistics

The slopes of the calibration curves were calculated by linear regression analysis. Non-linear regression analysis was used for all other curves. Arithmetic mean ($\bar{x}$), standard deviation (SD), and standard error (SE) of the mean were obtained using Equation 2.20, 2.21, and 2.22 respectively.

$$\bar{x} = \frac{\sum_{i=1}^{i=n} x_i}{n} \qquad 2.20$$

$$SD = \sqrt{\frac{\sum_{i=1}^{i=n} (x_i - \bar{x})^2}{n-1}} \qquad 2.21$$

$$SE = \frac{SD}{\sqrt{n}} \qquad 2.22$$

x_i: Value of sample i

n: Number of measurements

The coefficient of variation (CV) in percent was obtained using Equation 2.23.

$$CV = \frac{SD}{\bar{x}} \cdot 100 \qquad 2.23$$

Error propagation of SE was calculated according to Equations 2.24 - 2.27 as described in Sachs (1973).

In case of an addition ($\overline{X}_1 + \overline{X}_2$) or a subtraction ($\overline{X}_1 - \overline{X}_2$) of stochastic independent means, SE was calculated as follows:

$$SE = \sqrt{SE_1^2 + SE_2^2} \qquad 2.24$$

In case of a division ($\frac{\overline{X}_1}{\overline{X}_2}$), SE was:

$$SE = \frac{\sqrt{\overline{X}_1^2 \cdot SE_2^2 + \overline{X}_2^2 \cdot SE_1^2}}{\overline{X}_2^2} \qquad 2.25$$

In case of a multiplication ($\overline{X}_1 \times \overline{X}_2$), SE was:

$$SE = \sqrt{\overline{X}_1^2 \cdot SE_2^2 + \overline{X}_2^2 \cdot SE_1^2} \qquad 2.26$$

In case of $\overline{X}_1 \times \overline{X}_2 \times \overline{X}_3$, SE was:

$$SE = \sqrt{\overline{X}_1^2 \cdot \overline{X}_2^2 \cdot SE_3^2 + \overline{X}_1^2 \cdot \overline{X}_3^2 \cdot SE_2^2 + \overline{X}_2^2 \cdot \overline{X}_3^2 \cdot SE_1^2} \qquad 2.27$$

Comparisons of differences between kinetic parameters were done using one-way ANOVA. The level of statistical significance was set at < 0.05.

The program Prism 5 for Macintosh was used to calculate the parameters describing the curves together with the SEs of these parameters. It was also used to perform the statistical tests.

3 RESULTS

3.1 Method validation studies

3.1.1 The NADPH regenerating system

In gas uptake studies with ET, either an NADPH solution (e.g., Csanády et al., 1992) or an NADPH regenerating system (e.g., Kreuzer et al., 1991) was injected to the microsomal incubations. In order to test which of both procedures yielded the most effective EO production, both kinds of NADPH administration were compared using an ET exposure concentration of about 3000 ppm (for methodology see 2.2.4.2). The EO production was monitored in the gas phase using GC/FID. The concentration-time courses of EO obtained in hepatic microsomes of mice and rats are shown in Figure 3.1.

When injecting NADPH directly, the selection of the initial NADPH concentration was based on *in vivo* data. For a normal rat liver, it was reported that the sum of $NADP^+$ and NADPH is 0.4 mmol/l (Ferris and Clark, 1971) and NADPH represents by far the predominant form (Veech et al., 1969). In the presently used NADPH regenerating system, the initial concentration of $NADP^+$ was 1 mmol/l. Kreuzer et al. (1991), using an NADP regeneration system, showed that the rate of the microsomal oxidation of an olefin was independent of the $NADP^+$ concentration in the range between 0.1 and 1 mmol/l.

For both animal species, the initial EO formation rates were similar in both incubations systems. After direct injection of NADPH (0.5 mmol/l, final concentration), the EO formation rates decreased after about 6 minutes and the EO concentrations reached plateaus, probably because of complete consumption of NADPH. In incubation systems that contained the NADPH regeneration system, continuous increases in the EO concentrations were observed. Because of this result, all further ET incubations were carried out using the NADPH regenerating system.

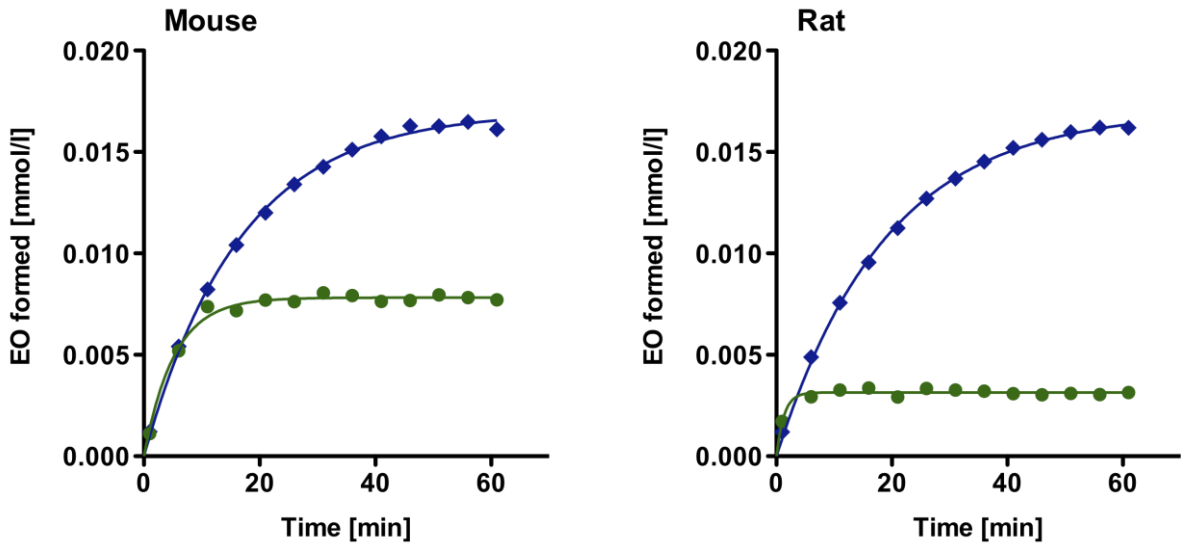

Figure. 3.1 Concentration-time courses of ethylene oxide (EO) formed in closed incubation vials (~38 ml) containing atmospheric ethylene exposure concentrations of ~3000 ppm and incubation media (4 ml) that consisted of pooled native hepatic microsomes from 50 B6C3F1 mice or 10 Fischer 344 rats and either an NADPH-regenerating system (◆) or a NADPH solution (●; 0.5 mmol/l). EO is given as EO concentrations in the liquid phase of the incubation vial. Symbols: single values calculated from measured data; lines: fits to the data using Equation 2.15. Each concentration-time course represents 1 experiment carried out in 1 vial.

3.1.2 Distribution between liquid phase and air

The thermodynamic distribution coefficient incubation medium-to-air (K_{eq}) of ET or EO and the steady-state concentration ratio incubation medium-to-air of EO, the distribution factor (K_{st}), were obtained from measured data as described in 2.2.4.4.

Distribution coefficient

Figure 3.2A shows a typical concentration-time course of ET in the gas phase of a non-shaken vial that contained an initial ET exposure concentration of 9.2 ppm and a liquid medium with heat-inactivated rat liver microsomes. From the exponential curve fitted to the data, the K_{eqET} value was calculated using Equations 2.6a and 2.6b. Figure 3.2B shows concentration-time courses of EO in the gas phases of two vials into both of which the same amount of gaseous EO was administered. Only one of the vials contained in addition to EO a liquid medium with heat-inactivated rat liver microsomes. Both vials were continuously heavily shaken. K_{eqEO} was obtained from the difference between the constant concentrations measured during the exposure period in both vials. The K_{eq} values are shown in Table 3.1.

When required for calculations, K_{eqET} of 0.2 and K_{eqEO} of 68.4 (microsomal incubation media) and of 75.9 (cytosolic incubation media) were used.

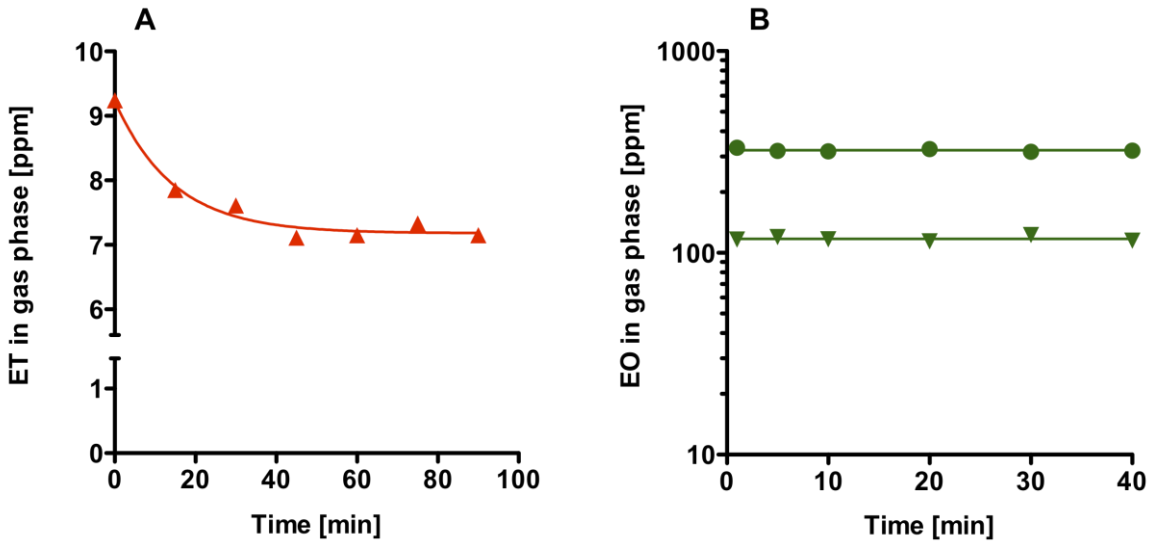

Figure 3.2 Concentration-time courses (A) of ethylene (ET) in the atmosphere of a non-shaken headspace vial (37°C) containing incubation medium with heat-inactivated Fischer 344 rat liver microsomes or (B) of ethylene oxide (EO) in the atmospheres of heavily shaken headspace vials (37°C) containing only EO (●) or EO and incubation medium with heat-inactivated Fischer 344 rat liver microsomes (▼). Symbols: single values; lines: means (green colored) or fit to the data (red colored) using Equation 2.10. Each concentration-time course represents 1 experiment carried out in 1 vial.

Table 3.1 Distribution coefficients incubation medium-to-air (K_{eq}) of ethylene (ET) and ethylene oxide (EO)

Compound	Incubation medium	Protein [mg/ml]	K_{eq} (mean ± SD)	n
ET	Microsomes	2.5	0.20 ± 0.06	3
	Microsomes	5.0	0.18 ± 0.03	4
EO	Microsomes	2.5	71.1 ± 0.3	3
	Microsomes	5.0	68.4 ± 0.6	3
	Microsomes	10	68.3 ± 0.1	3
	Cytosol	3.0	75.9 ± 3.1	3

Distribution factor

The distribution factor of EO (K_{stEO}) was measured in three incubation experiments in order to test whether in heavily shaken vials with cytosolic incubations the distribution of EO between liquid and air phase was fast enough to consider it as instantaneous, even under conditions of metabolic elimination. The results are shown in Table 3.2. From the similarity between K_{stEO} (65.5 ± 6.2; mean ± SD) and K_{eq} one can conclude that EO distributed so rapidly between both phases that it was justified to neglect the distribution rates when the rates of metabolic elimination were calculated from the data obtained in EO incubation studies in cytosol.

Table 3.2 Distribution factors incubation medium-to-air (K_{stEO}) of ethylene oxide (EO) in heavily shaken vials containing cytosolic incubations and GSH

EO in gas phase [ppm]	K_{stEO} [a)]
520	62.1
150	61.8
80	72.7

[a)]: one determination at each concentration

3.1.3 Microsomal and cytosolic viability tests

CYP2E1 activity

In order to verify the NADPH dependent CYP activity in hepatic microsomes over the incubation time, the rapidly metabolized olefin ST (Csanády et al., 1994) was chosen as a test substance because ST, in contrast to other terminal olefins, is known to destroy its metabolizing CYP species extremely slowly (reviewed in Correia and Ortiz de Montellano, 2005). ST gas uptake studies were performed using pooled microsomes from mouse and rat as described in 2.2.4.1. The concentration-time courses followed continuously first-order decays for the whole time periods of up to 65 minutes without any sign of loss of activity (Figure 3.3). In incubations that contained native microsomes (2 mg protein/ml), the slopes of the curves were 0.046 min^{-1} in mouse liver microsomes and 0.031 min^{-1} in rat liver microsomes. Drastically flatter curves with slopes of 0.0019 min^{-1} (mouse liver) and of 0.0010 min^{-1} (rat liver) were obtained when using heat-inactivated microsomes (2 mg protein/ml).

When comparing the CYP2E1 specific metabolism of chlorzoxazone to 6-hydroxy-chlorzoxazone in pooled liver microsomes (5 mg protein/ml) with a chlorzoxazone concentration of 1 µmol/l, formation rates of 4.27 and 4.28 nmol/min/mg protein were obtained in mouse microsomes (n=2) and of 2.56 ± 0.097 nmol/min/mg protein in rat microsomes (n=7). In their classical study, Court et al. (1997) obtained 6-hydroxy-chlorzoxazone formation rates of 3.9 nmol/min/mg protein in mouse and of 2.5 nmol/min/mg protein in rat liver microsomes when using a maximum chlorzoxazone concentration of 1 µmol/l. Based on the results obtained with ST and with chlorzoxazone, it was concluded that the microsomes were intact over the whole exposure period and that the CYP activity of the microsomes used for the investigation of the CYP mediated metabolism of ET and EO was excellent.

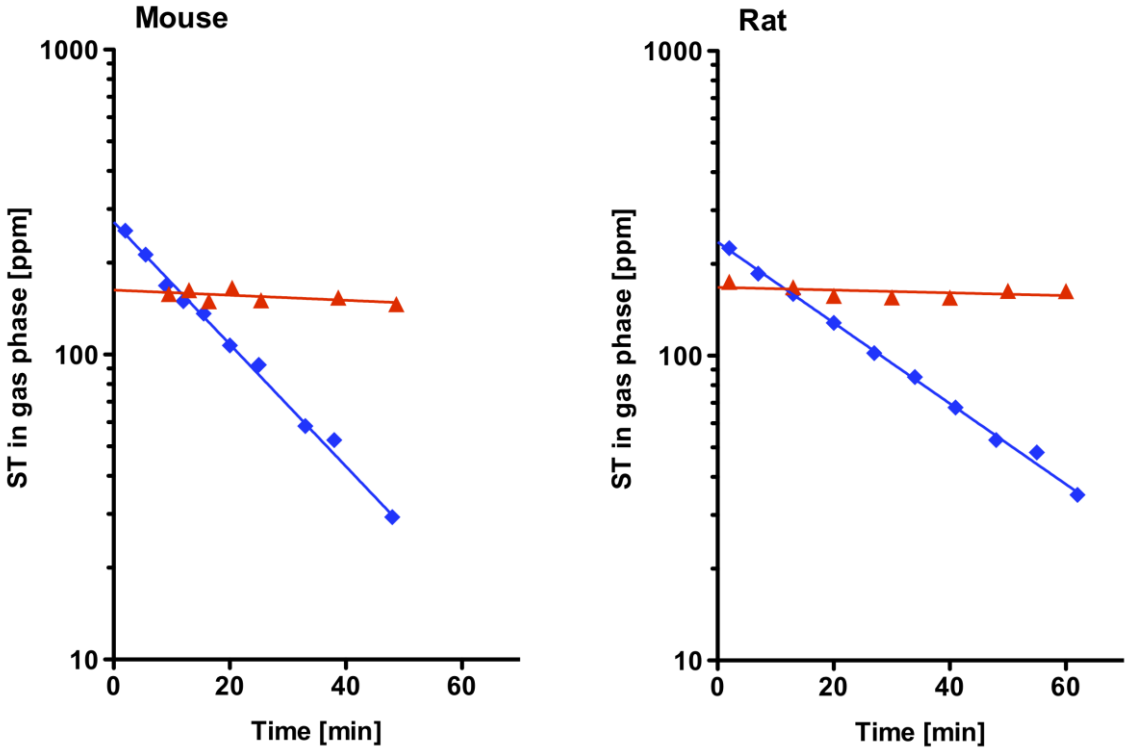

Figure 3.3 Concentration-time courses of gaseous styrene (ST) in the atmospheres of closed vials (8 ml) containing incubation media (1 ml) that consisted of pooled heat-inactivated (▲) or native (◆) microsomes (2 mg protein/ml) from livers of 50 B6C3F1 mice or 10 Fischer 344 rats. Symbols: single values; lines: fits to the data using Equation 2.10. Each concentration-time course represents 1 experiment carried out in 1 vial.

Microsomal EH activity

In order to verify the EH activity in liver microsomes, some gas uptake studies were conducted with PO using the same native pooled liver microsomes (3 mg protein/ml) of

mice or rats and liver microsomes (3 mg protein/ml) of a male human subject as were used for the EO experiments. PO was chosen because it has similar amphiphilic properties as EO. The octanol/water partition coefficient ($P_{o/w}$) of PO is 1.1 (calculated from log $P_{o/w}$ given in NIOSH 2009) and that of EO is 0.50 (calculated from log $P_{o/w}$ given in NIOSH 2001). The accumulation of both epoxides in the liquid phase of the incubation vials is similar as evidenced by the K_{eq} values of 63.7 (PO; Faller et al., 2001) and 68.4 (EO, see above). Figure 3.4 shows the concentration-time courses of PO in the atmosphere of vials containing microsomal incubations. PO was continuously eliminated according to first-order kinetics over the whole time period of 65 minutes. Only a very small decay of the PO concentration was observed in heat-inactivated microsomes. In incubations with native microsomes, the rate constants were calculated to be 0.011 min^{-1} for mouse, 0.012 min^{-1} for rat and 0.029 min^{-1} for human. Using these rate constants, the K_{eq} value of PO, the volumes of air phase and of incubation medium, and the protein concentrations, the metabolic clearances of PO are calculated to be 5.4 µl/min/mg protein (mouse), 5.9 µl/min/mg protein (rat), and 14.9 µl/min/mg protein (human). Considering that similar findings were published by Faller et al. (2001), the microsomes were considered to be intact with respect to their EH activity.

GST activity

In order to verify the cytosolic GST activity, some gas uptake studies were conducted with PO using GSH- or DEM-containing native pooled liver cytosol of mice or rats and liver cytosol of a male human subject.

Figure 3.5 shows the concentration-time courses of PO in the atmosphere of vials containing cytosolic incubations. In the presence of GSH, PO was continuously eliminated over the whole time period of 65 minutes. Only a very small concentration decay was observed in DEM containing heat-inactivated cytosol. In the incubations with GSH-containing native cytosol, the rate constants were calculated to be 0.050 min^{-1} for mouse, 0.027 min^{-1} for rat and 0.023 min^{-1} for human. The corresponding metabolic clearance of PO is calculated to be 26.0 µl/min/mg protein (mouse), 10.3 µl/min/mg protein (rat) and 8.2 µl/min/mg protein (human). Considering the similar values (mouse: 33; rat: 13; human: 12 and 13 µl/min/mg protein) obtained by Faller et al. (2001), the cytosol is considered to be viable with respect to the GST activity.

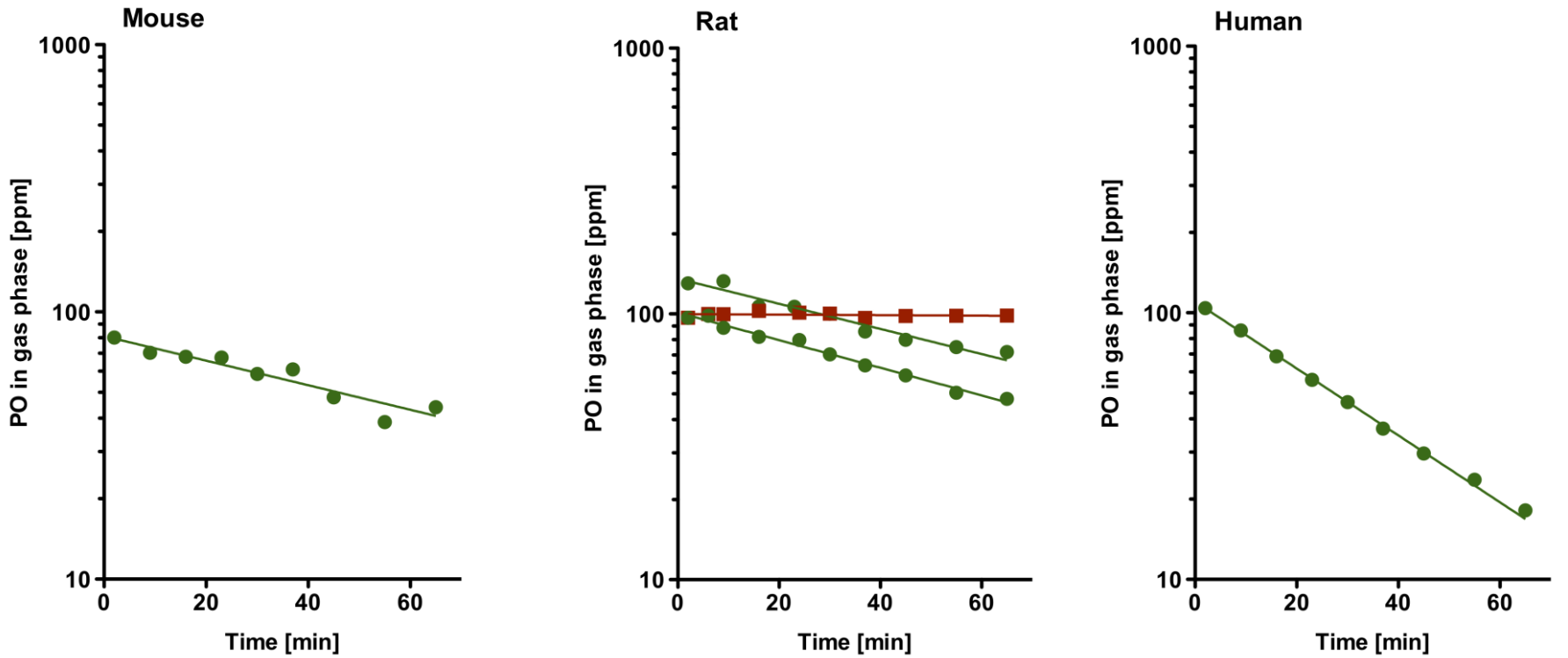

Figure 3.4 Concentration-time courses of propylene oxide (PO) in the atmospheres of closed vials (~38 ml) containing incubation media (1 ml) that consisted of native (●) or heat-inactivated (■) microsomes (3 mg protein/ml) from pooled livers of 50 B6C3F1 mice, 10 Fischer 344 rats, or from a liver of a 22 year-old male human subject. Symbols: single values; lines: fits to the data using Equation 2.10. Each concentration-time course represents 1 experiment carried out in 1 vial.

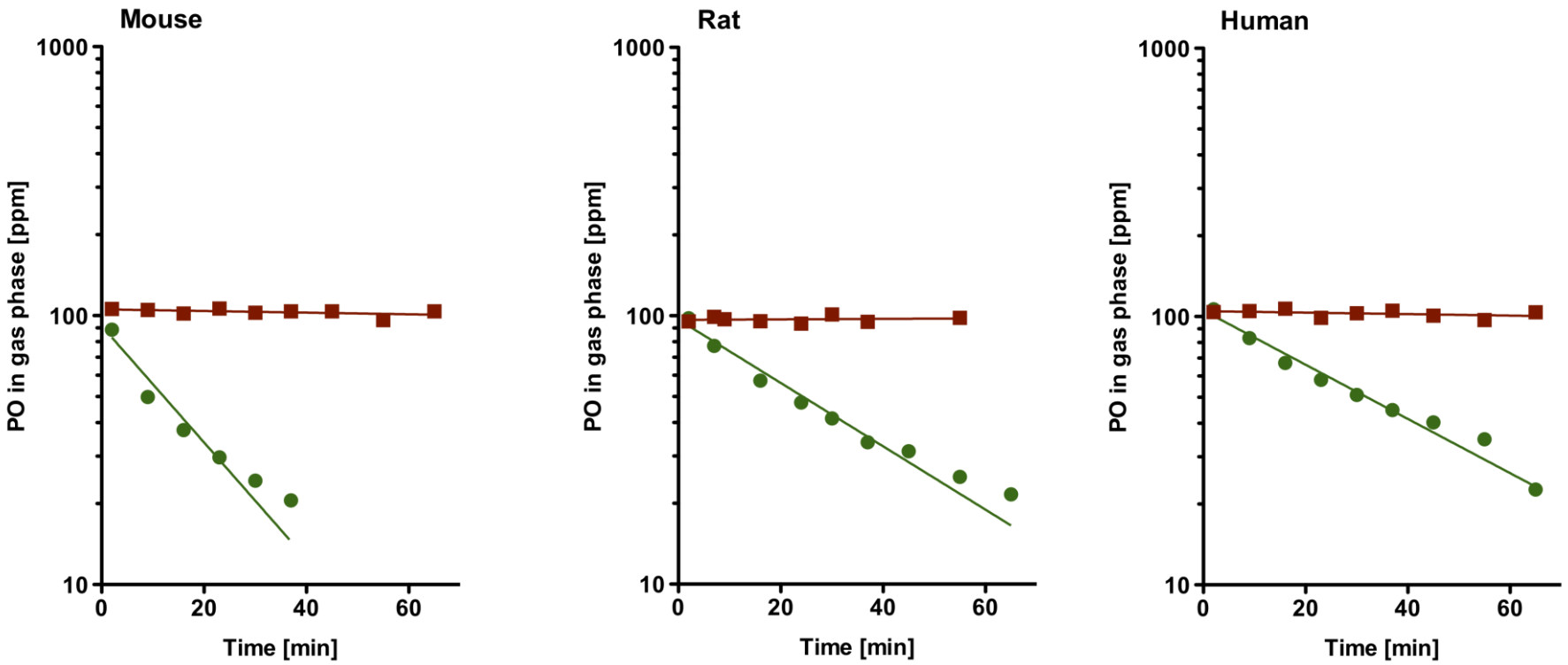

Figure 3.5 Concentration-time courses of propylene oxide (PO) in the atmospheres of closed vials (~38 ml) containing incubation media (1 ml) that consisted of GSH- or DEM-containing pooled hepatic cytosol (3 mg protein/ml) from 50 B6C3F1 mice, 10 Fischer 344 rats, or of hepatic cytosol (3 mg protein/ml) from a 22-year old male human subject.
Symbols: single values; heat-inactivated cytosol in presence of DEM (3 mmol/l; ■) or native cytosol in presence of GSH (15 mmol/l; ●); lines: fits to the data using Equation 2.10. Each concentration-time course represents 1 experiment carried out in 1 vial.

3.1.4 Genotyping

According to The Jackson Laboratory (2009), in PCR analysis amplicons with 280 DNA base pairs are characteristic for CYP2E1 knockout (CYP2E1 -/-) mice and amplicons with 125 DNA base pairs are characteristic for wild-type (CYP2E1 +/+) mice. PCR analyses confirmed that the offspring of the 129/Sv-Cyp2e1^{tm1Gonz}/J mice obtained from The Jackson Laboratory were indeed knocked out for CYP2E1 (Figure 3.6).

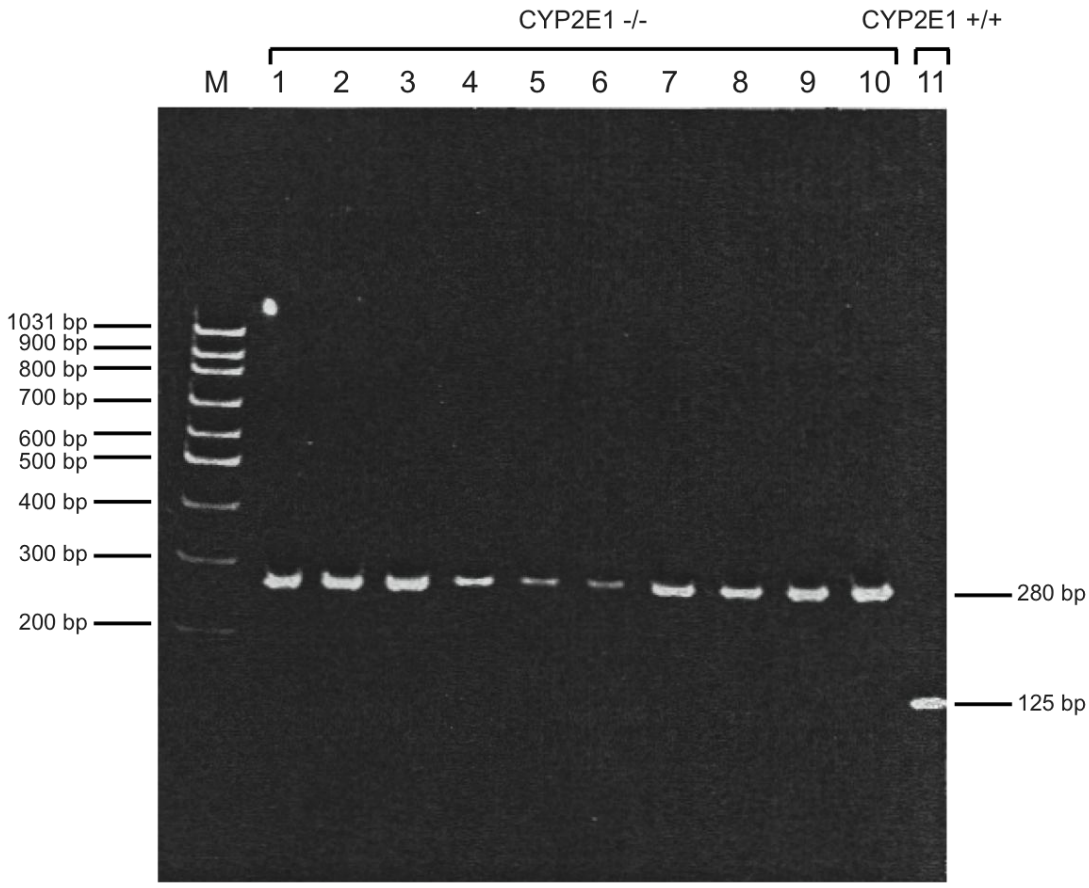

Figure 3.6 Photograph of an illuminated polyacrylamide gel containing a DNA ladder (lane M) and PCR-products characteristic for the CYP2E1 knockout (-/-) gene (10 mice, lanes 1 to 10) or the CYP2E1 wild-type (+/+) gene (one mouse, lane 11); bp means base pairs.

3.2 Incubation studies

3.2.1 Gas uptake studies with ethylene in microsomal incubations

3.2.1.1 Elimination of ethylene

In order to investigate metabolic ET elimination by means of gas uptake studies, a protein concentration of 5 mg/ml was used at first. However, ET elimination was so slow that there was no distinguishable difference between heat-inactivated and native microsomes (Figure 3.7A). After increasing the amount of protein by a factor of 5, differences in the concentration-time courses between heat-inactivated and native microsomes became visible (Figures 3.7B and 3.7C). The slopes of the curves fitted to the data in native microsomes flattened with the exposure time and after about 20 minutes become parallel to the curves fitted to the data with heat-inactivated ones. The small decay of the latter curves results from the ET loss due to the sampling of the gas probes. The curves gained with native microsomes leveled off with time demonstrating the well-known suicide inactivation of the ET metabolizing CYP species as a result of the NADPH dependent activation of ET (Ortiz de Montellano and Mico, 1980). From the e-functions describing the curves in Figures 3.7B and 3.7C, initial rates of ET elimination were calculated. In mouse liver microsomes, the initial metabolic ET elimination was 0.069 nmol/min/mg protein at an ET exposure concentration in the vial atmosphere of 170 ppm. In rat liver microsomes, initial rates were 0.022 and 0.051 nmol/min/mg protein at an ET concentration of 200 ppm (two experiments) and 0.005 nmol/min/mg protein at an ET concentration of 30 ppm. Within this concentration range, the metabolic ET elimination seems to be linearly dependent on the ET exposure concentration. However, the determination of the metabolic elimination was rather vague. This becomes evident from Figures 3.7B and 3.7C, which show that the differences between the curves with heat-inactivated and native microsomes were only small. In addition, very large amounts of microsomal protein (100 mg/incubation) were required. Therefore, the experimental procedure was revised. Instead of determining the elimination of ET, the formation of its metabolite EO was measured in ET-exposed microsomes.

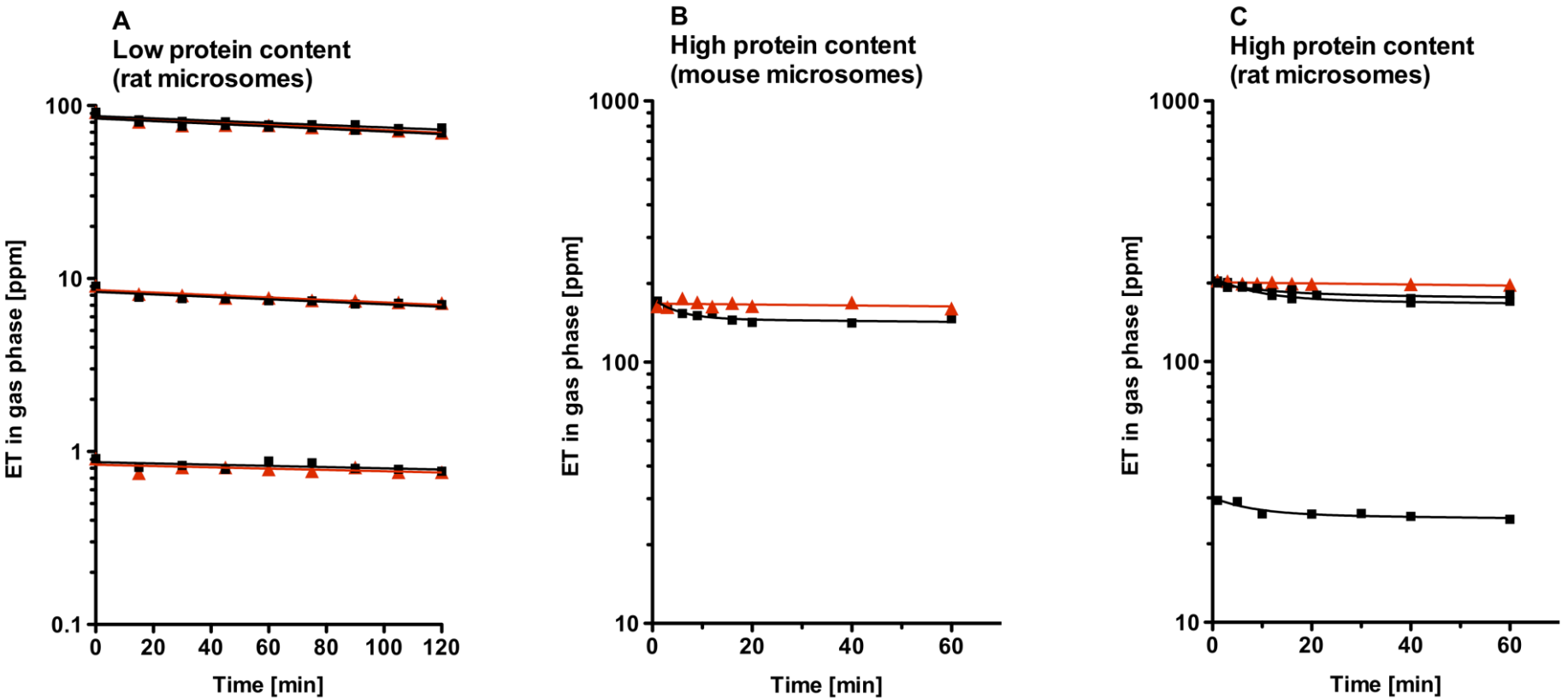

Figure 3.7 Concentration-time courses of gaseous ethylene (ET) of several initial concentrations in the atmospheres of closed vials containing incubation media with low or high microsomal protein content. A: Low protein content: 5 mg protein/ml, incubation volume 4 ml, vessel volume 8 ml; B, C: high protein content: 10 mg protein/ml, incubation volume 10 ml, vessel volume 38 ml. Symbols: single values obtained with pooled hepatic heat-inactivated (▲) or native (■) microsomes from 50 B6C3F1 mice or 10 Fischer 344 rats; lines: fits to the data using Equation 2.10. Each concentration-time course represents 1 experiment carried out in 1 vial.

3.2.1.2 Quantitative description of the suicide inactivation of CYP2E1 by ethylene; development of a suicide inhibition model

Principal experimental procedure

At first, the formation of EO was investigated in two vials containing ET-exposed (7600 ppm) rat liver microsomes using protein concentrations of 2 and 5 mg/ml. After starting the ET metabolism by injecting the NADPH-regenerating system, concentration-time courses of metabolically formed EO were monitored in the atmosphere of the vials. Figure 3.8 presents the hereof-calculated exposure time dependent EO concentration that is related to the liquid phase (see Equation 2.14). The curves were fitted by e-functions of the general form $y = y_{\infty} \cdot (1 - e^{-k \cdot t})$ (see Equation 2.15). In both curves, the values of k were very similar (lower curve: 0.06 [min^{-1}], higher curve: 0.08 [min^{-1}]). The y_{∞}-values were 0.01 [mmol/l] (lower curve) and 0.02 [mmol/l] (upper curve), and the ratio of both values were close to the ratio of the protein concentrations. The initial EO formation rates (Equation 2.16) were 0.45 [nmol/min/mg protein] (lower curve) and 0.44 [nmol/min/mg protein] (upper curve). The plateaus of the curves show that the EO formation was completely inhibited after about 50 min. This is in agreement with the concept of the above discussed suicide inactivation of the ET metabolizing CYP species. In order to explain quantitatively the concentration-time courses of the metabolically formed EO, the following model was developed which describes the suicide inhibition of CYP2E1 by ET during the formation of EO.

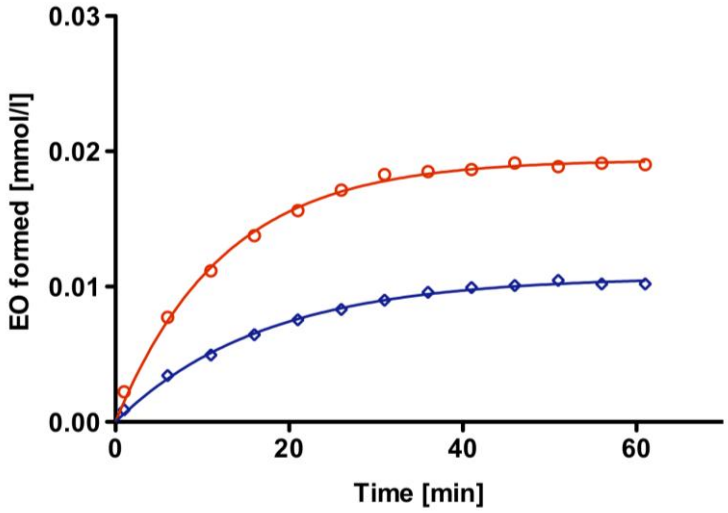

Figure 3.8 Concentration-time courses of ethylene oxide (EO) formed during exposures to ethylene (~7600 ppm) in closed vials (38 ml) containing incubation media (4 ml) consisting of pooled hepatic microsomes from 10 Fischer 344 rats at a protein concentration of 2 mg/ml (◇) or 5 mg/ml (O). EO is given as EO concentrations in the liquid phase of the incubation vial. Symbols: single values; lines: fits to the data using Equation 2.15. Each concentration-time course represents 1 experiment carried out in 1 vial.

Development of a suicide inhibition model

The CYP-mediated metabolic production of EO from ET together with the irreversible inactivation of CYP by N-hydroxyethylation of the pyrrole ring D (see, for example, Correia and Ortiz de Montellano, 2005) was described by the following reaction scheme (adapted from Collman et al., 1990), which incorporates the metabolite formation via the enzyme-substrate complex ES and the simultaneous suicide inactivation of ES.

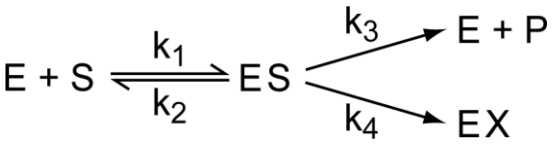

3.1

The concentration of the ET metabolizing CYP species is given by E, that of the substrate ET by S, and that of the product EO by P. EX stands for irreversibly inactivated CYP. The rate constants of the four reactions shown in Equation 3.1 are represented by k_1, k_2, k_3, and k_4. In the literature, k_3 is often named "k_{cat}" and k_4, the inactivation constant, "k_{inact}". The co-substrates O_2 and NADPH are not considered because O_2 was in excess and NADPH was assumed to be constant during the exposure period because the NADPH regeneration system was used. According to Equation 3.1, the change of ES over time (t) is described by:

$$\frac{dES}{dt} = k_1 \cdot S \cdot E - (k_2 + k_3 + k_4) \cdot ES \qquad 3.2$$

When the rate of the suicide inhibition

$$\frac{dEX}{dt} = k_4 \cdot ES \qquad 3.3$$

is zero, Equation 3.2 reads

$$\frac{dES}{dt} = k_1 \cdot S \cdot E - (k_2 + k_3) \cdot ES \qquad 3.4$$

As discussed by Briggs and Haldane (1925), dES/dt in Equation 3.4 can be considered to be negligibly small. Taking this assumption of a very fast quasi-steady state into account and considering dEX/dt (see Equation 3.3) being much slower than the time to reach the quasi-steady state, Equation 3.2 can be reformulated to:

$$\frac{dES}{dt} = -k_4 \cdot ES \qquad 3.5$$

At the beginning of the microsomal incubations, the ES complex was already formed in the pre-incubation phase before the reaction was started by addition of NADPH regenerating system. During this phase, both k_3 and k_4 are evidently not existent (compare Equation 3.1); the ES complex ES_0 at t=0 (the end of the pre-incubation phase, when the reaction starts) is given by:

$$k_1 \cdot E \cdot S = k_2 \cdot ES_0 \qquad 3.6a$$

or

$$ES_0 = \frac{k_1 \cdot E \cdot S}{k_2} \qquad 3.6b$$

At the end of the pre-incubation phase, the total enzyme concentration (E_t) is given by:

$$E_t = ES_0 + E \qquad 3.7$$

Combining Equation 3.6b with Equation 3.7 and canceling E, one obtains ES_0 as a function of E_t, S, and the rate constants k_1 and k_2:

$$ES_0 = \frac{E_t \cdot k_1 \cdot S}{k_2 + k_1 \cdot S} \qquad 3.8$$

It can be derived from Equation 3.8 that ES_0 equals E_t at very high concentrations of S because k_2 can be neglected if compared with $k_1 \cdot S$ for such exposure conditions.
The solution of the differential Equation 3.5 is:

$$ES = ES_0 \cdot e^{-k_4 \cdot t} \quad 3.9$$

Equation 3.1 shows that the rate of the EO formation during the ET exposure (dP/dt) is represented by:

$$\frac{dP}{dt} = k_3 \cdot ES \quad 3.10$$

or with Equation 3.9:

$$\frac{dP}{dt} = k_3 \cdot ES_0 \cdot e^{-k_4 \cdot t} \quad 3.11$$

Because ES_0 equals E_t at very high concentrations of S, the maximum rate of metabolite formation dP_{max}/dt at the time point $t = 0$ ($t_{(0)}$), when the reaction is started, is given by:

$$\frac{dP_{max}}{dt} = k_3 \cdot E_t \quad 3.12$$

The concentration-time course of P at a given constant concentration of S is obtained by integrating Equation 3.11 and considering that $P = 0$ at $t_{(0)}$:

$$P = \frac{k_3}{k_4} \cdot ES_0 \cdot [1 - e^{-k_4 \cdot t}] \quad 3.13$$

The term (k_3/k_4) is called partition ratio and represents the number of products formed per one inactivation event. The partition ratio is constant, independent of the substance concentration. Both reactions ($k_3 \cdot ES$) and ($k_4 \cdot ES$) follow saturation kinetics.

Linkage of the suicide inhibition model with experimental parameters

Because of the very low K_{eqET} of 0.2 (see 3.1.2), the amount of ET was much greater in the relatively large atmospheric volumes of the closed vials than in the small liquid phase, where the reaction took place. Consequently and also because of the relatively

slow metabolic ET elimination, the substrate concentration ET remained almost constant during the exposure periods. The maximum EO production V_{maxEO} could be obtained experimentally as described in the text to Equation 3.1. Considering ET to be metabolized exclusively by CYP2E1, mean microsomal CYP2E1 contents (pmol/mg microsomal protein) of 96 (SD = 12; n=3), 35.8 (SD = 8.3; n=3), and 70.5 (SD = 17; n=30; weighted means and SD of 10 samples, each measured 3 times) in livers of male B6C3F1 mice, male Sprague-Dawley rats, and humans (male and female Caucasians), respectively (Seaton et al., 1995), were taken as the species specific total amounts of enzyme E_t. Replacing dP_{max}/dt in Equation 3.12 by the maximum EO formation rate (V_{maxEO}) and E_t by the CYP2E1 content, Equation 3.14 was used to calculate the value of k_3:

$$k_3 = \frac{V_{maxEO}}{CYP2E1} \qquad 3.14$$

Equation 3.13 has the same structure as Equation 2.15. Therefore, the value of the inactivation constant k_4 equals the experimentally obtained value of k in Equation 2.15. The concentration $k_3/k_4 \cdot ES_0$ (Equation 3.13) stays for the experimental EO plateau concentration C_1 (see Equation 2.16) which, when multiplied with k_4, equals the initial EO production rate (see Equation 3.11) at a given ET exposure concentration and a microsomal protein content.

It has to be stressed that the K_{map} values and the rate constants k_i dealt with in the present work are apparent constants because the experiments were not performed with purified enzymes. The use of microsomal and cytosolic suspensions is however preferable to that of purified enzymes because the translation of in-vitro results to the in-vivo situation requires fewer assumptions when using microsomal data.

3.2.1.3 Formation of ethylene oxide

When measuring the formation of EO in ET exposed microsomes, chromatograms like those shown in Figure 3.9 (for a high and a low ET exposure concentration) were obtained. The signal which is characteristic for EO was always clearly separated from other signals such as the one for AA.

Figure 3.10 shows the concentration-time courses of ET in those incubation experiments with pooled liver microsomes of mice, rats, and humans that were carried out in order to study the formation kinetics of metabolically produced EO. The slopes of the ET concentration-time courses result predominantly from the repeated collection of air samples of 50 µl and 500 µl required for determining ET and EO, respectively. This is evidenced by the concentration-time curves that represent e-functions calculated by considering only the removal of gas samples. The extent of metabolic elimination of ET from the vial atmospheres was too slight to become discernible.

Figures 3.11 - 3.14 present concentration-time courses of EO that are related to the liquid incubation medium. The concentrations were calculated from the corresponding measured atmospheric EO concentrations (see Equation 2.14). Data in Figure 3.11 was obtained when determining the EO formation in the ET incubation studies shown in Figure 3.10 using pooled liver microsomes of mice, rats, or humans. Figure 3.12 shows the EO formation in ET exposed liver microsomes of individual human subjects and Figure 3.13 that in pooled lung microsomes of mice or rats. In ET exposures with heat-inactivated liver microsomes of the three species, no EO formation was detected (data not shown). Figure 3.14 presents the concentration-time courses of EO formed in ET exposed pooled hepatic microsomal suspensions of CYP2E1 knockout mice and of their wild-type counter parts**.**

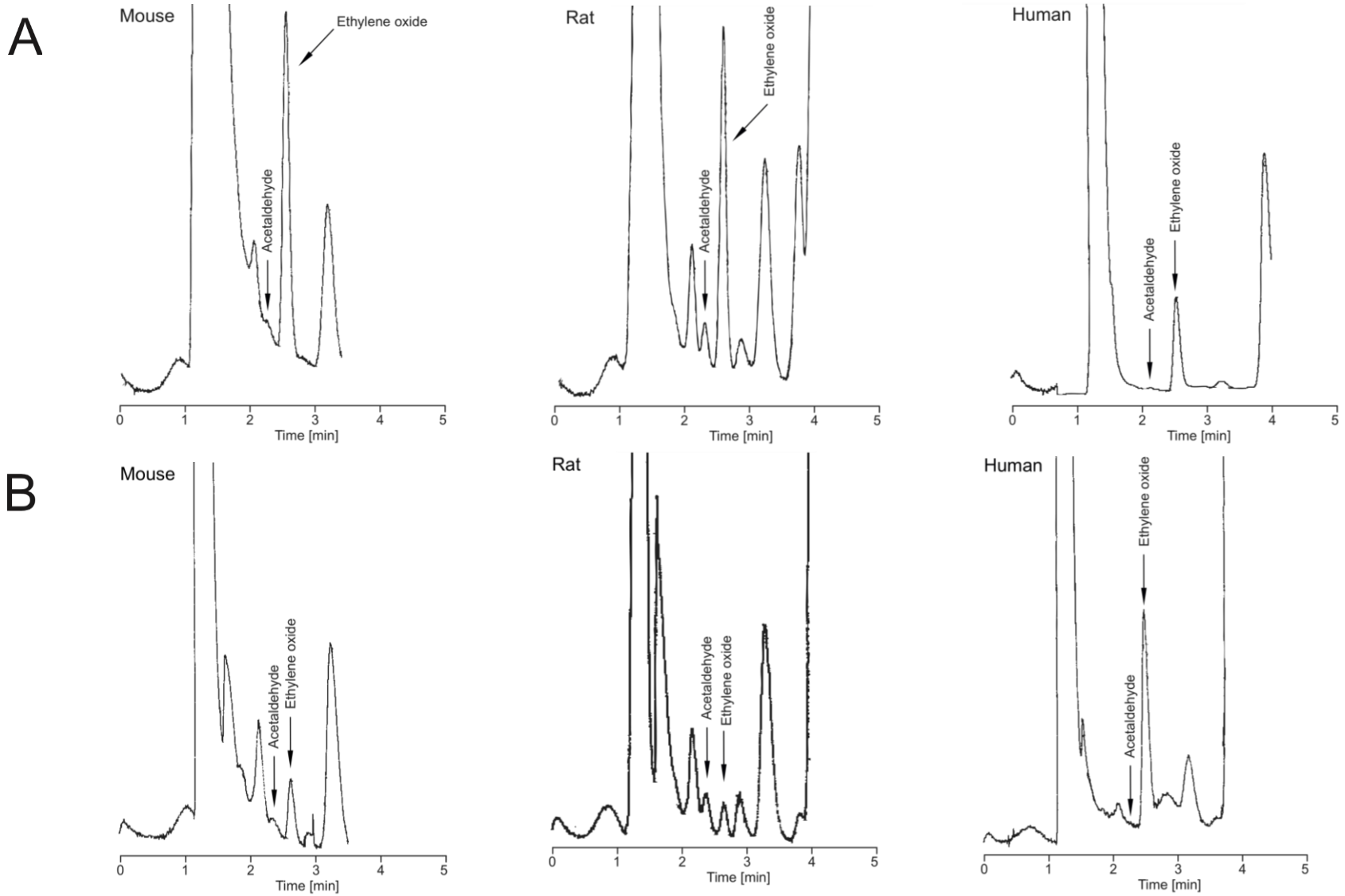

Figure 3.9 GC/FID chromatograms of ethylene oxide detected after 11 min of exposure to ethylene (A, ~3000 ppm; B, ~200 ppm) in the atmosphere of closed vials (38 ml) containing incubation media which consisted of pooled hepatic microsomes from B6C3F1 mice, Fischer 344 rats, and humans. Integrator attenuations are always zero except the chromatogram obtained at the high ethylene concentration in human microsomes (attenuation 3). The GC settings are given in Table 2.6

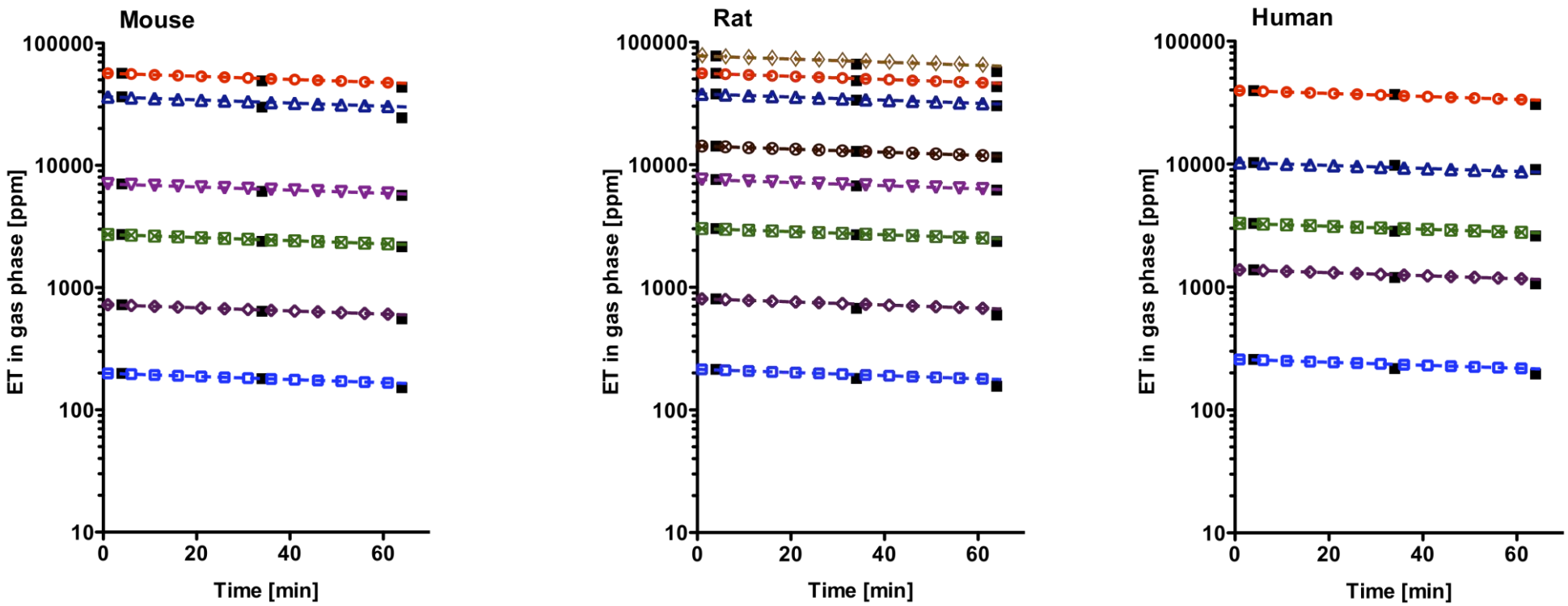

Figure 3.10 Concentration-time courses (■; measured single values) of various ethylene (ET) of several initial concentrations in the atmospheres of closed vials (38 ml) containing incubation media that consist of native pooled hepatic microsomes from 50 B6C3F1 mice (2.5 mg protein/ml, incubation volume 4 ml), 10 Fischer 344 rats (5 mg protein/ml, incubation volume 4 ml), or 25 humans (10 mg protein/ml, incubation volume 2 ml). Each concentration-time course represents 1 experiment carried out in 1 vial.
Open symbols: time points at which gas samples were collected for measuring metabolically formed ethylene oxide (see Figure 3.11). Dashed lines: predicted by taking into account the loss of ET from the vial during the sampling procedure. Initial ET exposure concentrations were:
Mouse: 200 ppm (□), 720 ppm (◇), 2720 ppm (⊠), 7040 ppm (▽), 36300 ppm (△), 56700 ppm (○)
Rat: 210 ppm (□), 810 ppm (◇), 3010 ppm (⊠), 7580 ppm (▽), 14200 ppm (⊗), 37800 ppm (△), 55700 ppm (○), 76900 ppm (◈)
Human: 260 ppm (□), 1380 ppm (◇), 3300 ppm (⊠), 10300 ppm (△), 39700 ppm (○)

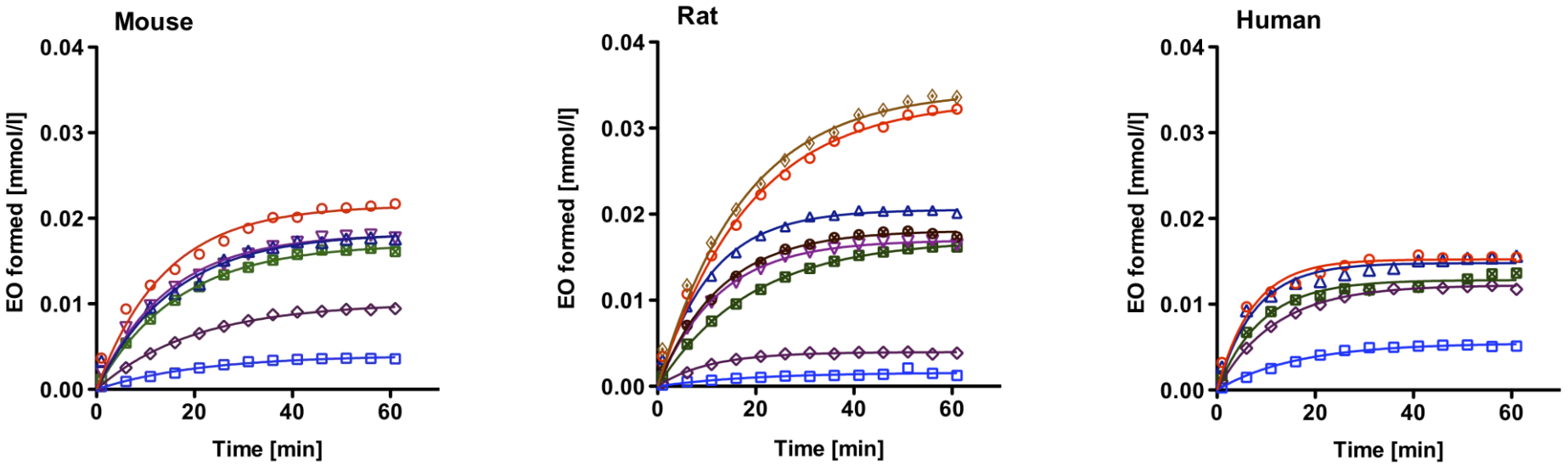

Figure 3.11 Concentration-time courses of metabolically formed ethylene oxide (EO) at various quasi-constant atmospheric concentrations of ethylene (ET) in closed vials (38 ml) containing incubation media that consisted of pooled hepatic microsomes from 50 B6C3F1 mice (2.5 mg protein/ml, incubation volume 4 ml), 10 Fischer 344 rats (5 mg protein/ml, incubation volume 4 ml), or 25 humans (10 mg protein/ml, incubation volume 2 ml). EO is given as EO concentrations in the liquid phase of the incubation vial. Symbols: single values; lines: fits to the data using Equation 2.15. Each concentration-time course represents 1 experiment carried out in 1 vial.
The colors of the open symbols represent the ET uptake experiments (Figure 3.10) in which the EO formation was determined. Initial ET exposure concentrations were:
Mouse: 200 ppm (□), 720 ppm (◇), 2720 ppm (⊠), 7040 ppm (▽), 36300 ppm (△), 56700 ppm (○)
Rat: 210 ppm (□), 810 ppm (◇), 3010 ppm (⊠), 7580 ppm (▽), 14200 ppm (⊗), 37800 ppm (△), 55700 ppm (○), 76900 ppm (◈)
Human: 260 ppm (□), 1380 ppm (◇), 3300 ppm (⊠), 10300 ppm (△), 39700 ppm (○)

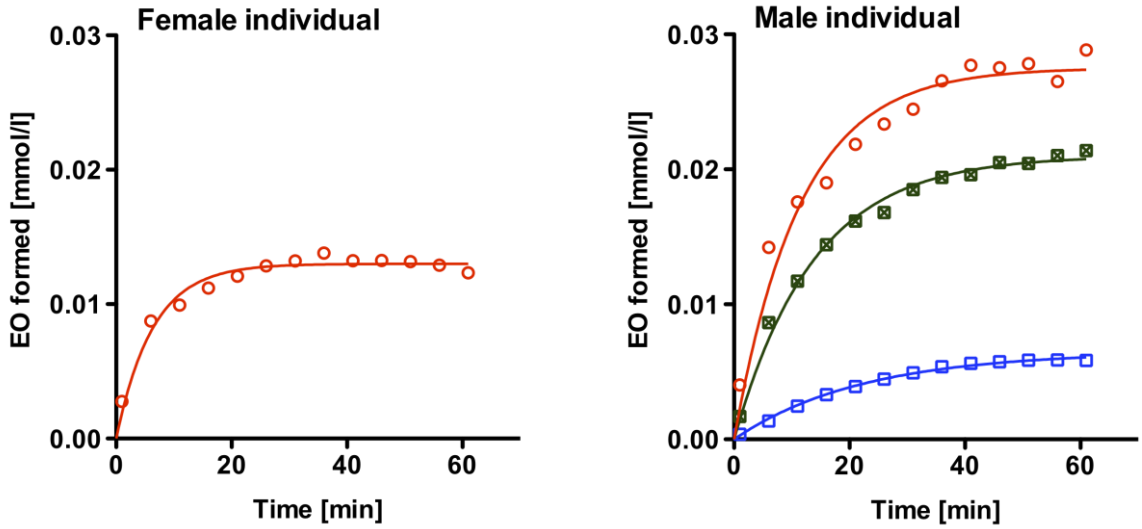

Figure 3.12 Concentration-time courses of metabolically formed ethylene oxide (EO) at various quasi-constant atmospheric concentrations of ethylene (ET) in closed vials (38 ml) containing incubation media (2 ml) that consisted of hepatic microsomes (10 mg protein/ml) of a 75-year old female and a 22-year old male human subject. EO is given as EO concentrations in the liquid phase of the incubation vial. Symbols: single values; lines: fits to the data using Equation 2.15. Each concentration-time course represents 1 experiment carried out in 1 vial.
Initial ET exposure concentrations were:
Female: 66300 ppm (O)
Male: 270 ppm (□), 3110 ppm (⊠), 38600 ppm (O)

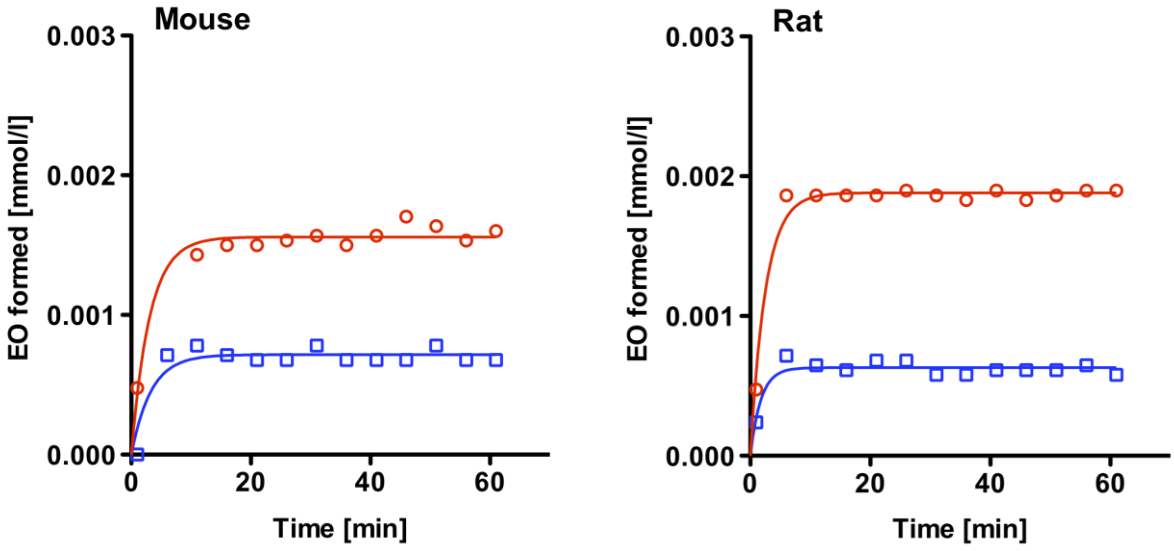

Figure 3.13 Concentration-time courses of metabolically formed ethylene oxide (EO) at quasi-constant atmospheric concentrations of ethylene (ET) in closed vials (38 ml) containing incubation media (2 ml each) that consisted of pooled pulmonary microsomes from 150 B6C3F1 mice (5 mg protein/ml) and 50 Fischer 344 rats (10 mg protein/ml). EO is given as EO concentrations in the liquid phase of the incubation vial. Symbols: single values; lines: fits to the data using Equation 2.15. Each concentration-time course represents 1 experiment carried out in 1 vial.
Initial ET exposure concentrations were:
Mouse: 16500 ppm (□), 75400 ppm (O)
Rat: 18600 ppm (□), 57800 ppm (O)

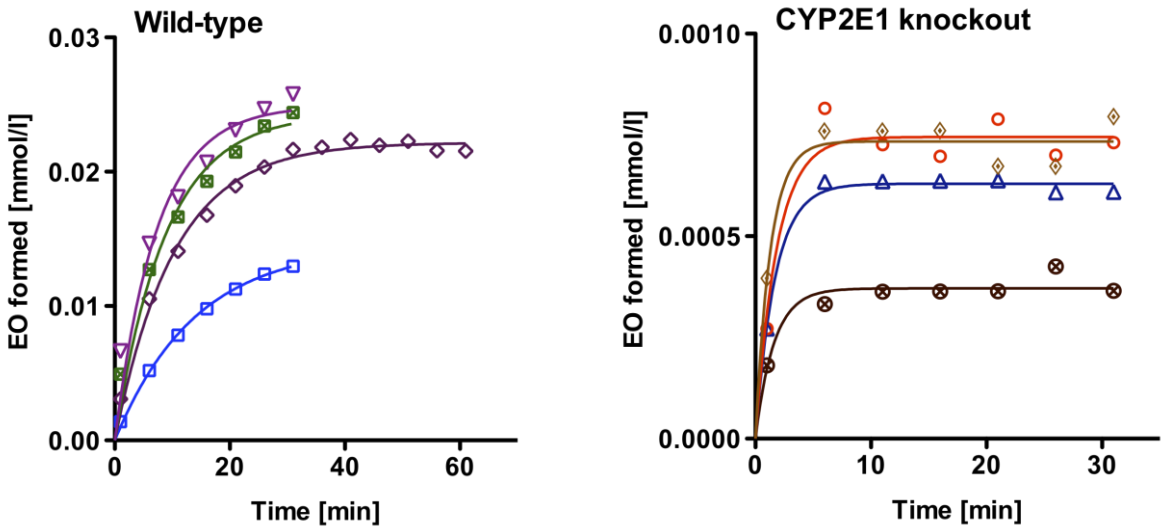

Figure 3.14 Concentration-time courses of metabolically formed ethylene oxide (EO) at various quasi-constant atmospheric concentrations of ethylene (ET) in closed vials (38 ml) containing incubation media that consisted of pooled hepatic microsomes from 50 wild-type mice (2.5 mg protein/ml, incubation volume 4 ml) or 50 CYP2E1 knockout mice (10 mg protein/ml, incubation volume 2 ml). EO is given as EO concentrations in the liquid phase of the incubation vial. Symbols: single values; lines: fits to the data using Equation 2.15. Each concentration-time course represents 1 experiment carried out in 1 vial.
Initial ET exposure concentrations were:
Wild-type: 1200 ppm (□), 3420 ppm (◇), 8910 ppm (⊠), 39800 ppm (▽)
CYP2E1 knockout: 10600 ppm (⊗), 20100 ppm (△), 30800 ppm (○), 38300 ppm (◈)

Figure 3.15 shows EO concentrations determined by GC/MSD in two incubation experiments with rat liver microsomes exposed to 60000 ppm ET. For comparison, the EO concentration-time course obtained by GC/FID analysis in the microsomal incubation study with an ET concentration of 55700 ppm (Figure 3.11, rat) is also presented. Both analytical methods give very similar results. Although the GC/MSD method is more specific for the determination of EO than the GC/FID method, the latter was generally used because it was much faster than the GC/MSD method (5 min versus 20 min) thereby delivering more data for the EO concentration-time courses.

The curves plotted to the concentration-time data in Figures 3.11 - 3.14 were fitted by the function given in Equation 2.15. Based on the fits to the EO concentration-time data, the initial EO formation rates (v_{init}) were calculated and are presented versus the ET exposure concentrations in Figure 3.16. The data obtained in lung microsomes at high ET concentrations of 16500 and 75400 (mice) and of 18600 and 57800 ppm (rats) probably represent the V_{maxEO} values of 0.073 nmol/min/mg protein (mean value, mice) and 0.055 nmol/min/mg protein (mean value, rats). The non-linear curves in Figure 3.16

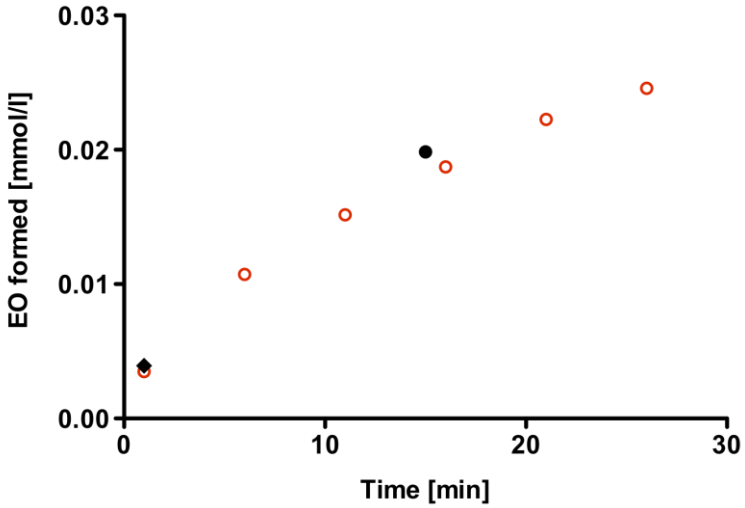

Figure 3.15 Concentrations of metabolically formed ethylene oxide (EO) at quasi-constant atmospheric concentrations of ethylene (ET) in 2 closed vials (38 ml) containing incubation media that consisted of pooled hepatic microsomes from 10 Fischer 344 rats (5 mg protein/ml, incubation volume 4 ml). EO is given as EO concentrations in the liquid phase of the incubation vial. Symbols: single values measured at an ET exposure concentration of 55700 ppm by GC/FID (○) or in two experiments at an ET exposure concentration of 60000 ppm by GC/MSD (◆, ●).

are fits to the data gained from liver microsomes prepared from wild-type mice, CYP2E1 knockout mice, B6C3F1 mice, rats, and humans considering saturation kinetics according to Michaelis and Menten. They were constructed by means of the program Prism 5 for Macintosh. The derived V_{maxEO} and their apparent Michaelis-constants (K_{map}) are given in Table 3.3. The highest V_{maxEO} value was found in wild-type and the lowest one in CYP2E1 knockout mice. In pooled microsomes, ratios of V_{maxEO} values mouse/human and rat/human were 2.6 and 1.8. Almost identical ratios can be read out from the Figure 2 of the publication of Court et al. (1997) in which the CYP2E1 activities were investigated in liver microsomes of several species using chlorzoxazone as substrate. CYP2E1 is the predominant ET metabolizing CYP species in the liver as can be concluded from the findings that V_{maxEO} was about 15 times higher in liver microsomes of wild-type mice than that in the CYP2E1 knockout mice. Even higher (340) was the ratio of V_{maxEO}/K_{map} in wild-type mice to V_{maxEO}/K_{map} in CYP2E1 knockout mice. In rats, it had been shown earlier that ET is metabolized by CYP2E1 (Fennell et al., 2004). Considering that the ratios of the maximum EO formation rates (present work) and of the CYP2E1 mediated chlorzoxazone hydroxylation (Court et al., 1997) in liver microsomes were identical between mice, rats, and humans, one has to

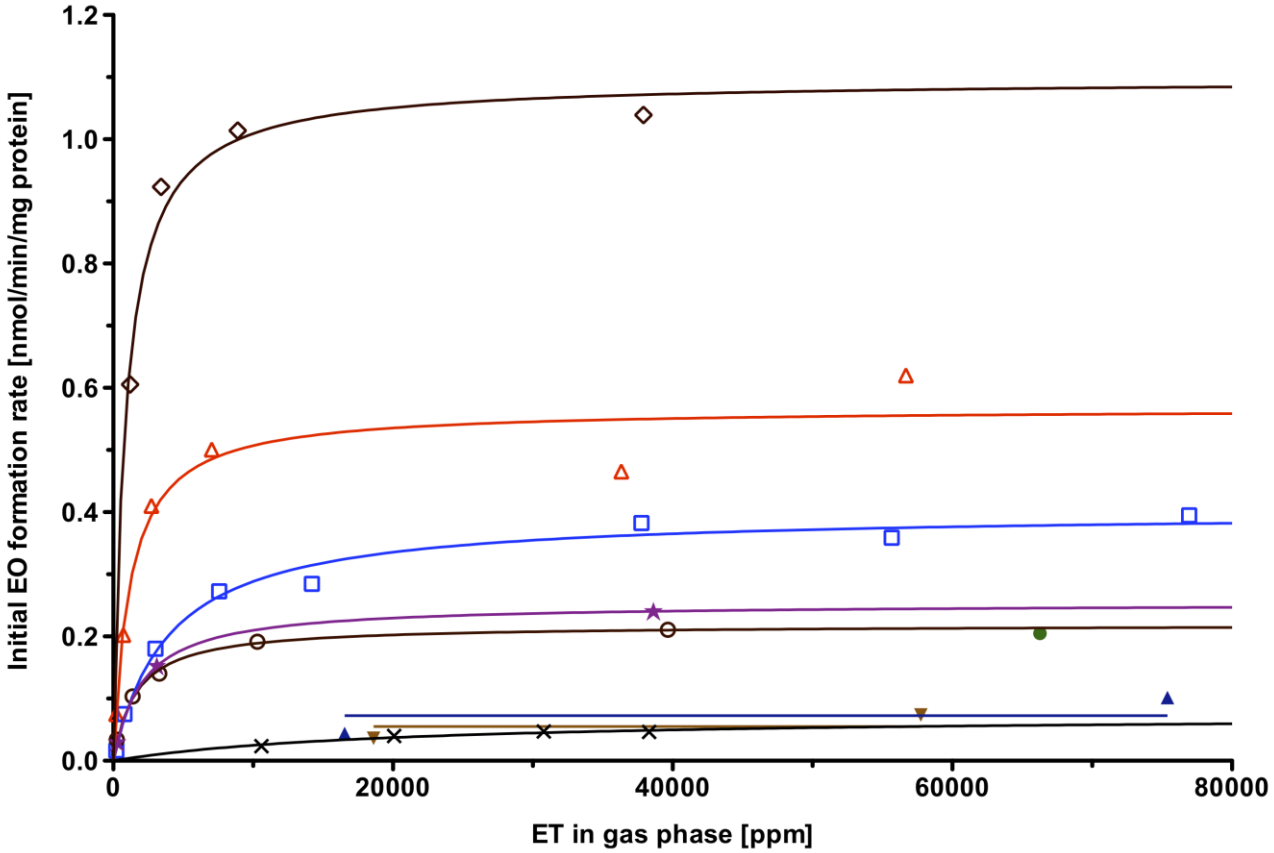

Figure 3.16 Initial formation rates of ethylene oxide (EO) in microsomal incubations at various atmospheric concentrations of ethylene (ET) as calculated from the EO concentration-time curves shown in Figures 3.11-3.14. Pooled liver microsomes from wild-type mice (CYP2E1 +/+; ◇), CYP2E1 knockout mice (×), B6C3F1 mice (△), Fischer 344 rats (□), or humans (○); liver microsomes from a 75-year old human female (●) and a 22-year old male (★) human subject; pooled lung microsomes from B6C3F1 mice (▲) and Fischer 344 rats (▼). Symbols: calculated from measured data (single values); lines: mean (lung data) or fits to the data according to Michaelis-Menten kinetics (liver data).

conclude that CYP2E1 is quantitatively the most relevant ET metabolizing CYP-species in humans, too.

The K_{map} value in humans is lower than that in rats and higher than that in mice. The almost same K_{map} value in B6C3F1 and wild-type mice demonstrates that CYP2E1 is the predominant ET metabolizing CYP in both strains. Accordingly, the amount of CYP2E1 in liver microsomes of the wild-type mouse is assumed to be 1.9-fold higher than in those of the B6C3F1 mouse as can be derived from the ratio of the corresponding V_{maxEO} values. The remaining CYP affinity in microsomes of CYP2E1 knockout mice is 22 times less than that of wild-type mice, as evidenced by the ratio of the K_{map} values in CYP2E1 knockout to wild-type mice. When comparing the ratios V_{maxEO}/K_{map}, human and rat liver microsomes show almost the same values which are about 4 times lower than those in B6C3F1 mice and roughly 10 times lower than those in wild-type mice.

Table 3.3 Maximum ethylene oxide formation rates (V_{maxEO}) and apparent Michaelis constants (K_{map}) in ethylene (ET) exposed hepatic microsomes from mice, rats, and humans (mean ± SE, obtained from curve fitting)

Species (strain)	V_{maxEO} [nmol/min/mg protein]	K_{map} [mmol/l ET]	V_{maxEO}/K_{map} [µl/min/mg protein]	n[a)]
Mouse[b)] (Wild-type)*	1.096 ± 0.042	0.007 ± 0.001	162 ± 34.7	5
Mouse[b)] (CYP2E1 knockout)[#]	0.074 ± 0.014	0.156 ± 0.066	0.48 ± 0.22	5
Mouse[b)] (B6C3F1)	0.567 ± 0.038	0.009 ± 0.003	60.9 ± 21.0	7
Rat[b)] (Fischer 344)	0.401 ± 0.013	0.031 ± 0.005	13.1 ± 2.01	9
Human[b)]	0.219 ± 0.005	0.013 ± 0.001	17.2 ± 1.50	6
Human[c)]	0.253 ± 0.0002	0.016 ± 0.0001	15.6 ± 0.12	4

[a)]: available numbers (ethylene oxide production rates) that were used to fit a Michaelis-Menton function; [b)]: pooled from the livers of 50 male mice, 10 male rats, or 25 humans of both genders; [c)]: from one male individual; *: 129S1/SvImJ; [#]: 129/Sv-Cyp2e1^{tm1Gonz}/J.

Table 3.4 shows the rate constants of the EO formation k_3, of the suicide inhibition k_4, and the ratios k_3/k_4. The values of k_3 were calculated by dividing V_{maxEO} (Table 3.3) by the CYP2E1 content (see 3.2.1.2).

The suicide inactivation rate constant k_4 of the ET metabolizing CYP species was obtained from the curve fits to the EO formation data shown in Figures 3.11, 3.13 and 3.14 (for explanation, see 3.2.1.2). The values of k_4, reflecting a reaction occurring within the porphyrin ring, are rather similar in the CYP2E1 containing liver microsomes. Those of k_3 are highest in rat and lowest in human livers. These findings might be caused by species differences in amino acid residues in the active site of CYP2E1 (Lewis et al., 1997). The values of the presently determined partition ratios k_3/k_4 are in agreement with the common observed values of less than 300 in unconjugated terminal olefins (Correia and Ortiz de Montellano, 2005).

The values of k_4 in lung microsomes of mice and rats are 5 and 8 times higher than those in liver microsomes of both species. These high k_4 values are unlikely to result from a bias in the interpretation of the EO concentration-times curves because these microsomes were stable and metabolically active during the exposure time as was tested using the model substance ST (see 3.1.3). These k_4 values are similar to that in liver microsomes of CYP2E1 knockout mice. It seems probable that not CYP2E1 but another CYP species metabolizes ET in mouse and rat lung.

Table 3.4 Ethylene-specific catalytic rate constants k_3, suicide inactivation rate constants k_4, and partition ratios k_3/k_4 in liver or lung microsomes from mice, rats, and humans (mean ± SE, n: number of determinations)

Species (strain)	Organ	k_3 [min^{-1}]	k_4 [min^{-1}]	k_3/k_4	n
Mouse (Wild-type) *	Liver [a)]	5.9 ± 0.5 [c)]	0.104 ± 0.013	60 ± 8	4
Mouse (CYP2E1 knockout) [#]	Liver [a)]	n.a.	0.633 ± 0.051	n.a.	4
Mouse (B6C3F1)	Liver [a)]	5.9 ± 0.6	0.060 ± 0.005	100 ± 9	6
	Lung [b)]	n.a.	0.306; 0.326	n.a.	2
Rat (Fischer 344)	Liver [a)]	11.2 ± 1.5	0.070 ± 0.006	169 ± 15	8
	Lung [b)]	n.a.	0.573; 0.392	n.a.	2
Human	Liver [a)]	3.2 ± 0.2	0.098 ± 0.013	39 ± 6	5

*: 129S1/SvImJ; [#]: 129/Sv-Cyp2e1^{tm1Gonz}/J; [a)]: pooled from the livers of 50 male mice, 10 male rats, or 25 humans of both genders; [b)]: pooled from lungs of 150 male mice or 50 male rats; [c)]: calculated assuming the CYP2E1 content to be 1.9 times the CYP2E1 content in B6C3F1 mice (based on the values of V_{maxEO}, see Table 3.3); n.a.: not available.

3.2.1.4 Acetaldehyde, a possible ethylene metabolite?

Olefins can be metabolized by CYP not only to epoxides but also to aldehydes (Mansuy et al., 1984). In all ET experiments conducted to study the formation of EO, a small peak was detected in the chromatograms of the samples collected from the atmosphere of the microsomal incubations containing vials, which showed the same retention time as acetaldehyde (Figure 3.9). It appeared immediately after adding the NADPH regenerating system to a microsomal incubation (with or without ET). The heights of the peaks were not dependent on the ET exposure concentration as exemplarily shown in ET exposed rat liver microsomal incubations (Figure 3.17). They also remained almost constant over the exposure period in contrast to the increasing EO peak. Possibly, the commercial isocitrate dehydrogenase used in the NADPH regenerating system was somewhat contaminated, maybe by acetaldehyde. The large variations in the peak heights are due to the low signal response and the incomplete separation of the Acetaldehyde- and ET-characteristic peaks, particularly at high ET concentrations (see Figure 3.9). In any case, there was no hint for acetaldehyde as a possible oxidation product of ET.

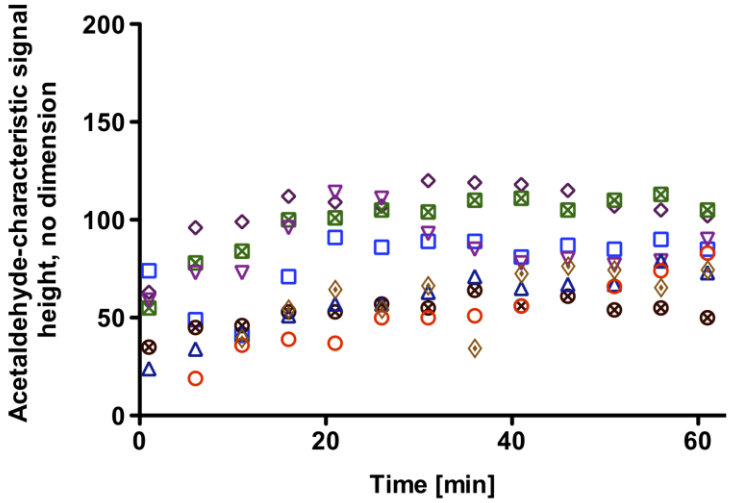

Figure 3.17 Time courses of a signal characteristic for acetaldehyde, which appeared in the GC/FID chromatograms obtained for ethylene oxide in incubations with ethylene (ET) exposed rat liver microsomes. Each concentration-time course represents 1 experiment carried out in 1 vial.
Exposure conditions: closed vials (38 ml) containing incubation media (4 ml) consisting of pooled hepatic microsomes from 10 Fischer 344 rats (5 mg protein/ml); ET exposure concentrations: 210 ppm (□), 810 ppm (◇), 3010 ppm (⊠), 7580 ppm (▽), 14200 ppm (⊗), 37800 ppm (△), 55700 ppm (○), 76900 ppm (◈)

3.2.2 Gas uptake studies with ethylene oxide in subcellular fractions

3.2.2.1 Ethylene oxide in microsomal incubations

Figures 3.18 and 3.19 show the results of EO uptake experiments in native and heat-inactivated pooled hepatic microsomes of mice, rats, and humans, in hepatic microsomes of two human individuals (one adult of each gender), and in pooled lung microsomes of mice and rats. The slopes of the curves demonstrating the EO elimination from the gas phase of the vials containing native hepatic or pulmonary rodent microsomes were not distinguishable from those with heat-inactivated microsomes that represent the spontaneous hydrolysis of EO. This means that no EH catalyzed EO elimination was found in liver and lung microsomes of both rodent species. In pooled native human liver microsomes however, the EO elimination was faster at low EO concentrations than in the heat-inactivated ones. The concentration dependent flattening of the slopes hints to saturation kinetics of the EO elimination (Figure 3.18). From the best fits to these data by means of the software Berkeley Madonna, a V_{maxEH} value of 14.35 nmol/min/mg protein was derived for the EH activity to EO. The K_{mapEH} value in the microsomal environment was 12.74 mmol/l (corresponding to 4735 ppm in gas phase), and the ratio of V_{maxEH} to K_{mapEH} was 1.13 µl/min/mg protein. When calculating the EO formation rates in microsomal incubations with ET (Table 3.3), the microsomal elimination of EO and the EO loss by spontaneous hydrolysis was not considered for. However, the hereof-resulting error in the maximum production rates given for rodents is negligible and does not exceed 10% of the maximum EO formation rate given for humans.

The slopes of the EO concentration-time curves in liver microsomes prepared from the two adults (female: 0.0036 min^{-1} and male: 0.0032 min^{-1}, Figure. 3.18, human individual) were almost identical with the one obtained in pooled human microsomes at 100 ppm (0.0034 min^{-1}, see Figure 3.18, human pooled).

In order to investigate whether EO was metabolized by cytochrome P450 dependent monooxygenases, one incubation medium (1 ml) consisting of rat liver microsomes (5 mg protein/ml) and a NADPH-regenerating system was exposed to EO (100 ppm) in a closed vial (38 ml). No CYP-mediated EO elimination could be detected because the slope of the obtained concentration-time curve (data not shown) did not differ from that found in heat-inactivated microsomes.

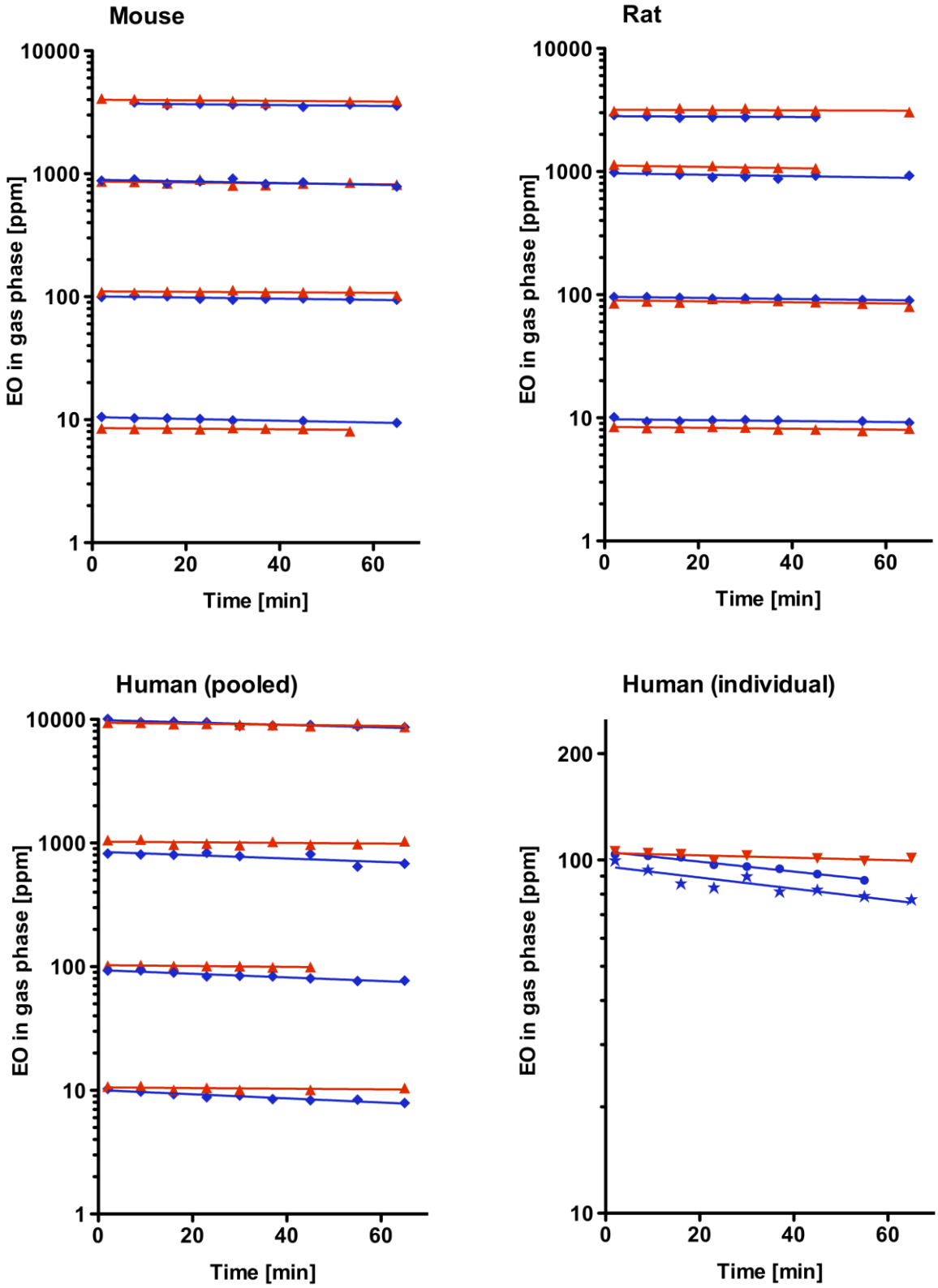

Figure 3.18 Concentration-time courses of ethylene oxide (EO) of various initial concentrations in the atmosphere of closed vials (38 ml) containing incubation media (1 ml) that consisted of pooled hepatic microsomes (5 mg protein/ml) from 50 B6C3F1 mice, 10 Fischer 344 rats, or 25 humans, and hepatic microsomes from two human individuals.
Symbols: red colored, heat-inactivated microsomes; blue colored, native microsomes; (▼, ●), 22-year old male human subject; (★), 75-year old female human subject; lines: fits to the data using Equation 2.10. Each concentration-time course represents 1 experiment carried out in 1 vial.

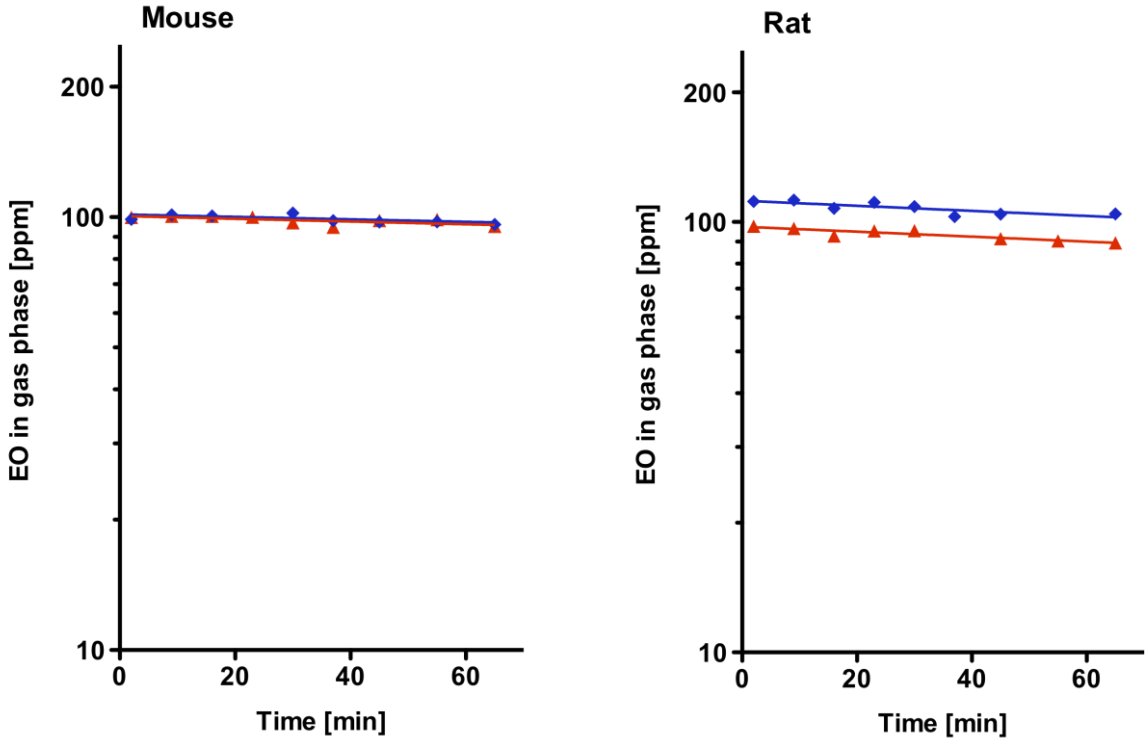

Figure 3.19 Concentration-time courses of ethylene oxide (EO) in the atmosphere of closed vials (38 ml) containing incubation media (1 ml) that consisted of pooled pulmonary heat-inactivated (▲) or native (◆) microsomes (5 mg protein/ml) from 150 B6C3F1 mice or 50 Fischer 344 rats. Symbols: single values; lines: fits to the data using Equation 2.10. Each concentration-time course represents 1 experiment carried out in 1 vial.

3.2.2.2 Ethylene oxide in cytosolic incubations

Figures 3.20 and 3.21 depict time courses of atmospheric EO concentrations in incubations of GSH- or DEM-containing native or heat-inactivated pooled hepatic cytosol from mice, rats, and humans or GSH- or DEM-containing native or heat-inactivated pooled pulmonary cytosol from mice and rats.

The slopes of the EO-concentration time courses in the GSH containing incubations with native cytosol are clearly different from those with GSH depleted heat-inactivated cytosol. With the same amount of cytosolic protein in all probes, the conjugation rates are highest in mouse and lowest in human liver cytosol. In the semi-logarithmic plots, the elimination curves are parallel over the whole exposure ranges up to about 3000 ppm (9 mmol/l) in liver cytosol and about 4000 ppm in lung cytosol, respectively, and do not show any hint to saturation kinetics. In spite of this, the conjugation reaction was catalyzed by GST, as has to be concluded from the evidently flatter slopes of the curves obtained in heat-inactivated, GSH containing cytosolic EO incubations. They

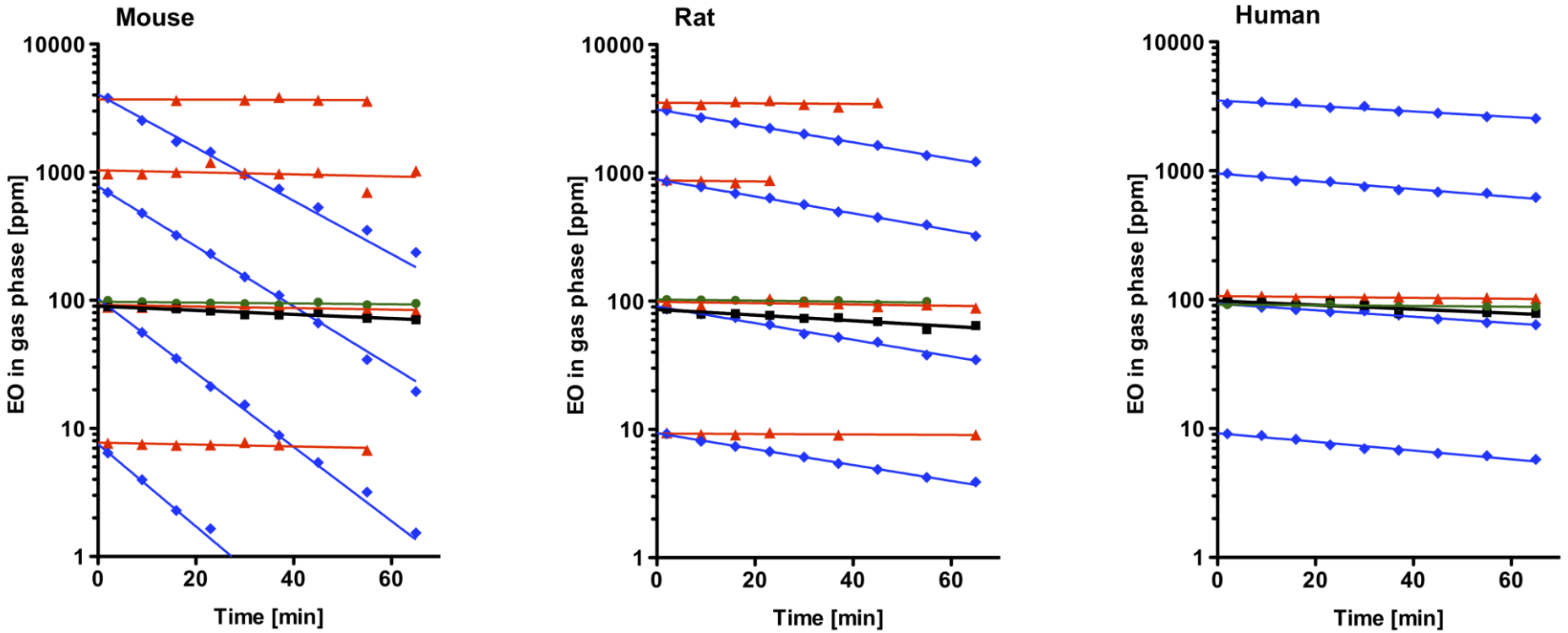

Figure 3.20 Concentration-time courses of ethylene oxide (EO) of various initial concentrations in the atmosphere of closed vials (~38 ml) containing incubations media (1 ml) that consisted of GSH- or DEM-containing pooled hepatic cytosol (3 mg protein/ml) from 50 B6C3F1 mice, 10 Fischer 344 rats, or 11 humans.
Symbols: single values; heat-inactivated cytosol in presence of DEM (3 mmol/l; ▲), native cytosol in presence of DEM (3 mmol/l; ●), heat-inactivated cytosol in presence of GSH (15 mmol/l; ■), native cytosol in presence of GSH (15 mmol/l; ◆); lines: fits to the data using Equation 2.10. Each concentration-time course represents 1 experiment carried out in 1 vial.

represent the sum of both the spontaneous EO hydrolysis and the nonenzymatic conjugation of EO with GSH. The elimination rate constant resulting solely from the nonenzymatic conjugation reaction of EO with GSH is calculated to be $k_{ceGSH} = 3.12 \cdot 10^{-3} \pm 3.0 \cdot 10^{-4}$ min^{-1} (mean ± SE, n=8; three data sets obtained with heat-inactivated liver cytosol from human individuals included, data not shown) corresponding to a mean half-life of 3.7 h at a GSH concentration of 15 mmol/l.

The slopes of the curves obtained with heat-inactivated, DEM containing or with native, DEM containing liver or lung cytosol did not differ significantly within and between each species. They were also not different from those obtained in Figures 3.18 and 3.19 with heat-inactivated microsomal EO incubations ($p<0.05$; one-way ANOVA) representing the spontaneous hydrolysis. When calculating the parameters of enzyme-catalyzed reactions, nonenzymatic GSH conjugation and spontaneous hydrolysis were accounted for. The rate constant of the spontaneous EO hydrolysis was $k_{eHyd} = 9.3 \cdot 10^{-4} \pm 7 \cdot 10^{-5}$ min^{-1} (mean ± SE, n=36). No catalytic activity at all could be allocated to the cytosolic EH.

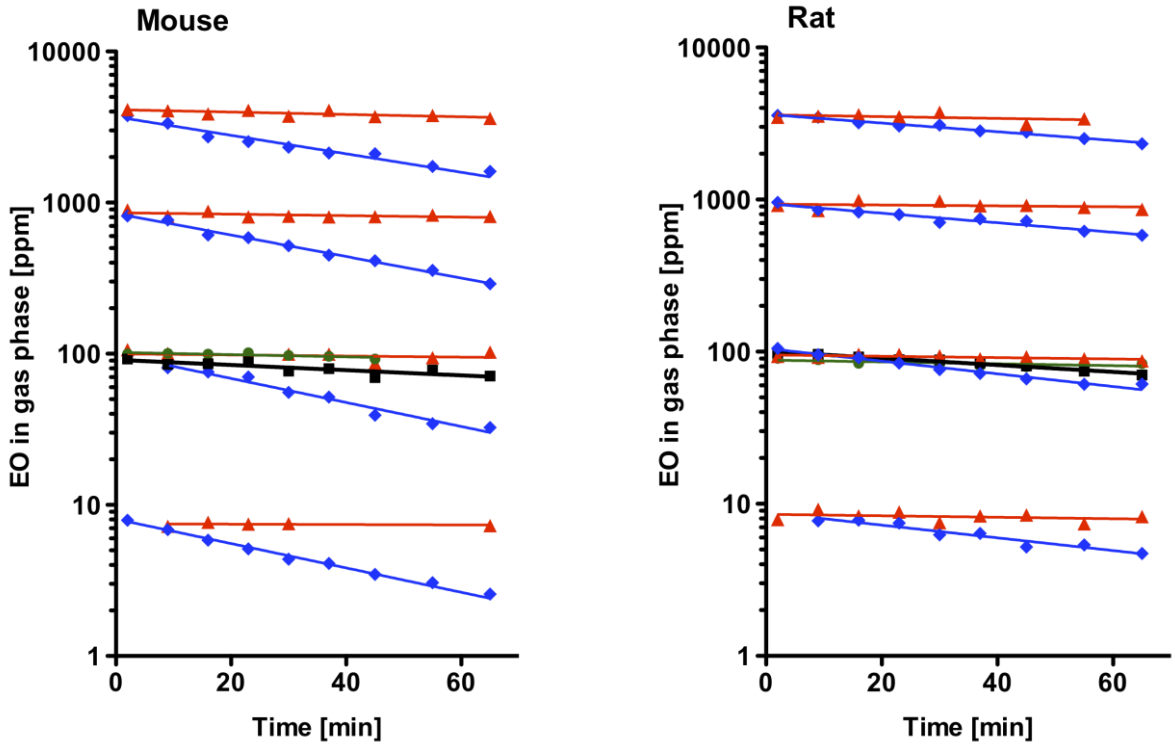

Figure 3.21 Concentration-time courses of ethylene oxide (EO) of various initial concentrations in the atmosphere of closed vials (~38 ml) containing incubations media (1 ml) that consisted of GSH- or DEM-containing pooled pulmonary cytosol (3 mg protein/ml) from 150 B6C3F1 mice or 50 Fischer 344 rats. Symbols: single values; heat-inactivated cytosol in presence of DEM (3 mmol/l; ▲), native cytosol in presence of DEM (3 mmol/l; ●), heat-inactivated cytosol in presence of GSH (15 mmol/l; ■), native cytosol in presence of GSH (15 mmol/l; ◆); lines: fits to the data using Equation 2.10. Each concentration-time course represents 1 experiment carried out in 1 vial.

Considering the polymorphism of the EO eliminating human GST-theta (GSTT1; Föst et al., 1991, 1995) and its influence on the genotoxicity of EO (Hallier et al., 1993), the GST-mediated conjugation of EO with GSH was additionally investigated in liver cytosol of 6 male and 7 female individuals of between 16 and 78 years of age. The results are summarized in Table 3.5 together with those obtained in pooled liver cytosol of mice, rats, and humans and in pooled lung cytosol of mice and rats. Only the ratio V_{maxGST}/K_{mapGST} is shown because the GST catalyzed EO elimination followed in all experiments first-order kinetics over the whole concentration range of EO. The ratio was calculated according to Equation 2.19. Organ specific GST catalyzed EO elimination was highest in mouse and lowest in human cytosol. In human liver cytosol, pooled activity was reasonably in the middle between the lowest individual GST activity (zero) and the highest one (2.87 µl/min/mg protein). The time span between death and autopsy did presumably not influence the GST activity because out of the 13 hepatic cytosol samples obtained from non-Asian individuals, highest GST activities were found in the samples of a 22-year and a 42-year old man, who died 6.5 h and 29 h, respectively, prior to autopsy. Two samples (15%) did not show any GST activity to EO. The percentage agrees with that of the GSTT1*0 carriers reported for non-Asians (between 10 and 25%; Bolt and Thier, 2006).

The observed first-order decays in the EO concentrations signify that the rate of the GST-mediated EO elimination was directly proportional to the EO exposure concentration the highest of which was 4000 ppm in the atmosphere (Figure 3.20). This corresponds to an EO concentration of 12 mmol/l in the cytosolic suspension. Considering the GST catalyzed conjugation of GSH with EO to follow saturation kinetics according to a sequentially ordered ping-pong mechanism (Johanson and Filser, 1993; Csanády and Filser, 2007), the K_{mapGST} concentration of EO in livers or lungs of mice and rats and in livers of humans can be concluded to be ≥ 12 mmol/l. The GST catalyzed EO elimination rate is almost independent of the GSH concentration for concentrations >1 mmol/l because the K_{map} of GSH is only about 0.1 mmol/l (Johanson and Filser, 1993; Csanády and Filser, 2007). Taking into account a K_{mapGST} value of 12 mmol/l tissue for the GST substrate EO, V_{max} values of 335, 63.6, and 13.7 nmol/min/mg protein are obtained for the GST-mediated GSH conjugation with EO in mouse, rat, and human pooled liver cytosol, respectively. Corresponding values for mouse and rat lung cytosol are 75.9 and 21.3 nmol/min/mg protein.

Table 3.5 Clearance (V_{maxGST}/K_{mapGST}; related to the cytosolic environment) of glutathione S-transferase-mediated elimination of ethylene oxide from mouse and rat hepatic and pulmonary cytosol and from human hepatic cytosol

Tissue	Species	Gender	Age [year]	V_{maxGST}/K_{mapGST} [a)] [µl/min/mg protein]	Time prior to autopsy [h]
Liver	Mouse [b)]	Male	0.25	27.90 ± 2.87	0
Liver	Rat [b)]	Male	0.25	5.30 ± 0.10	0
Liver	Human [c)]	Both	1.9 - 70	1.14 ± 0.32	n.a.
Liver	Human	Female	51	0.00 ± 0.00	n.a.
Liver	Human	Female	54	0.00 ± 0.00	25
Liver	Human	Male	36	0.50 ± 0.25	23
Liver	Human	Male	63	0.54 ± 0.29	n.a.
Liver	Human	Male	16	0.75 ± 0.26	24
Liver	Human	Female	75	0.81 ± 0.34	0 [e)]
Liver	Human	Female	78	1.21 ± 0.16	n.a.
Liver	Human	Female	42	1.36 ± 0.18	n.a.
Liver	Human	Male	58	1.49 ± 0.32	17
Liver	Human	Female	53	1.62 ± 0.32	n.a.
Liver	Human	Female	48	1.76 ± 0.46	n.a.
Liver	Human	Male	42	1.82 ± 0.51	29
Liver	Human	Male	22	2.87 ± 0.57	6.5
Lung	Mouse [d)]	Male	0.25	6.32 ± 0.52	0
Lung	Rat [d)]	Male	0.25	1.78 ± 0.33	0

[a)]: mean ± SE, n = 4; [b)]: pooled from livers of 50 mice or 10 rats; [c)]: pooled from livers of 5 male and 6 female humans; [d)]: pooled from lungs of 150 mice or 50 rats; [e)]: liver sample collected during transplantation; n.a.: not available

3.2.3 Gas uptake studies with ethylene oxide in tissue homogenates

EO elimination was investigated in the atmosphere of closed vials that contained incubation media consisting of native homogenates (25% w/v, 1 ml) of livers from mice and rats or of kidneys, brains, lungs and blood from rats in absence or presence of GSH or DEM. In the vigorously shaken vials concentration-time courses of atmospheric

EO were monitored (see 2.2.4.5). The obtained data were fitted by an exponential function. Typical results are shown in Figure 3.22 for livers and in Figure 3.23 for the other tissues investigated.

In none of the DEM containing incubations, the loss of the EO concentration was higher than that resulting from spontaneous hydrolysis. This finding is in agreement with the results obtained with subcellular fractions in which no EH-mediated EO elimination was found (see 3.2.2).

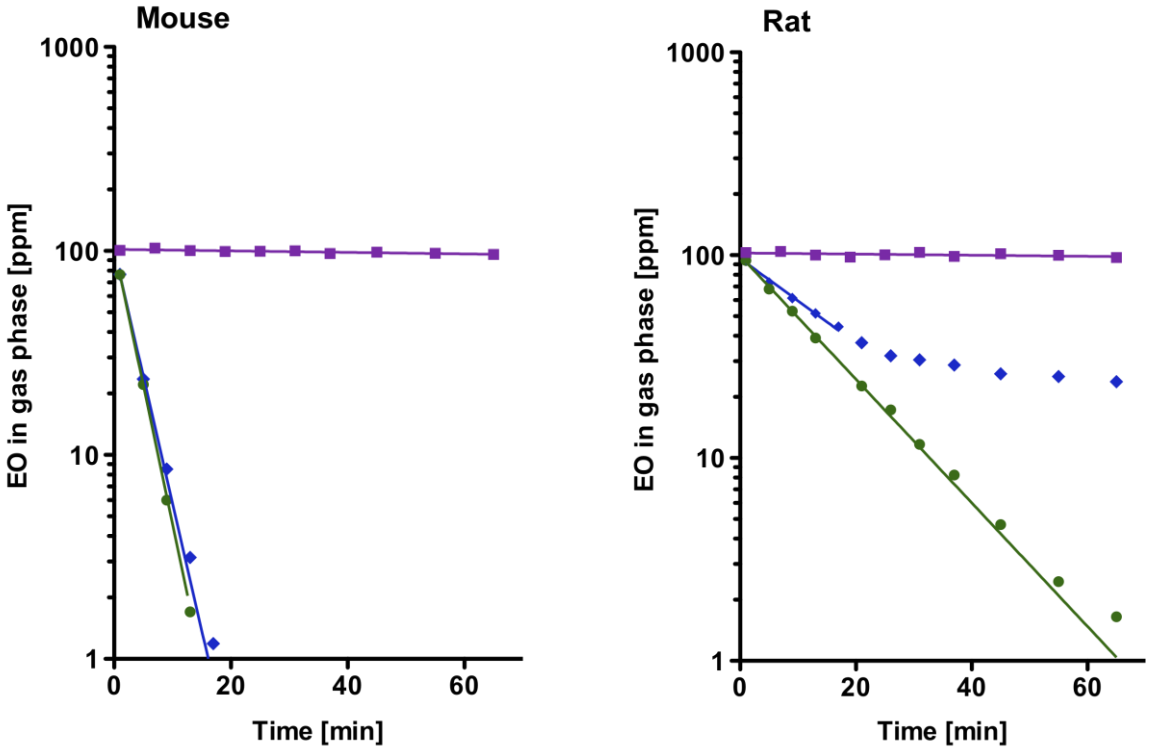

Figure 3.22 Concentration-time courses of ethylene oxide (EO) of several initial concentrations in the atmosphere of closed vials (~38 ml) containing liver homogenates (25% w/v, 1 ml) from 3 B6C3F1 mice or 3 Fischer 344 rats (pooled homogenate).
Symbols: single values; native homogenate in presence of DEM (3 mmol/l; ■), native homogenate (◆), native homogenate in presence of GSH (15 mmol/l; ●); lines: fits to the data using Equation 2.10. Each concentration-time course represents 1 experiment carried out in 1 vial.

In native homogenates with no addition of GSH or DEM, the EO elimination was faster than in the DEM containing ones. This hints to the presence of residual GSH when starting the exposures. In the rat liver, the slope of the EO concentration-time course flattened after about 20 min. In native mouse liver homogenate, the fast EO elimination could be monitored for only 17 min because the EO concentrations approached the detection limit. The shapes of the concentration-time courses of EO obtained in native

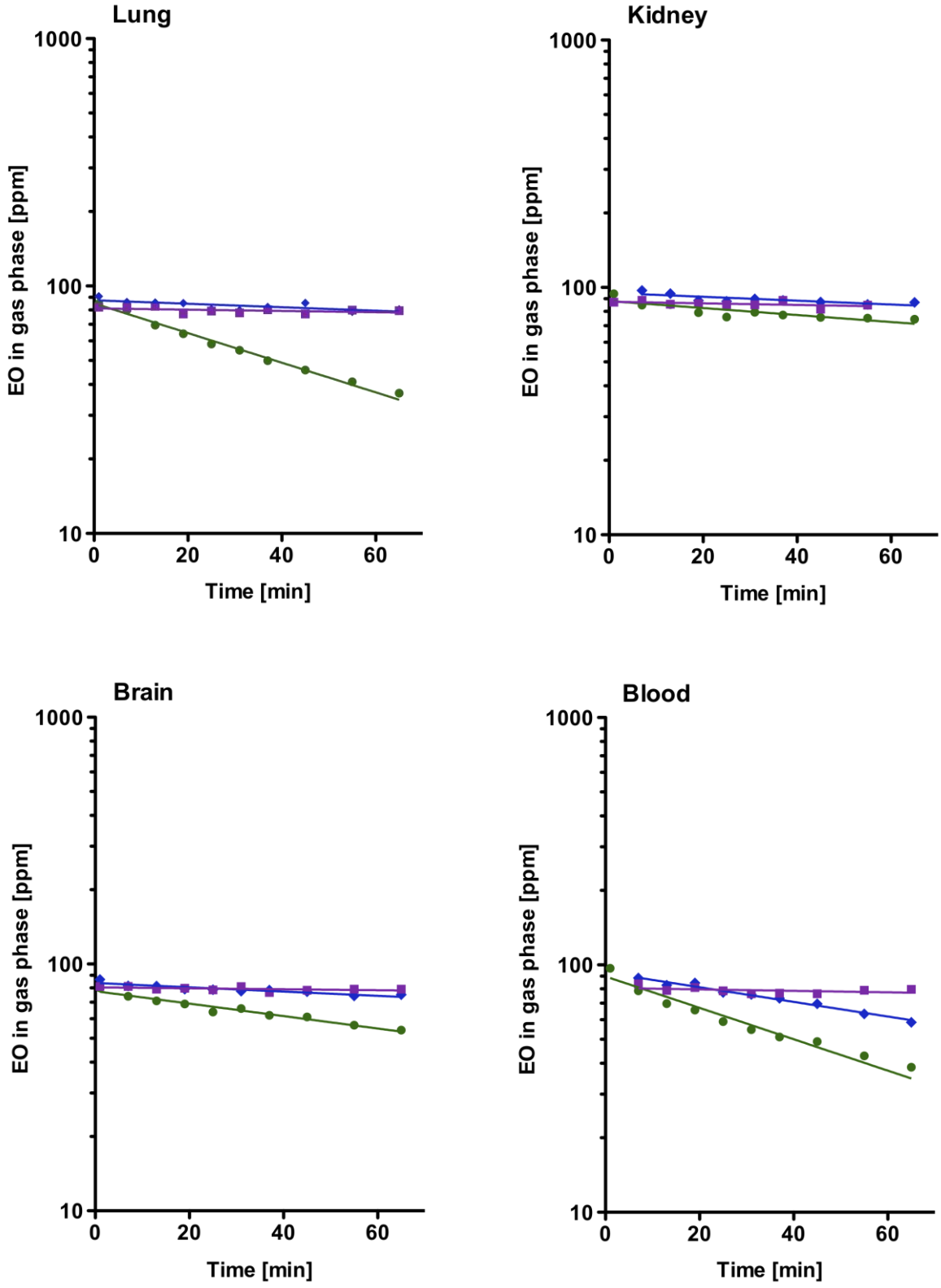

Figure 3.23 Concentration-time courses of ethylene oxide (EO) of several initial concentrations in the atmosphere of closed vials (~38 ml) containing pooled blood tissue homogenates (25% w/v, 1 ml) from 3 Fischer 344 rats.
Symbols: single values; native homogenate or blood in presence of DEM (3 mmol/l; ■), native homogenate or blood (◆), native homogenate or blood in presence of GSH (15 mmol/l; ●); lines: fits to the data using Equation 10. Each concentration-time course represents 1 experiment carried out in 1 vial.

liver homogenates may originate from the loss of the initial GSH concentration (2.0 mmol/l and 1.8 mmol/l in rat and mouse, respectively) resulting from the GST-mediated GSH conjugation with EO. Also in native rat blood, the slope of the EO concentration-time curve differs clearly from the one obtained in DEM pretreated blood. Here, no deviation from linearity is recognizable. Possibly, the GST-mediated EO elimination is too slow to deplete the residual GSH pool. The very flat slopes (rate constants 0.0015 to 0.0022 min^{-1}) of the concentration–time curves of EO obtained in the homogenates of rat lung, kidney, and brain differ barely from the slopes of the curves obtained with DEM pretreated tissue homogenates.

Table 3.6 Parameters used to calculate the organ-specific ethylene oxide (EO) clearance from the slopes (k_{ce})* of the EO concentration-time curves obtained in rat and mouse liver homogenates (Figure 3.22) and rat tissue homogenates and blood (Figure 3.23) with additional GSH (15 mmol/l)

Species	Organ	k_{ce} [min^{-1}]	n	Cytosolic protein [mg/g organ]
Mouse	Liver [a)]	0.31	1	95 [b)]
Rat	Liver [a)]	0.073 ± 0.002	3	95 [b)]
	Lung [a)]	0.011 ± 0.0018	3	28.6 [c)]
	Kidney [a)]	0.0029 ± 0.0003	3	n.a.
	Brain [a)]	0.0059 ± 0.0001	3	41.2 [d)]
	Blood	0.015 ± 0.0003	3	77.8 [e)]

[a)]: Homogenates were prepared in phosphate buffer (4-fold dilution); [b)]: from Kreuzer et al. (1991); [c)]: from Faller (1998); [d)]: from Ayers et al. (1996); [e)]: from Feuers et al. (1997); n.a.: not available; *: mean ± SE (n= number of determinations).

After adding GSH (15 mmol/l) to the homogenates and to rat blood, distinct increases in the slopes of the EO concentration-time curves were seen in all incubations except that of the rat kidney. The slopes of these curves and the organ-specific cytosolic protein contents (see Table 3.6) were used to calculate the clearance (V_{maxGST}/K_{mapGST}) of the GST-mediated EO elimination by means of Equations 2.9, 2.18 and 2.19. Further parameters required as inputs in theses equations were K_{eq} (61 for blood (Csanády et al., 2000) and 68.4 for all other tissues according to 3.1.2), the volumes of the liquid (1 ml) and the gaseous (37 ml) phase, as well as the rate constants k_{ceGSH}

($3.12 \cdot 10^{-3}$ min^{-1}) and k_{eHyd} ($9.3 \cdot 10^{-4}$ min^{-1}) that were obtained in the gas uptake studies with EO in cytosolic incubations (see 3.2.2.2). The obtained V_{maxGST}/K_{mapGST} values are given in Table 3.7. As expected, the values V_{maxGST}/K_{mapGST} obtained in the homogenates of livers from mice and rats, and of lungs from rats are close to the corresponding values obtained in cytosol (Table 3.5). The highest GST activity was found in homogenates of the livers. In rat kidney homogenate, GST activity could not be detected. In homogenates of rat brain and blood, very low GST activities were detected and the values were similar.

Table 3.7 Clearance (V_{maxGST}/K_{mapGST}) of glutathione S-transferase-mediated elimination of ethylene oxide (EO) in homogenates from livers of 3 mice or 3 rats, or from various organs of 3 rats (mean ± SE, n: number of determinations)

Species	Organ	V_{maxGST}/K_{mapGST} [µl/min/mg organ]	V_{maxGST}/K_{mapGST} [µl/min/mg protein]	n
Mouse	Liver	1903	20.0	1
Rat	Liver	428 ± 11	4.50 ± 0.12	3
	Lung	42 ± 11	1.59 ± 0.39	3
	Kidney	n.d.	n.d.	3
	Brain	11 ± 0.8	0.28 ± 0.02	3
	Blood	17 ± 0.4	0.22 ± 0.01	3

n.d.: not detected because the elimination rate constant k_{ce} (Table 3.6) could not be differentiated from the sum of the spontaneous hydrolysis of EO and the nonenzymatic GSH conjugation of EO at the GSH concentration of 15 mmol/l (see Equation 2.18).

4 DISCUSSION

4.1 Cytochrome P450 suicide inactivation

A large number of chemical compounds are known to inhibit CYP during their metabolic activation. The mostly irreversible suicide inhibition of CYP occurs generally during or after the oxygenation step in the catalytic cycle of CYP. The inhibition can be highly isoenzyme specific because reversible binding of the substrate and its activation is required (Correia and Ortiz de Montellano, 2005). It was demonstrated in the present work that it is CYP2E1 which metabolizes ET and which is suicide-inactivated by ET. Characteristic substructures of suicide inactivators are furans, thiophenes, halogenated ethylenes, secondary amines, benzodioxolones, isothiocyanates, thioamides, dithiocarbamates, terminal and $\omega-1$ acetylenes, and terminal olefins. According to Correia and Ortiz de Montellano (2005), epoxides are no inhibitors of CYP. Irreversible CYP inactivation can result from four mechanisms: alkylation of the porphyrin ring of the prosthetic heme, covalent binding to protein, virtually irreversible binding to the prosthetic heme iron, and degradation of the prosthetic heme to protein reactive products. Terminal olefins and acetylenes inactivate CYP by the first mechanism (Correia and Ortiz de Montellano, 2005; Fontana et al., 2005).

Already in 1971 the association of CYP mediated metabolism of a terminal olefin (2-allyl-2-isopropylacetamide) and the loss of metabolically active CYP together with the accumulation of a green pigment was recognized (De Matteis, 1971). With ET, the green pigment was detected in rats after pretreatment of the animals with the CYP inducing agent phenobarbital before exposure to ET (Ortiz de Montellano and Mico, 1980). The pigment was later identified as the alkylation product of the prosthetic heme N-(2-hydroxyethyl)protoporphyrin IX (Ortiz de Montellano et al., 1981). If there is a steric hindrance or the double bond is not terminally situated or is part of a conjugated system, CYP is not inactivated as was demonstrated by Ortiz de Montellano and Mico (1980) using 2-methyl-1-heptene, 2-hexene, and styrene, or the inactivation is very slow as compared to the epoxidation. For terminal olefins, the partition ratio (the rate constant of product formation per rate constant of CYP inactivation) ranges from about 40 (this work, human CYP2E1) to about 300 (Collman et al., 1990; Correia and Ortiz de Montellano, 2005). In a metalloporphyrin model system, it was 100 for 1-decene, but

800 for methylenecyclohexane and even 10000 to 12000 for styrene (Collman et al., 1986).
For epoxidation and N-alkylation, several mechanisms have been proposed: formation of “an olefin-oxo π-complex, an acyclic cation or radical, an electron-transfer species followed by collapse to a radical or cation, a metallacarbene, or a metallacycle” (Collman et al., 1986). A more recent formulated mechanism considers a two-state reactivity scenario (Shaik et al., 2002; Shaik and Visser, 2005). An overview of the possible mechanisms is given by Correia and Ortiz de Montellano (2005). However, as stated by the authors “the heme alkylation details, the parameters that govern partitioning between epoxidation and heme alkylation, and the relationships between the mechanism of heme alkylation vs. epoxide formation remain to be clarified.”

In the present work the straightforward function 3.13 was theoretically derived from a suicide inactivation model taking into account the quasi-steady-state assumption of Briggs and Haldane (1925) that has meanwhile be proven to be a law (Li et al., 2008). Using a more empirical procedure, Collman et al. (1990) derived the same equation when investigating the kinetics of the epoxidation and of the heme N-alkylation by styrene. The authors compared the accuracies of the rate constants “k_{cat}” (here named k_3) and “k_{inact}” (here named k_4) that were obtained by fitting the function to the monitored concentration-time course of epoxide formed to the accuracies of these parameters obtained by the “classical” procedure. The latter is based on measuring, at diverse substrate concentrations, the concentration of product formed when the also measured concentration of inactivated CYP is completed. In the classical procedure, the partition ratio is obtained by the ratio of product concentration to the concentration of inactivated CYP. The values of K_{map} and k_4 are usually obtained by fitting a Michaelis-Menten equation to the concentration specific average CYP inactivation rates. Also, the concentration specific average product formation rates are determined (e.g., Walsh, 1982). Collman et al. (1990) stated that fitting the function to the concentration-time course of the formed epoxide gave “more accurate partition numbers” than the classical procedure. This is due to the fact that fitted curves are based on a series of time-dependent data gained at each substrate concentration. A further advantage of the present procedure is that K_{map} values are obtained on the basis of these curves, when extrapolated to the time point zero. Finally, the measurement of CYP inactivation is not required. In spite of these advantages, the

more laborious, less exact classical procedure is still generally being used (e.g. Hopkins et al., 1992; Mayhew et al., 2000; Regal et al., 2000; Ghanbari et al., 2006). Maybe, this will change in the future because now the theoretical explanation of the inactivation function and the easy experimental procedure for obtaining k_3, k_4, and K_{map} is available.

4.2 Toxicokinetics of ethylene

Principally, the first step in the metabolism of an olefin can result in both the formation of an epoxide and of an aldehyde (reviewed in, e.g. Guengerich, 2001). ET however, is metabolized in liver microsomes only to EO as first metabolite and not to AA as demonstrated in the present work. Therefore, EO formation rates equal ET elimination rates, i.e., $|V_{maxEO}|$ equals $|V_{maxET}|$ and K_{map} of EO formation equals K_{map} of ET elimination. In Table 4.1, maximum rates of ET elimination and atmospheric K_{map} concentrations, calculated for *in vivo* conditions from the *in vitro* results given in Table 3.3, are compared with corresponding parameters obtained *in vivo* from gas uptake studies. On average, the predicted maximum ET elimination rates are around three times higher than those observed *in vivo*. At a first glance, these results seem to be inconsistent. If, however, one bears in mind the values of the suicide inactivation constant k_4 of the ET metabolizing CYP2E1 (Table 3.4), one has to expect that the amount of active hepatic CYP2E1 decreases in between 11 min (humans) and 18 min (mice) to about 1/3 of the initial status at very high ET concentrations at which CYP2E1 is saturated. In gas uptake studies with ET in rats (Bolt et al., 1984) or mice (Artati, 2010), in which the elimination of ET in the gas phase was monitored, this effect could not be recognized from the atmospheric concentration-time courses of ET because it occurs within the time span of the initial exposure phase in which the gas enriches in the organism.

Predicted K_{map} concentrations in the atmosphere are 3.8- to 7.4-fold higher than actually determined *in vivo* (Table 4.1). However, the predicted species-specific ratio V_{maxET}/K_{map} does not differ by more than a factor of two from the corresponding ratio obtained *in vivo* (Table 4.1). This ratio, which reflects the clearance of metabolism, is a direct measure of the metabolic elimination of ET at low atmospheric ET concentrations at which the ET elimination rate is proportional to the exposure concentration.

Table 4.1 Kinetic parameters of metabolic ethylene (ET) elimination in mouse, rat, and human as predicted from *in vitro* data on metabolically produced ethylene oxide (EO) [a)] and as determined *in vivo*

Species	Predicted from *in vitro* data [b)]			Determined *in vivo*		
	V_{maxET} [c)] [µmol/h/kg]	K_{map} [d)] [ppm in air]	V_{maxET}/K_{map} [µmol/h/kg/ppm]	V_{maxET} [µmol/h/kg]	K_{map} [ppm in air]	V_{maxET}/K_{map} [µmol/h/kg/ppm]
Mouse	42.9	400	0.11	15 [e)]	105 [e)]	0.14
Rat	28.9	1516	0.02	8.5 [f)]	204 [f)]	0.04
				8.6 [g)]	218 [g)]	0.04
Human	9.8	963	0.01	n.d.	n.d.	0.005 [h)]

Abbreviations: V_{maxET}, maximum metabolic elimination rate of ET; K_{map}, apparent Michaelis constant of the metabolic ET elimination, given as ET exposure concentration in air; n.d., not determined.
[a)]: It is assumed that the maximum rate of ethylene oxide formation (V_{maxEO}) equals -V_{maxET} and that the K_{map} concentrations of EO production and ET elimination are identical. [b)]: The parameters were predicted using the V_{maxEO} and K_{map} values obtained in pooled liver microsomes (Table 3.3). [c)]: V_{maxET} *in vivo* was derived from V_{maxEO} (*in vitro*; Table 3.3) as described in Kreuzer et al. (1991) taking into account a microsomal protein content of 30 mg/g liver, liver weights of 1 g (mouse), 10 g (rat), and 1.5 kg (human), and body weights of 25 g (mouse), 250 g (rat), and 70 kg (human). [d)]: K_{map} (ppm) was calculated by dividing the in Table 3.3 given K_{map} (mmol/l supension) by the *in vivo* obtained steady-state bioaccumulation factor K_{st}, which gives the ratio of the average ET concentration in the body at low ET exposure concentrations to the ET exposure concentration in the atmosphere – K_{st}=0.55 (mouse, Artati, 2010), K_{st}=0.50 (rat, Bolt et al., 1984), and K_{st}=0.33 (human, Filser et al., 1992) – and by multiplication with 24460 ml, the molar volume of an ideal gas at 25°C. [e)]: From Artati (2010); [f)]: from Bolt and Filser (1987); [g)]: from Andersen et al. (1980). [h)]: The value was calculated by dividing the "clearance of metabolism (related to atmosph. concn.)" of 9.3 l/h (Table 2 in Filser et al., 1992) by 24.46 l, the molar volume of an ideal gas at 25°C, and by a body weight of 70 kg.

The agreement between the predicted and the *in vivo* obtained V_{maxET}/K_{map} values is striking. Because the *in vivo*-derived values of V_{maxET} were obviously too low – not reflecting the suicide inhibition –, the corresponding *in vivo* K_{map} values had also to be too low in order to describe correctly the metabolic elimination at low ET concentrations. For the same reason, an extremely small value of 0.0005 mmol/l was used for the apparent Michaelis constant of the ET oxidation in the liver compartment of the physiological toxicokinetic ET model of Csanády et al. (2000).

4.3 Toxicokinetics of ethylene oxide

The present results obtained in subcellular fractions of mouse and rat livers can be compared with those of Brown et al. (1996) who investigated the ethylene glycol formation in liver microsomes and cytosol of both species. In microsomal incubations, the authors detected a maximum rate of hydrolysis of only 1.5 - 2 nmol/min/mg protein at an EO concentration of 15 mmol/l. The rate was at best (assuming a protein concentration of 2 mg/ml incubate) 2 times faster than that of the nonenzymatic hydrolysis. The Michaelis constant for this reaction could only be estimated “due to the high rate of nonenzymatic hydrolysis relative (to) the enzymatic rate”. One could argue, that the analytical method of Brown et al. (1996) was more sensitive than the present one in which only EO was quantified. However, the rate constant of the nonenzymatic elimination could well be determined in the present work. It is almost identical with the value of 0.001 min^{-1} that can be calculated from the data given by Brown et al. (1996).
EO is for a long time considered to be a poor substrate for microsomal EH (Goldberg, 1986). This view results from findings of Dent and Schnell (1981) who investigated the competitive inhibition of the rat liver microsomal EH mediated hydrolysis of styrene-7,8-oxide by EO, PO and other 1,2-epoxyalkanes of low molecular weight. The authors found that very high concentrations (in the molar range) of each of both epoxides were required for a 50% inhibition of the hydroxylation of styrene-7,8-oxide (2 mmol/l). The authors suggested, too, that glutathione conjugation should be more relevant for the metabolic elimination of linear C_2 - C_4 1,2-epoxyalkanes than EH mediated hydrolysis. This interpretation was later falsified for PO. Both microsomal EH and cytosolic GST metabolize PO similarly well (Faller et al., 2001). Possibly, the inhibition of styrene-7,8-oxide hydroxylation by PO is only partly competitive. For EO, the conclusion of Dent and Schnell (1981) has now been verified in mice, rats, and humans by the here

presented direct measurements of EH and GST catalyzed EO elimination and for mice and rats by the studies conducted by Brown et al. (1996).

In agreement with Brown et al. (1996), EO elimination takes place almost completely in the cytosol and is catalyzed by GST. The reported V_{maxGST} and K_{mapGST} values for GSH conjugation with EO in liver cytosol of mice and rats are very similar to those obtained in the present work. As shown in 3.2.3, the ratios V_{maxGST}/K_{mapGST} are also in agreement with the ones obtained in liver homogenates of both species. In the present work, the GST catalyzed EO elimination was also detected in homogenates of rat lungs, brains, and blood, albeit with lower values of V_{maxGST}/K_{mapGST}. Taking into account that the blood flow through the lung is around four times that through the liver, one has to conclude that the GSH conjugation of EO in the lung may contribute substantially to the EO metabolism in the body. In contrast to Brown et al. (1996) who reported the rate of cytosolic GSH conjugation of EO in rat kidney to be almost four fifth of that in rat liver, EO elimination in kidney homogenate of the same rat strain was too low to be detected in the present work (see Table 3.7). Using the standard substrate DTNB, Jurczuk et al. (2006) found the GST activity in the rat kidney to be around one tenth of that in the liver. In the light of these findings, the GSH conjugation of EO reported by Brown et al. (1996) for kidney cytosol is probably too high.

From the high K_{mapGST} value of at least 12 mmol/l in liver cytosol (mice, rats, and humans; this work) or 10 - 13 mmol/l (mice and rats; Brown et al., 1996), the EO metabolism *in vivo* can be expected to be proportional to the EO exposure concentration until the consumption of GSH will be too high to be counterbalanced by the rate of its synthesis. Indeed, in single EO gas uptake studies with Sprague-Dawley or Fischer rats, EO elimination from the chamber atmosphere followed first-order kinetics up to EO concentrations of about 600 ppm. At exposure concentrations of about 1000 ppm, the concentration-time courses flattened with increasing exposure time (Csanády et al., 2000). Depletion of GSH was most probably the cause for this effect considering that McKelvey and Zemaitis (1986) observed a concentration-dependent decrease of GSH in Fischer rats exposed for 4 h to constant EO concentrations of 100, 600, or 1200 ppm. At the highest EO concentration, GSH levels in the livers decreased to less than 20% of the control value. In B6C3F1 mice exposed for 4 h to constant EO concentrations of up to 200 ppm, EO blood levels were linearly related to the exposure concentration (Brown et al., 1998). At exposure concentrations of 300 and 400 ppm however, the EO blood levels increased over-proportional when

related to the exposure concentration. The authors linked these findings to the depletion of GSH that declined at both highest EO concentrations in the livers to less than 22% of the control value (Brown et al., 1998).

The question arises why EO is a very poor substrate for microsomal EH in contrast to PO and other unbranched 1,2-epoxyalkanes, independently of their enantiomeric nature (Bellucci et al., 1989; Wistuba and Schurig, 1992). From the findings that epoxides with small lipophilic substituents were weak inhibitors of the microsomal EH catalyzed hydrolysis of styrene-7,8-oxide in contrast to other epoxides with large substituents like 1,2-epoxy-n-octane, Oesch et al. (1971) postulated hydrophobic interactions of the substituent with enzyme residues near to the active site. The idea of a hydrophobic pocket for the substituent, by which the epoxide becomes sterically presented to the catalytic center (the catalytic triad consisting of three amino acid residues; Arand et al., 1999) was supported by a series of studies (e.g., Armstrong et al., 1981; Bellucci et al., 1980, 1989; Sayer et al., 1985) and is now enlarged and experimentally proven (Gomez et al., 2004). Considering that EO is missing any substituent, one can imagine that gaining the right position in the active center of EH to become hydrolyzed will be time consuming thereby resulting in a slow rate of hydrolysis.

Microsomal EH-catalyzed hydrolysis of EO is expected to represent at least one fourth of the overall EO metabolism in humans. This ratio is obtained taking into account a protein content of 30 mg/g liver in microsomes and of 95 mg/g liver in cytosol (Kreuzer et al., 1991) as well as a V_{maxEH} to K_{mapEH} ratio of the EH-catalyzed EO elimination in microsomes of 1.13 µl/min/mg protein (see 3.2.2.1) and of the GST-catalyzed conjugation reaction in pooled cytosol of 1.14 µl/min/mg protein (Table 3.5). Neglecting extrahepatic metabolism, one can therefore expect for EO exposed humans of the GSTT1*0/0 genotype the EO tissue burden to be at most 4 times higher than in equally exposed humans carrying the active GSTT1 form. This conclusion of a quantitatively relevant role of microsomal EH on the elimination of EO in humans is supported by the results of a thoroughly conducted study on smokers. Hydroxyethyl adduct levels to the N-terminal valine of hemoglobin were on average 1.61 times higher in GSTT1-null individuals than in GSTT1 carriers (Fennell et al., 2000).

4.4 Ethylene oxide burden during exposure to ethylene

From the present parameters of EO formation, CYP2E1 inhibition, and EO metabolism, one has to expect to find in mice, rats and humans, when exposed to high ET concentrations, an early EO peak in blood followed by a rather rapid decline to a plateau characterized by a distinctly lower equilibrium between CYP2E1 neosynthesis and elimination as compared to the initial CYP2E1 status. In the atmosphere of a closed exposure chamber, the changes of the concentrations of exhaled EO have to be slower and less drastic than the rapid ones of EO in blood because the chamber behaves like a deep compartment. The reported pictures of initial EO peaks in blood and EO maxima in exhaled air of rats and mice exposed to ET concentrations > 300 ppm and > 30 ppm, respectively (Artati, 2010; Erbach, 2010; Fennell et al., 2004; Filser and Bolt, 1984; Maples and Dahl, 1993), are in support of this expectation. At low ET concentrations, the permanent resynthesis of CYP2E1 will be large as compared to the rate of suicide inhibition and the CYP2E1 turnover rate will not much change during exposure. In agreement with the observations made in rats (Maples and Dahl, 1993; Erbach, 2010) and in mice (Artati, 2010), EO in blood and in chamber atmosphere increases continuously until reaching a plateau that is simply characterized by the equilibrium between EO formation and EO elimination.

4.5 Outlook

A presently favored procedure to evaluate human health risks from chemicals uses toxicokinetic and toxicodynamic chemical-specific adjustment factors (CSAFs) in dose-response assessment (see, for example, Meek et al., 2002). Usually, the CSAF for the toxicokinetic uncertainty between species and that for the toxicokinetic uncertainty between human individuals is given a maximum number of $10^{0.6}$ and of $10^{0.5}$, respectively. In the laboratory of Prof. Filser, studies on the EO burden in ET exposed mice, rats, and human individuals are presently being conducted. The results together with the robust toxicokinetic parameters obtained in the present work will be used to improve a physiological toxicokinetic model for ET and EO in these three species (Csanády et al., 2000). Because of its strong inter-species and inter-individual data basis, one can expect to generate model predictions that will be reliable enough for reducing the toxicokinetic CSAFs to the minimum.

5 Summary / Zusammenfassung

5.1 Summary

Ethylene (ET), which is found ubiquitously in the environment, is the largest volume organic chemical produced worldwide. In mammals, it was neither mutagenic nor carcinogenic inspite of its metabolism to the mutagenic and carcinogenic ethylene oxide (EO). The negative results were explained by a too low sensitivity of classical long-term carcinogenicity studies. Because of the high industrial relevance of ET and EO, several working groups investigated the toxicokinetics and metabolism of both chemicals in laboratory animals. However, important toxicokinetic data on the ET metabolism mediated by cytochrome P450-dependent monooxygenase (CYP) and on the spontaneous and enzyme catalyzed elimination of EO are still missing. Furthermore, no toxicokinetic data on EO in humans have been published. Quantitative information is needed for the validation of a future physiological toxicokinetic model of ET and EO, which is required for estimating the risk of both chemicals to humans based on the outcome of the long-term animal studies with EO. Considering that metabolism of ET is related to the CYP isoenzyme 2E1 (CYP2E1) and metabolism of EO to epoxide hydrolases (EH) and glutathione S-transferases (GST), the aim of the present work was to investigate CYP2E1-mediated kinetics of ET as well as EH and GST catalyzed kinetics of EO in subcellular fractions prepared from livers of B6C3F1 mice, Fischer 344 rats or human donors or from lungs of mice or rats. CYP2E1 knockout mice were to be used to prove the relevance of CYP2E1 for the metabolism of ET.

At first, in-house bred CYP2E1 knockout mice were genotyped by means of the polymerase chain reaction in order to verify the knockout of this CYP-species. Then, gas chromatographic methods for the detection of ET and vapors of EO, acetaldehyde (AA; a possible ET metabolite), propylene oxide (PO), and styrene (ST; both compounds served for validating purposes) were evaluated. In order to determine the CYP2E1 activity in liver microsomes of mice and rats, the metabolic formation of 6-hydroxychlorzoxazone from the CYP2E1 specific substrate chlorzoxazone was determined by means of high performance liquid chromatography coupled to tandem

mass spectrometry (LC/MS/MS). For the determination of reduced glutathione (GSH), a spectrophotometrical method was established which is based on the reaction of GSH with 5,5'-dithiobis-(2-nitrobenzoic acid). After having established the analytical methods, kinetics of ET metabolism to EO and of elimination of EO were investigated at 37°C in headspace vessels containing incubations of subcellular fractions (microsomes or cytosol) or a tissue homogenate together with required coenzymes. Gaseous ET, EO, PO, or ST was injected into the atmosphere of the headspace vial in order to achieve a defined initial gas concentration. Thereafter, gas samples were taken periodically from the headspace and analyzed by gas chromatography.

The Results part starts with validation studies which confirmed that liver microsomes were intact over the whole exposure periods of up to 65 min (demonstrated with styrene) and that they exhibited full CYP2E1 activity as proven using the CYP2E1 specific chlorzoxazone test. EH activity was verified by using PO, a well-known substrate for microsomal EH. Cytosolic GST activity was verified by conducting gas uptake studies with the GST substrate PO using native pooled liver cytosol of mice or rats and liver cytosol of a male human subject, which contained GSH or the GSH depleting agent diethyl maleate.

CYP-associated metabolism of ET to EO was found in microsomes of each species. The possible ET metabolite AA was not detected. In order to describe the concentration-time courses of EO detected in the microsomal incubations of ET, a novel procedure for the kinetic analysis of these time courses was developed. It describes both CYP2E1 catalyzed formation of EO from ET according to Michaelis and Menten kinetics and the suicide inactivation of CYP2E1 by its substrate ET. In pooled liver microsomes, values of the maximum rate of EO formation (V_{max}; nmol/min/mg protein) and of the apparent Michaelis constant (K_{map}; mmol/l ET in the microsomal suspension) were 0.567 and 0.0093 (mouse), 0.401 and 0.031 (rat), and 0.219 and 0.013 (human), respectively. In pooled lung microsomes, V_{max} values were 0.073 (mouse) and 0.055 (rat). During ET exposure, the rates of EO formation decreased rapidly. Rate constants for CYP inactivation in liver microsomes were between 0.06 min^{-1} (mice) and 0.1 min^{-1} (humans). The values of the partition ratio, which represents the number of products formed per one inactivation event, were between 39 (humans) and 169 (rats) in liver microsomes. The relevance of CYP2E1 in the ET metabolism was evidenced by the very small EO formation rates in CYP2E1

knockout mice. There was no EH-related metabolism of EO detectable in pooled hepatic or pooled pulmonary microsomes of rats and mice but some in hepatic microsomes of humans, which obeyed saturation kinetics (V_{max}: 14.35 nmol/min/mg protein; K_{map}: 12.74 mmol/l EO in the microsomal suspension). No cytosolic EH activity at all was detected in cytosolic EO incubations. GST-related metabolism of EO was found in cytosol of each species. In pooled liver cytosol, GST activities to EO expressed as V_{max}/K_{map} (µl/min/mg protein) were 27.90 (mouse), 5.30 (rat), and 1.14 (human). In pooled lung cytosol of mice and rats, GST activities were 6.32 and 1.78 µl/min/mg protein, respectively. Considering the polymorphism of the EO eliminating human GST-theta, GST activities to EO were also investigated in individual hepatic cytosol preparations of 13 humans (both genders, between 16 and 78 years old). The activities ranged from 0.00 to 2.87 µl/min/mg protein. Finally, gas uptake studies were conducted with EO in mouse and rat tissue homogenates. In rat tissue homogenates, the highest GST activity was found in the liver. In mouse liver and rat liver and lung homogenates, the obtained GST activities V_{max}/K_{map} were close to the corresponding values obtained in cytosol. In rat kidney homogenate, GST activity could not be detected. In homogenates of rat brain and blood, GST activities were very low.

In the Discussion, some general reflections on the suicide inactivation of CYP are dealt with, in the light of the present results, for instance the well-known CYP specificity for the inactivating substrate that is characterized by a chemical subgroup such as a terminal olefin. It is mentioned that the here found inactivation of CYP2E1 by ET agrees with this picture. Then, the theoretically derived kinetic method for quantifying both CYP mediated catalysis and CYP inactivation (present work) is compared with the classical procedure that is based on measuring not only the product formed from the substrate but also the inactivation of the metabolizing CYP isoenzyme. It is argued why the kinetic method is not only more accurate but also less laborious than the hitherto used procedure. Thereafter, toxicokinetic parameters of ethylene, predicted from *in vitro* to *in vivo*, are opposed to corresponding values derived from studies *in vivo*. It is elucidated why the ratios of maximum rates of ET metabolism to apparent Michaelis constants can be well predicted from the *in vitro* parameters and why the predicted values of the maximum rates and apparent Michaelis constants differ from the values obtained *in vivo*. Concerning EO, the validity of the values of the kinetic parameters is demonstrated by a comparison with published data *in vitro* as well as *in vivo* and with

the results obtained in tissue homogenates. The finding that EO was a poor substrate of EH is explained in the light of the mechanism of the EH mediated hydroxylation of epoxides. However, concerning the polymorphism of GST-theta in humans, it is emphasized that the EH activity in human microsomes is relevant with respect to the EO elimination in humans *in vivo.* Finally, the hitherto only partly understood *in vivo* findings that an initial EO peak had been detected in blood of rats and mice when exposed to high ET concentrations is enlightened on the basis of the present *in vitro* results. In the outlook, it is stressed that the new quantitative data are of utmost importance concerning the reduction of uncertainties when evaluating a health risk from ET and EO on the basis of a future physiological toxicokinetic model.

5.2 Zusammenfassung

Ethylen (ET), das ubiquitär gefunden wird, ist die weltweit meistproduzierte Chemikalie. Vom Säuger wird das Olefin zu Ethylenoxid (EO) metabolisiert, das mutagen ist und im Tierversuch kanzerogen war. Im Gegensatz hierzu war ET in entsprechenden Untersuchungen negativ, was damit begründet wurde, dass die Belastungen durch metabolisch gebildetes EO zu niedrig waren, um mutagene bzw. kanzerogene Wirkungen erfassen zu können. Wegen der hohen industriellen Bedeutung von ET und EO haben mehrere Arbeitsgruppen die als Voraussetzung für eine Risikoermittlung erforderliche Toxikokinetik beider Stoffe untersucht. Dennoch fehlten bisher wichtige toxikokinetische Daten zum durch Cytochrom P450-abhängige Monooxygenasen (CYP) katalysierten ET-Metabolismus sowie zur EO-Elimination, vermittelt durch Epoxidhydrolase (EH) und Glutathion-S-transferase (GST). Deshalb sollten in der vorliegenden Arbeit mit beiden Stoffen die enzymspezifischen Parameter „maximale Metabolismusgeschwindigkeit“ (V_{max}) und „scheinbare Michaelis-Konstante“ (K_{map}) in subzellulären Fraktionen aus Lebern und Lungen von B6C3F1-Mäusen und Fischer 344 Ratten sowie aus Lebern menschlicher Donoren untersucht werden. Entsprechende Untersuchungen mit Mikrosomen von CYP2E1-Knockout- und entsprechenden Wildtyp-Mäusen sollten die quantitative Bedeutung von CYP2E1 (einem bestimmten CYP-Isoenzym) für den ET-Metabolismus beweisen. Weiterhin sollte in einigen Experimenten mit Gewebehomogenaten die quantitative Bedeutung bestimmter Gewebe für den EO-Metabolismus ermittelt werden.

Zuerst wurden Lungen- und Lebermikrosomen bzw. -zytsol von Fischer-344-Ratten, B6C3F1-Mäusen, Wildtyp-Mäusen (129S1/SvImJ) und CYP2E1-Knockout-Mäusen präpariert, nachdem bei letzteren der CYP2E1-Knockout durch „Genotyping“ bewiesen worden war. Von verschiedenen menschlichen Individuen gewonnene, vereinte („gepoolte“) subzelluläre Leberfraktionen wurden käuflich erhalten. Zusätzlich wurden Lebermikrosomen von einem und Leberzytosol von zwölf verstorbenen Personen präpariert sowie Mikrosomen und Zytosol aus einer Leber, die einem Patienten während der Transplantation entnommen wurde. Gewebehomogenate wurden aus den Lebern von B6C3F1-Mäusen und aus Lebern, Lungen, Nieren und Gehirnen von Fischer-344-Ratten hergestellt. Von letzteren Tieren wurden auch Blutproben gewonnen. Sodann wurden gaschromatographische Methoden zur Bestimmung von ET, EO, Acetaldehyd (einem möglichen ET-Metaboliten) Propylenoxid, und Styrol (beide für Validierungen eingesetzt) sowie spektrophotometrische Verfahren zur Ermittlung der Gehalte an Protein und reduziertem Glutathion (GSH) evaluiert. Zum Nachweis mikrosomaler CYP2E1-Aktivität wurde Chlorzoxazon verwendet, das durch CYP2E1 in 6-Hydroxychlorzoxazon überführt wird. Letzteres wurde mit einem an einen Tandem-Massenspektrometer gekoppelten Hochdruckflüssigkeitschromatographen bestimmt. Die kinetischen Untersuchungen zur CYP2E1-katalysierten EO-Bildung aus ET, zur Hydrolyse von EO (katalysiert durch die EH bzw. spontan ablaufend) sowie zur Konjugation von GSH mit EO (spontan bzw. durch die GST katalysiert) wurden in „Head-Space“-Gefäßen bei 37°C vorgenommen. Hierzu wurden die Gefäße, welche in Puffer suspendierte subzelluläre Fraktion, Gewebehomogenat oder nur Blut enthielten, mit oder ohne Co-Substrat (NADPH-regenerierendes System bzw. GSH) in Gegenwart definierter initialer Gaskonzentrationen von ET oder EO inkubiert. Kontrolluntersuchungen zur metabolischen Aktivität der subzellulären Fraktionen wurden mit Styrol und mit Propylenoxid vorgenommen. Die Konzentrations-Zeitverläufe der aufgeführten Stoffe wurden anhand der Analyse von Gasproben, die zu festgelegten Zeitpunkten während der Inkubationen entnommen wurden, ermittelt.

Im Ergebnisteil werden zuerst Validierungsexperimente aufgeführt, die zeigen, dass die ET- und EO-metabolisierenden Enzyme in den subzellulären Gewebefraktionen metabolisch aktiv waren (Untersuchung der Aktivität des CYP2E1 mit Styrol und Chlorzoxazon, der EH mit Propylenoxid sowie der GST mit Propylenoxid in Gegenwart von GSH). In Anwesenheit von NADPH setzten die Mikrosomen aller drei Spezies über einen CYP-katalysierten Schritt ET zu EO um. Acetaldehyd wurde nicht gefunden.

Dass der ET-Metabolismus tatsächlich durch CYP2E1 katalysiert wird, wurde anhand von ET-Inkubationen in Lebermikrosomen von CYP2E1-Knockout-Mäusen gezeigt. Zur kinetischen Analyse der Konzentrations-Zeitkurven von bei den ET-Expositionen gebildetem EO wurde ein neues kinetischen Verfahren entwickelt. Es beruht auf einem enzymatischen Modell, das sowohl die durch CYP2E1-vermittelte Bildung von EO aus ET entsprechend einer Kinetik nach Michaelis und Menten als auch die ET-induzierte Suizidhemmung von CYP2E1 beinhaltet. Hiermit ergaben sich für die EO-Bildung in ET-exponierten gepoolten Lebermikrosomen V_{max}-Werte (nmol/min/mg Protein) von 0,567 (Maus), 0,401 (Ratte) und 0,219 (Mensch). Die entsprechenden K_{map}-Werte (mmol ET/l mikrosomale Suspension) betrugen 0,0093, 0,031 und 0,013. In den gepoolten Lungenmikrosomen konnten nur die V_{max}-Werte mit 0,073 (Maus) und 0,055 (Ratte) quantifiziert werden. Während der ET-Inkubationen nahmen die EO-Bildungsgeschwindigkeiten rasch ab. Die hieraus ermittelten Geschwindigkeitskonstanten der Suizidhemmung des CYP2E1 in Lebermikrosomen lagen zwischen 0,06 min^{-1} (Maus) und 0,1 min^{-1} (Mensch). Pro CYP2E1-Inaktivierungsereignis wurden in den Lebermikrosomen zwischen 39 (Mensch) und 169 (Ratte) Moleküle ET in EO überführt. EH-Aktivität mit EO als Substrat konnte nur in Humanlebermikrosomen nachgewiesen werden (V_{max}, 14,35 nmol/min/mg Protein; K_{map}, 12.74 mmol EO/l Suspension). Konjugation von GSH mit EO, sowohl spontan als auch GST-katalysiert, fand sich in den zytosolischen Gewebsfraktionen aller drei Spezies. In gepooltem Leberzytosol betrugen die GST-Aktivitäten mit EO als Substrat, ausgedrückt als V_{max}/K_{map} (µl/min/mg Protein) 27,90 (Maus), 5,30 (Ratte) und 1,14 (Mensch). In gepooltem Lungenzytosol von Maus und Ratte betrugen sie 6,32 und 1,78. Berücksichtigend, dass beim Menschen EO durch die polymorphe GST-theta umgesetzt wird, wurde die Aktivität dieses Enzyms mit EO als Substrat auch individuell in Leberzytosolproben von 13 Personen beider Geschlechter bestimmt. Es zeigte sich eine große Streuung mit Werten zwischen 0,00 und 2,87 µl/min/mg Protein. Die GST-Aktivitäten in Mäuseleberhomogenat und in den Homogenaten von Rattenleber und -lunge waren sehr ähnlich wie die Werte, die in entsprechendem Zytosol gefunden wurden. Deutlich geringere Aktivitäten als in der Rattenlunge fanden sich in Blut und Gehirn. In der Rattenniere war keine GST-Aktivität nachweisbar.

Die Diskussion befasst sich zunächst mit einigen generellen Aspekten der Suizidhemmung von CYP; es wird gezeigt, dass die hier erarbeiteten Ergebnisse mit den vorliegenden Erkenntnissen zur Hemmung durch Stoffe mit terminalen

olefinischen Gruppen in Einklang stehen. Sodann wird ein Vergleich des in der vorliegenden Arbeit erstmals theoretisch abgeleiteten Verfahrens zur Ermittlung der kinetischen Parameter für metabolische Umsetzung und Suizidhemmung mit der allgemein angewandten Methode vorgenommen. Es zeigt sich, dass die hier gewählte Vorgehensweise weniger arbeitsaufwändig ist und die kinetischen Parameter genauer bestimmbar sind. Anschließend werden, ausgehend von den *in vitro* erhaltenen toxikokinetischen ET-Parametern, Extrapolationen von V_{max} und K_{map} auf die *in-vivo*-Bedingung vorgenommen und diese veröffentlichten *in-vivo*-Parametern gegenübergestellt und die Differenzen erläutert. Die Validität der für EO erhaltenen Parameter werden ebenfalls im Lichte der Literatur und auch anhand der eigenen Befunde mit Leberhomogenat diskutiert. Der Befund, dass EO kein bzw. nur ein schlechtes Substrat für die EH darstellt, wird anhand von Litertaturdaten zum Mechanismus der EH-katalysierten Hydrolyse erklärt. Weiterhin wird hergeleitet und mit Literaturdaten belegt, dass beim Menschen, wegen des Polymorphismus der GST-Theta, die EH-Aktivität für die EO-Elimination bedeutsam sein kann. Schließlich wird der bis dato nicht recht verstandene Befund des initialen EO-Peaks diskutiert, der im Blut von Tieren bei hoher ET-Expositionskonzentration auftritt. Er wird als Folge einer wegen der Suizidhemmung von CYP2E1 nur anfänglich hohen ET-Metabolisierung gedeutet. Für niedrige ET-Konzentrationen wird die ET-bedingte Hemmung des Enzyms als zu gering im Vergleich zu seiner Neusynthese angenommen. Somit wäre es verständlich, dass hier kein EO-Peak auftrat.

Im Ausblick wird klargestellt, dass die hier gewonnenen, quantitativen Daten, zusammen mit den Ergebnissen gerade laufender Arbeiten zur EO-Belastung ET-exponierter Freiwilliger, für die Erstellung eines physiologisch-toxikokinetischen Modells verwendet werden sollen. Mit Hilfe dieses Modell sollte es möglich werden, die Unsicherheiten bei der Abschätzung des in ET- und EO-Expositionen bestehenden Gesundheitsrisikos drastisch zu reduzieren.

6 ABBREVIATIONS

Frequently used abbreviations:

AA	Acetaldehyde
b.w.	Body weight
CYP	Cytochrome P450-dependent monooxygenase
DEM	Diethyl maleate
EH	Epoxide hydrolase
EO	Ethylene oxide
ET	Ethylene
GSH	Glutathione
GST	Glutathione S-transferase
k_{ce}	Rate constant of overall elimination in cytosolic incubations
k_{ceGSH}	Rate constant of non-enzymatic GSH conjugation
k_{eHyd}	Rate constant of non-enzymatic spontaneous hydrolysis
K_{eq}	Distribution coefficient incubation medium-to-air
K_{map}	Apparent Michaelis constant
K_{st}	Distribution factor at steady state
PO	Propylene oxide
$P_{o/w}$	Octanol/water partition coefficient
Pr	Amount of protein
ST	Styrene
V_d	Volume of distribution
V_g	Volume of the gas phase of the headspace vial
V_l	Volume of the liquid phase
V_{max}	Maximum rate of metabolism

7 REFERENCES

Abeles, F. B. and Dunn, L. J. (1985). Ethylene-enhanced ethylene oxidation in *Vicia faba*. *J. Plant Growth Regul.* **4,** 123–128.

ACGIH (2005). American Conference of Governmental Industrial Hygienists. TLVs and BEIs. Threshold Limit Values for Chemical Substances and Physical Agents and Biological Exposure Indices. Cincinnati, Ohio, USA.

ACGIH (2011). American Conference of Governmental Industrial Hygienists. TLVs and BEIs. Threshold Limit Values for Chemical Substances and Physical Agents and Biological Exposure Indices. Cincinnati, Ohio, USA.

Alberta Environment (2003). Assessment report on ethylene for developing ambient air quality objectives. *http://www3.gov.ab.ca/env/protenf/standards/index.html* (downloaded on Sept. 13, 2011).

Alberta's Ethylene Crop Research Project (2002). Alberta's Ethylene Crop Research Project, Fact sheet–research result. *http://www.novachem.com/Joffre/docs/Ethyl11.pdf* (downloaded on Sept. 13, 2011).

Amoore, J. E. and Hautala, E. (1983). Odor as an aid to chemical safety: odor threshold compared with threshold limit values and volatilities for 214 industrial chemicals in air and water dilution. *J. Appl. Tox.* **36,** 272–290.

Andersen, M. E., Gargas, M. L., Jones, R. A., and Jenkins, L. J. Jr. (1980). Determination of the kinetic constants for metabolism of inhaled toxicants *in vivo* using gas uptake measurements. *Toxicol. Appl. Pharmacol.* **54,** 100–116.

Angerer, J., Bader, M., and Krämer, A. (1998). Ambient and biochemical effect monitoring of workers exposed to ethylene oxide. *Int. Arch. Occup. Environ. Health* **71,** 14–18.

Arand, M., Müller, F., Mecky, A., Hinz, W., Urban, P., Pompon, D., Kellner, R., and Oesch, F. (1999). Catalytic triad of microsomal epoxide hydrolase: replacement of Glu404 with Asp leads to a strongly increased turnover rate. *Biochem. J.* **337,** 37–43.

Arms, A. D. and Travis, C. C. (1988). *Reference Physiological Parameters in Pharmacokinetic Modeling* (Report No EPA 600 6-88/004), Washington DC, US Environmental Protection Agency.

Armstrong, R. N., Kedzierski, B., Levin, W., and Jerina, D. M. (1981). Enantioselectivity of microsomal epoxide hydrolase toward arene oxide substrates. *J. Biol. Chem.* **256,** 4726–4733.

Artati, A. (2010). Toxicokinetics of ethylene and ethylene oxide in the male B6C3F1 mouse. PhD thesis, Lehrstuhl für Chemisch-Technische Analyse und Chemische Lebensmitteltechnologie, Technische Universität München.

Ayers, N. A., Kapás, L., and Krueger, J. M. (1996). Circadian variation of nitric oxide synthase activity and cytosolic protein levels in rat brain. *Brain Res.* **707,** 127–130.

Bellucci, G., Berti, G., Ingrosso, G., and Mastrorilli, E. (1980). Stereoselectivity in the epoxide hydrase catalyzed hydrolysis of the stereoisomeric 4-tert-butyl-1,2-epoxycyclohexanes. *J. Org. Chem.* **45,** 299–303.

Bellucci, G., Chiappe, C., Conti, L., Marioni, F., and Pierini, G. (1989). Substrate enantioselection in the microsomal epoxide hydrolase catalyzed hydrolysis of monosubstituted oxiranes. Effects of branching of alkyl chains. *J. Org. Chem.* **54,** 5978–5983.

Bleecker, A. B. and Kende, H. (2000). Ethylene: a gaseous signal molecule in plants. *Annu. Rev. Cell Dev. Biol.* **16,** 1–18.

Bolt, H. M. and Filser, J. G. (1987). Kinetics and disposition in toxicology. Example: carcinogenic risk estimate for ethylene. *Arch. Toxicol.* **60,** 73–76.

Bolt, H. M. and Filser, J. G. (1984). Olefinic hydrocarbons: A first risk estimate for ethene. *Toxicol. Pathol.* **12,** 101–105.

Bolt, H. M., Filser, J. G., and Störmer, F. (1984). Inhalation pharmacokinetics based on gas uptake studies V. Comparative pharmacokinetics of ethylene and 1,3-butadiene in rats. *Arch. Toxicol.* **55,** 213–218.

Bolt, H. M. and Thier, R. (2006). Relevance of the deletion polymorphisms of the glutathione S-transferases GSTT1 and GSTM1 in pharmacology and toxicology. *Curr. Drug Metab.* **7,** 613–628.

Boogaard, P. J., Rocchi, P. S. J., and van Sittert, N. J. (1999). Biomonitoring of exposure to ethylene oxide and propylene oxide by determination of hemoglobin adducts: correlations between airborne exposure and adduct levels. *Int. Arch. Occup. Environ. Health* **72,** 142–150.

Boyland, E. and Chasseaud, L. F. (1970). The effect of some carbonyl compounds on rat liver glutathione levels. *Biochem. Pharmacol.* **19,** 1526–1528.

Briggs, G. E. and Haldane, J. B. S. (1925). A note on the kinetics of enzyme action. *Biochem. J.* **19,** 338–339.

Brown, C. D., Asgharian, B., Turner, M. J., and Fennell, T. R. (1998). Ethylene oxide dosimetry in the mouse. *Toxicol. Appl. Pharmacol.* **148,** 215–221.

Brown, C. D., Wong, B. A., and Fennell, T. R. (1996). *In vivo* and *in vitro* kinetics of ethylene oxide metabolism in rats and mice. *Toxicol. Appl. Pharmacol.* **136,** 8–19.

Brugnone, F., Perbellini, L., Faccini, G., and Pasini, F. (1985). Concentration of ethylene oxide in the alveolar air of occupationally exposed workers. *Am. J. Ind. Med*. **8,** 67–72.

Brugnone, F., Perbellini, L., Faccini, G. B., Pasini, F., Bartolucci, G. B., and DeRosa, E. (1986). Ethylene oxide exposure. Biological monitoring by analysis of alveolar air and blood. *Int. Arch. occup. environ. Health* **58,** 105–112.

Burgaz, S., Rezanko, R., Kara, S., and Karakaya, A. E. (1992). Thioethers in urine of sterilization personnel exposed to ethylene oxide. *J. Clin. Pharm. Ther.* **17,** 169–172.

Chittur S. V. and Tracy, T. S. (1997). Rapid and sensitive high-performance liquid chomatographic assay for 6-hydroxychlorzoxazone and chlorzoxazone in liver microsomes. *J. Chromatogr. B* **693,** 479–483.

Clemens, M. R., Einsele, H., Frank, H., Remmer, H., and Waller, H. D. (1983). Volatile hydrocarbons from hydrogen peroxide-induced lipid peroxidation of erythrocyte and their cell compounds. *Biochem. Pharmacol*. **32,** 3877–3878.

Coggon, D., Harris, E. C., Poole, J., and Palmer, K. T. (2004). Mortality of workers exposed to ethylene oxide: extended follow up of a British cohort. *Occup. Environ. Med.* **61,** 358–362.

Collman, J. P., Hampton, P. D., and Brauman, J. I. (1986). Stereochemical and mechanistic studies of the ‘‘suicide’’ event in biomimetic P-450 olefin epoxidation. *J. Am. Chem. Soc.* **108,** 7862–7864.

Collman, J. P., Hampton, P. D., and Brauman, J. I. (1990). Suicide inactivation of cytochrome P-450 model compounds by terminal olefins. 1. A mechanistic study of heme N-alkylation and epoxidation. *J. Am. Chem. Soc.* **112,** 2977–2986.

Correia, M. M. and Ortiz de Montellano, P. R. (2005). Inhibition of cytochrome P450 enzymes. In: Cytochrome P450: Structure, Mechanism, and Biochemistry (Ortiz de Montellano P. R., ed.), Kluwer Academic/Plenum Publishers, New York.

Court, M. H., Von Moltke, L. L., Shader, R. I., and Greenblatt, D. J. (1997). Biotransformation of chlorzoxazone by hepatic microsomes from humans and ten other mammalian species. *Biopharm. Drug Dispos.* **18,** 213–226.

Csanády, Gy. A., Denk, B., Pütz, C., Kreuzer, P. E., Kessler, W., Baur, C., Gargas, M. L., and Filser, J. G. (2000). A physiological toxicokinetic model for exogenous and endogenous ethylene and ethylene oxide in rat, mouse, and human: formation of 2-hydroxyethyl adducts with hemoglobin and DNA. *Toxicol. Appl. Pharmacol.* **165,** 1–26.

Csanády, Gy. A., Guengerich, F. P., and Bond, J. A. (1992). Comparison of the biotransformation of 1,3-butadiene and its metabolite, butadiene monoepoxide, by hepatic and pulmonary tissues from humans, rats and mice. *Carcinogenesis* **13,** 1143–1153.

Csanády, Gy. A. and Filser, J. G. (2007). A physiological toxicokinetic model for inhaled propylene oxide in rat and human with special emphasis on the nose. *Toxicol. Sci.* **95,** 37–62.

Csanády, Gy. A., Mendrala, A. L., Nolan, R. J., and Filser, J. G. (1994). A physiologic pharmacokinetic model for styrene and styrene-7,8-oxide in mouse, rat and man. *Arch. Toxicol.* **68,** 143–157.

De Bont, J. A. M. and Albers, R. A. J. M. (1976). Microbial metabolism of ethylene. (1976). *Antonie van Leeuwenhoek* **42,** 73–80.

De Matteis F. (1971). Loss of haem in rat liver caused by the porphyrogenic agent 2-allyl-2-isopropylacetamide. *Biochem. J.* **124,** 767–77.

Dellarco, V. L., Generoso, W. M., Sega, G. A., Fowle, J. R., 3rd, and Jacobson-Kram, D. (1990). Review of the mutagenicity of ethylene oxide. *Environ. Mol. Mutagen.* **16,** 85–103.

Dent, J. G. and Schnell, S. R. (1981). Inhibition of microsomal-membrane bound and purified epoxide hydrolase by C2-C8 1,2-alkene oxides. *Biochem. Pharmacol.* **30,** 1712–1714.

DFG (1993). Deutsche Forschungsgemeinschaft. Ethylen. In: Gesundheitsschädliche Arbeitsstoffe. Toxikologisch-arbeitmedizinische Begründungen von MAK-Werten, Wiley-VCH, Weinheim.

Dunkelberg, H. (1981). Carcinogenic activity of ethylene oxide and its reaction products 2-chloroethanol, 2-bromoethanol, ethylene glycol and diethylene glycol. I. Carcinogenicity of ethylene oxide in comparison with 1,2-propylene oxide after subcutaneous administration in mice. *Zentralbl. Bakteriol. Mikrobiol. Hyg. B* **174,** 383–404.

Dunkelberg, H. (1982). Carcinogenicity of ethylene oxide and 1,2-propylene oxide upon intragastric administration to rats. *Br. J. Cancer* **46,** 924–933.

Duus, U., Osterman-Golkar, S., Törnqvist, M., Mowrer, J., Holm, S., and Ehrenberg, L. (1989). Studies of determinants of tissue dose and cancer risk from ethylene oxide exposure. Proceedings of the Symposium on Management of Risk from Genotoxic Substances in the Environment. Solna, 1989, pp. 141–153.

Ehrenberg, L., Hiesche, K. D., Osterman-Golkar, S., and Wenneberg, I. (1974). Evaluation of genetic risks of alkylating agents: tissue doses in the mouse from air contaminated with ethylene oxide. *Mutat. Res.* **24,** 83–103.

Ehrenberg, L., Osterman-Golkar, S., Segerbäck, D., Svensson, K., and Calleman, C. J. (1977). Evaluation of genetic risks of alkylating agents. III. Alkylation of haemoglobin after metabolic conversion of ethene to ethene oxide in vivo. Mutat. Res. 45, 175–184.

Eide, I., Hagemann, R., Zahlsen, K., Tareke, E., Törnqvist, M., Kumar, R., Vodicka, P., and Hemminki, K. (1995). Uptake, distribution, and formation of hemoglobin and DNA adducts after inhalation of C2-C8 1-alkenes (olefins) in the rat. *Carcinogenesis* **16,** 1603–1609.

Erbach, E. (2010). Toxikokinetische Studien zur Bildung von Ethylenoxid aus Ethylen bei männlichen Sprague-Dawley- und Fischer-344-Ratten. PhD thesis, Lehrstuhl für Chemische Lebensmitteltechnologie and Institut für Toxikologie und Umwelthygiene, Technische Universität München.

Eyer, F. and Podhradsky, D. (1986). Evaluation of the micromethod for determination of glutathione using enzymatic cycling and Ellman's reagent. *Anal. Biochem.* **153,** 57–66.

Faller, T. H. (1998). Unterschungen zur Toxikokinetik von Propenoxid:
– Glutathionkonzentrationen in Leber und Nasenmucosa exponierter Ratten
– Kinetik in Zellfraktionen aus Leber und Lunge von Ratte, Maus und Mensch sowie aus Nasenmucosa der Ratte. PhD thesis, Fakultät für Chemie, Biologie und Geowissenschaften, Technische Universität München.

Faller, T. H., Csanády, G. A., Kreuzer, P. E., Baur, C. M., and Filser, J. G. (2001). Kinetics of propylene oxide metabolism in microsomes and cytosol of different organs from mouse, rat, and humans. *Toxicol. Appl. Pharmacol.* **172,** 62–74.

Farmer, P. B., Sepai, O., Lawrence, R., Autrup, H., Sabro Nielsen, P., Vestergård, A. B., Waters, R., Leuratti, C., Jones, N. J., Stone, J., Baan, R. A., van Delft, J. H. M., Steenwinkel, M. J. S. T., Kyrtopoulos, S. A., Souliotis, V. L., Theodorakopoulos, N., Bacalis, N. C., Natarajan, A. T., Tates, A. D., Haugen, A., Andreassen, Å., Øvrebø, S., Shuker, D. E. G., Amaning, K. S., Schouft, A., Ellul, A., Garner, R. C., Dingley, K. H., Abbondandolo, A., Merlo, F., Cole, J., Aldrich, K., Beare, D., Capulas, E., Rowley, G., Waugh, A. P. W., Povey, A. C., Haque, K., Kirsch-Volders, M., van Hummelen, P., and Castelain, P. (1996). Biomonitoring human exposure to environmental carcinogenic chemicals. *Mutagenesis* **11,** 363–381.

Fennell, T. R. and Brown, C. D. (2001). A physiologically based pharmacokinetic model for ethylene oxide in mouse, rat, and human. *Toxicol. Appl. Pharmacol.* **173,** 161–175.

Fennell, T. R., MacNeela, J. P., Morris, R. W., Watson, M., Thompson, C. L., and Bell, D. A. (2000). Hemoglobin adducts from acrylonitrile and ethylene oxide in cigarette smokers: effects of *glutathione S-transferase T1*-null and *M1*-null genotypes. *Cancer Epidemiol. Biomarkers Prev.* **9,** 705–712.

Fennell, T. R., Snyder, R. W., Parkinson, C., Murphy, J., and James, R. A. (2004). The effect of ethylene exposure on ethylene oxide in blood and on hepatic cytochrome P450 in Fischer rats. *Toxicol. Sci.* **81,** 7–13.

Ferris, G. M. and Clark, J. B. (1971). Nicotinamide nucleotide synthesis in regenerating rat liver. *Biochem. J.* **131,** 655–662.

Feuers, R. J. Weindruch, R., Leakey, J. E. A., Duffy, P. H., and Hart, R. W. (1997) Increased effective activity of rat liver catalase by dietary restriction. *Age* **20,** 215–220.

Filser, J. G. (1992). The closed chamber technique-uptake, endogenous production, excretion, steady-state kinetics and rates of metabolism of gases and vapors. *Arch. Toxicol.* **66,** 1–10.

Filser, J. G. and Bolt, H. M. (1983). Exhalation of ethylene oxide by rats on exposure to ethylene. *Mutat. Res.* **120,** 57–60.

Filser, J. G. and Bolt, H. M. (1984). Inhalation pharmacokinetics based on gas uptake studies. VI. Comparative evaluation of ethylene oxide and butadiene monoxide as exhaled reactive metabolites of ethylene and 1,3-butadiene in rats. *Arch. Toxicol.* **55,** 219-223.

Filser, J. G., Denk, B., Tornqvist, M., Kessler, W., and Ehrenberg, L. (1992). Pharmacokinetics of ethylene in man; body burden with ethylene oxide and hydroxyethylation of hemoglobin due to endogenous and environmental ethylene. *Arch. Toxicol.* **66,** 157–163.

Filser, J. G., Kreuzer, P. E., Greim, H., and Bolt, H. M. (1994). New scientific arguments for regulation of ethylene oxide residues in skin-care products. *Arch. Toxicol.* **68,** 401–405.

Filser, J. G., Schwegler, U., Csanády, Gy. A., Greim, H., Kreuzer, P. E., and Kessler, W. (1993). Species-specific pharmacokinetics of styrene in rat and mouse. *Arch. Toxicol.* **67,** 517–530.

Fishbein, L. (1979). Potential halogenated industrial carcinogenic and mutagenic chemicals III. Alkane halides, alkanols and ethers. *Sci. Total Environ.* **11,** 223–257.

Fontana, E., Dansette, P. M., and Poli, S. M. (2005). Cytochrome P450 enzymes mechanism based inhibitors: common sub-structures and reactivity. *Curr. Drug Metab.* **6,** 413–54.

Föst, U., Hallier, E., Ottenwälder, H., Bolt, H. M., and Peter, H. (1991). Distribution of ethylene oxide in human blood and its implications for biomonitoring. *Hum. Exp. Toxicol.* **10,** 25–31.

Föst, U., Törnqvist, M., Leutbecher, M., Granath, F., Hallier, E., and Ehrenberg, L. (1995). Effects of variation in detoxification rate on dose monitoring through adducts. *Hum. Exp. Toxicol.* **14,** 201–203.

Fraenkel-Conrat, H. (1944). The action of 1,2-epoxides on proteins. J. Biol. Chem. **152,** 227–238.

Frank, H., Hintze, T., Bimboes, D., and Remmer, H. (1980). Monitoring lipid peroxidation by breath analysis: endogenous hydrocarbons and their metabolic elimination. *Toxicol. Appl. Pharmacol.* **56,** 337–344.

Fu, P. C., Zic, V., and Ozimy, K., (1979). Studies of ethylene-forming system in rat liver extract. *Biochim. biophys. Acta* **585,** 427–434.

Garman, R. H., Snellings, W. M., and Maronpot, R. R. (1985). Brain tumors in F344 rats associated with chronic inhalation exposure to ethylene oxide. *Neurotoxicology* **6,** 117–137.

Ghanbari, F., Rowland-Yeo, K., Bloomer, J. C., Clarke, S. E., Lennard, M. S., Tucker, G. T., and Rostami-Hodjegan, A. (2006). A critical evaluation of the experimental design of studies of mechanism based enzyme inhibition, with implications for *in vitro-in vivo* extrapolation. *Curr. Drug Metab.* **7,** 315–334.

Goldberg, L. (1986). Hazard Assessment of Ethylene Oxide. CRC Press, Boca Raton, Florida.

Gomez, G. A., Morisseau, C., Hammock, B. D, and Christianson, D. W. (2004). Structure of human epoxide hydrolase reveals mechanistic inferences on bifunctional catalysis in epoxide and phosphate ester hydrolysis. *Biochemistry* **43,** 4716–4723.

Guengerich, F. P. (2001). Common and uncommon cytochrome P450 reactions related to metabolism and chemical toxicity. *Chem. Res. Toxicol.* **14,** 611–650.

Guengerich, F. P., Kim, D. H., and Iwasaki, M. (1991). Role of human cytochrome P-450 IIE1 in the oxidation of many low molecular weight cancer suspects. *Chem. Res. Toxicol.* **4,** 168–179.

Greim, H. and Filser, J. (1994). Risikoabschätzung in der Toxikologie. In: Fremdstoffmetabolismus und Klinische Pharmakologie (Dengler, H. J. and Mutschler, E., eds.), Gustav Fischer Verlag, Stuttgart.

Hagmar, L., Mikoczy, Z., and Welinder, H. (1995). Cancer incidence in Swedish sterilant workers exposed to ethylene oxide. *Occup. Environ. Med.* **52,** 154–156.

Hallier, E., Langhof, T., Dannappel, D., Leutbecher, M., Schröder, K., Goergens, H. W., Müller, A., and Bolt, H. M. (1993). Polymorphism of glutathione conjugation of methyl bromide, ethylene oxide and dichloromethane in human blood: influence on the induction of sister chromatid exchanges (SCE) in lymphocytes. *Arch. Toxicol.* **67,** 173–178.

Hamm, T. E., Guest, D., and Dent, J. G. (1984). Chronic toxicity and oncogenicity bioassay of inhaled ethylene in Fischer-344 rats. *Fundam. Appl. Toxicol.* **4,** 473–478.

Haufroid, V., Merz, B., Hofmann, A., Tschopp, A., Lison, D., and Hotz, P. (2007). Exposure to ethylene oxide in hospitals: Biological monitoring and influence of glutathione S-transferase and epoxide hydrolase polymorphisms. *Cancer Epidemiol. Biomarkers Prev*. **16,** 796–802.

Hopkins, N. E., Foroozesh, M. K., and Alworth, W. L. (1992). Suicide inhibitors of cytochrome P450 1A1 and P450 2B1. *Biochem. Pharmacol.* **44,** 787–796.

Högstedt, L. C. (1988) Epidemiological studies on ethylene oxide and cancer: An updating. In: Bartsch, H., Hemminki, K. & O'Neill, I.K., eds, *Methods for Detecting DNA Damaging Agents in Humans: Applications in Cancer Epidemiology and Prevention* (IARC Scientific Publications No. 89), Lyon, IARC, pp. 265–270.

Högstedt, C., Rohlen, O., Berndtsson, B. S., Axelson, O., and Ehrenberg, L. (1979). A cohort study of mortality and cancer incidence in ethylene oxide production workers. *Br. J. Ind. Med.* **36,** 276–280.

IARC (1994a). International Agency for Research on Cancer. Ethylene. In: Some Industrial Chemicals. *IARC Monogr. Eval. Carcinog. Risks Hum.* **60,** 45–71.

IARC (1994b). International Agency for Research on Cancer. Ethylene oxide. In: Some Industrial Chemicals. *IARC Monogr. Eval. Carcinog. Risks Hum.* **60,** 73–159.

IARC (2008). Ethylene oxide. In: 1,3-Butadiene, Ethylene Oxide and Vinyl Halides (Vinyl Fluoride, Vinyl Chloride and Vinyl Bromide) (International Agency for Research on Cancer, ed.) *IARC Monogr. Eval. Carcinog. Risks Hum.* **97,** 185–309.

IHS (2011a). World petrochemical report on ethylene. *http://www.sriconsulting.com/WP/Public/Reports/ethylene* (downloaded on Oct. 20, 2011).

IHS (2011b). World petrochemical report on ethylene oxide. *http://www.sriconsulting.com/WP/Public/Reports/eo* (downloaded on Sep. 30, 2011).

Johanson, G. and Filser, J. G. (1993). A physiologically based pharmacokinetic model for butadiene and its metabolite butadiene monoxide in rat and mouse and its significance for risk extrapolation. *Arch. Toxicol*. **67,** 151–163.

Johanson, G. and Filser, J. G. (1992). Experimental data from closed chamber gas uptake studies in rodents suggest lower uptake rate of chemical than calculated from literature values on alveolar ventilation. *Arch. Toxicol*. **66,** 291–295.

Jones, A. R. and Wells, G. (1981). The comparative metabolism of 2-bromoethanol and ethylene oxide in the rat. *Xenobiotica* **11,** 763–770.

Jurczuk, M., Moniuszko-Jakoniuk, J., and Rogalska, J. (2006). Glutathione-related enzyme activity in kiver and kidney of rats exposed to cadmium and ethanol. *Polish J. of Environ. Sud.* **15,** 861–868.

Kardos, L., Széles, G., Gombkötö, G., Szeremi, M., Tompa, A., and Ádány, R. (2003). Cancer deaths among hospital staff potentially exposed to ethylene oxide: An epidemiological analysis. *Environ. Mol. Mutagen.* **42,** 59–60.

Kautiainen, A., Törnqvist, M., Anderstam, B., and Vaca, C. E. (1991). *In vivo* hemoglobin dosimetry of malonaldehyde and ethene in mice after induction of lipid peroxidation. Effects of membrane lipid fatty acid composition. *Carcinogenesis* **12,** 1097–1102.

Kessler, W. and Remmer, H. (1990). Generation of volatile hydrocarbons from amino acids and proteins by an iron/ascorbate/GSH system. *Biochem. Pharmacol*. **39,** 1347–1351.

Kiesselbach, N., Ulm, K., Lange, H.J., and Korallus, U. (1990). A multicentre mortality study of workers exposed to ethylene oxide. *Br. J. ind. Med.* **47,** 182–188.

Kolman, A., Chovanec, M., and Osterman-Golkar, S. (2002). Genotoxic effects of ethylene oxide, propylene oxide and epichlorohydrin in humans: update review (1990-2001). *Mutat. Res.* **512,** 173–194.

Kreuzer, P. E., Kessler, W., Welter, H. F., Baur, C., and Filser, J. G. (1991). Enzyme specific kinetics of 1,2-epoxybutene-3 in microsomes and cytosol from livers of mouse, rat, and man. *Arch. Toxicol.* **65,** 59–67.

Krishnan, K., Gargas, M. L., Fennell, T. R., and Andersen, M. E. (1992). A physiologically based description of ethylene oxide dosimetry in the rat. *Toxicol. Ind. Health* **8,** 121–140.

Lawrence, G. D. and Cohen, G. (1985). *In vivo* production of ethylene from 2-keto-4-methylthiobutyrate in mice. *Biochem. Pharmacol.* **34,** 3231–3236.

Lewis, D. F. V., Bird, M. G., and Parke, D. V. (1997). Molecular modeling of CYP2E1 enzymes from rat, mouse and man: An explanation for species differences in butadiene metabolism and potential carcinogenicity, and rationalization of CYP2E substrate specificity. *Toxicology* **118,** 93–113.

Li, B., Shen, Y., and Li, B. (2008). Quasi-steady-state laws in enzyme kinetics. *J. Phys. Chem. A* **112,** 2311–2321.

Li, F., Segal, A., and Solomon, J. J. (1992). *In vitro* reaction of ethylene oxide with DNA and characterization of DNA adducts. *Chem.-biol. Interact.*, **83,** 35–54

Lide, D. R. (2006). CRC Handbook of Chemistry and Physics, 86th edition 2005-2006. CRC Press, Taylor and Francis, Boca Raton, Florida.

Lieberman, M., Kunishi, A. T., Mapson, L. W., and Wardale D. A. (1965). Ethylene production from methionine. *Biochem. J*. **97,** 449–459.

Loaharanu, P. (2003). Irradiated foods. Fifth edition. American Council on Science and Health. New York. *http://www.acsh.org/docLib/20040331_irradiated2003.pdf* (downloaded on Oct. 20, 2011).

Lynch, D. W., Lewis, T. R., Moorman, W. J., Burg, J. R., Groth, D. H., Khan, A., Ackerman, L. J., and Cockrell, B. Y. (1984). Carcinogenic and toxicologic effects of inhaled ethylene oxide and propylene oxide in F344 rats. *Toxicol. Appl. Pharmacol.* **76,** 69–84.

Mansuy, D., Leclaire, J., Fontecave, M., and Momenteau, M. (1984). Oxidation of monosubstituted olefins by cytochromes P-450 and heme models: evidence for the formation of aldehydes in addition to epoxides and allylic alcohols. *Biochem. Biophys. Res. Commun.* **119,** 319–325.

Maples, K. R. and Dahl, A. R. (1993). Levels of epoxides in blood during inhalation of alkenes and alkene oxides. *Inhal. Toxicol.* **5,** 43–54.

Martis, L., Kroes, R., Darby, T. D., and Woods, E. F. (1982). Disposition kinetics of ethylene oxide, ethylene glycol, and 2-chlorethanol in the dog. *J. Toxicol. environ. Health* **10,** 847–856.

Mayhew, B. S., Jones, D. R., and Hall, S. D. (2000). An *in vitro* model for predicting *in vivo* inhibition of cytochrome P450 3A4 by metabolic intermediate complex formation. *Drug Metab. Dispos.* **28,** 1031–1037.

McKelvey, J. A. and Zemaitis, M. A. (1986). The effects of ethylene oxide (EO) exposure on tissue glutathione levels in rats and mice. *Drug Chem. Toxicol.* **9,** 51–66.

Meek, M. E., Renwick, A., Ohanian, E., Dourson, M., Lake, B., Naumann, B. D., and Vu, V. (2002). Guidelines for application of chemical-specific adjustment factors in dose/concentration–response assessment. *Toxicology* **181–182,** 115–120.

Mendes, G. C. C., Brandao, T. R. S., and Silva, C. L. M. (2007). Ethylene oxide sterilization of medical devices: a review. *Am. J. Infect. Control* **35,** 574–81.

Mullis, K., Faloona, F., Scharf, S., Saiki, R., Horn, G., and Erlich, H. (1986). Specific enzymatic amplification of DNA *in vitro*: The polymerase chain reaction. *Cold Spring Harbor Symp. Quant. Biol.* **51,** 263–273.

NIOSH (2001). National Institute for Occupational Safety and Health. International chemical safety cards. Ethylene oxide, ICSC: 0155. *http://www.cdc.gov/niosh/ipcsneng/neng0155.html* (downloaded on February 16, 2011).

NIOSH (2009). National Institute for Occupational Safety and Health. International chemical safety cards. Propylene oxide, ICSC: 0192. *http://www.cdc.gov/niosh/ipcsneng/neng0192.html* (downloaded on February 16, 2011).

Norman, S. A., Berlin, J. A., Soper, K. A., Middendorf, B. F., and Stolley, P. D. (1995). Cancer incidence in a group of workers potentially exposed to ethylene oxide. *Int. J. Epidemiol.* **24,** 276–284.

NOVA Chemicals (2007). Product risk profile ethylene. *http://www.novachem.com/socialresp/prodsteward/docs/RP/ETHYLENERP.pdf* (downloaded on Sep. 13, 2011).

NTP, National Toxicology Program (1987). Toxicology and Carcinogenesis Studies of Ethylene Oxide (CAS No. 75-21-8) in B6C3F1 Mice (Inhalation Studies). *Natl. Toxicol. Program Tech. Rep. Ser.* **326,** 1–114.

OECD (1998). Organization for Economic Cooperation and Development. Ethylene. Screening Information Datasets (SIDS) for High Production Volume Chemicals. United Nations Environmental Programme (UNEP) Publications. *http://www.chem.unep.ch/irptc/sids/oecdsids/74851.pdf* (downloaded on Sept. 12, 2011).

Oesch, F., Kaubisch, N., Jerina, D. M, and Daly, J. W. (1971). Hepatic epoxide hydrase. Structure-activity relationships for substrates and inhibitors. *Biochemistry* **10,** 4858–4866.

Ortiz de Montellano, P. R., Beilan, H. S., Kunze, K. L., and Mico, B. A. (1981). Destruction of cytochrome P-450 by ethylene. Structure of the resulting prosthetic heme adduct. *J. Biol. Chem.* **256,** 4395–4399.

Ortiz de Montellano, P. R. and Correia, M. A. (1983). Suicidal destruction of cytochrome P-450 during oxidative drug metabolism. *Ann. Rev. Pharmacol. Toxicol.* **23,** 481–503.

Ortiz de Montellano, P. R. and Mico, B. A. (1980). Destruction of cytochrome *P-450* by ethylene and other olefins. *Mol. Pharmacol.* **18,** 128–135.

Osterman-Golkar, S., and Ehrenberg, L. (1982). Covalent binding of reactive intermediates to hemoglobin as an approach for determining the metabolic activation of chemicals – ethylene. *Drug Metabol. Rev.* **13,** 647–660.

Osterman-Golkar, S., Ehrenberg, L., Segerbäck, D., and Hällström, I. (1976). Evaluation of genetic risks of alkylating agents. II. Haemoglobin as a dose monitor. *Mutat. Res.* **34,** 1–10.

Osterman-Golkar, S., Farmer, P. B., Segerbäck, D., Bailey, E., Calleman, C. J., Svensson, K., and Ehrenberg, L. (1983). Dosimetry of ethylene oxide in the rat by quantitation of alkylated histidine in hemoglobin. *Teratog. Carcinog. Mutag.* **3,** 395–405.

Peqlab (2009). Direct PCR Lysis Reagent Tail_Manual. *http://www.peqlab.de/wcms/de/pdf/31-103-T_m.pdf* (downloaded on May 3, 2009).

Peter, R., Boecker, R., Beaune, P. H., Iwasaki, M., Guengerich, F. P., and Yang, C. S. (1990). Hydroxylation of chlorzoxazone as a specific probe for human liver cytochrome P-450IIE1. *Chem. Res. Toxicol.* **3,** 566–573.

Popp, W., Wahrenholz, C., Przygoda, H., Brauksiepe, A., Goch, S., Müller, G., Schell, C., and Norporth, K. (1994). DNA–protein cross-links and sister chromatid exchange frequencies in lymphocytes and hydroxyethyl mercapturic acid in urine of ethylene oxide-exposed hospital workers. *Int. Arch. occup. environ. Health*, **66,** 325–332.

Potter, D., Blair, D., Davies, R., Watson, W. P., and Wright, A. S. (1989). The relationship between alkylation of haemoglobin and DNA in Fischer 344 rats exposed to [^{14}C]ethylene oxide. *Arch. Toxicol. Suppl.* **13,** 254–257.

Ram Chandra, G. and Spencer, M. (1963). A micro-apparatus for absorption of ethylene and its use in determination of ethylene in exhaled gases from human subjects. *Biochim. Biophys. Acta.* **69,** 423–425.

Regal, K. A., Schrag, M. L., Kent, U. M., Wienkers, L. C., and Hollenberg, P. F. (2000). Mechanism-based inactivation of cytochrome P450 2B1 by 7-ethynylcoumarin: verification of apo-P450 adduction by electrospray ion trap mass spectrometry. *Chem. Res. Toxicol.* **13,** 262–270.

Ribeiro, L. R., Salvadori, D. M., Rios, A. C., Costa, S. L., Tates, A. D., Törnqvist, M., and Natarajan, A. T. (1994). Biological monitoring of workers occupationally exposed to ethylene oxide. *Mutat. Res.* **313,** 81–87.

Rusyn, I., Asakura, S., Li, Y., Kosyk, O., Koc, H., Nakamura, J., Upton, P. B., and Swenberg, J. A. (2005). Effects of ethylene oxide and ethylene inhalation on DNA adducts, apurinic/apyrimidinic sites and expression of base excision DNA repair genes in rat brain, spleen, and liver. *DNA Repair* **4,** 1099–1110.

Sagai M. and Ichinose T. (1980). Age-related changes in lipid peroxidation as measured by ethane, ethylene, butane, and pentane in respired gases of rats. *Life Sciences* **27,** 731–738.

Sachs, L. (1973). *Angewandte Statistik; Planung und Auswertung; Methoden und Modelle*. Fourth edition. Springer-Verlag, Berlin.

Sarto, F., Clonfero, E., Bartolucci, G. B., Franceschi, C., Chiricolo, M., and Levis, A. G. (1987). Sister chromatid exchanges and DNA repair capability in sanitary workers exposed to ethylene oxide: evaluation of the dose–effect relationship. *Am. J. Ind. Med*. **12,** 625–637.

Sarto, F., Cominato, I., Pinton, A. M., Brovedani, P. G., Faccioli, C. M., Bianchi, V., and Levis, A. G. (1984). Cytogenetic damage in workers exposed to ethylene oxide. *Mutat. Res.* **138,** 185–195.

Sarto, F., Törnqvist, M. A., Tomanin, R., Bartolucci, G. B., Osterman-Golkar, S. M., and Ehrenberg, L. (1991). Studies of biological and chemical monitoring of low-level exposure to ethylene oxide. *Scand. J. Work. Environ. Health* **17,** 60–64.

Sawada, S., and Totsuka, T. (1986). Natural and anthropogenic sources and fate of atmospheric ethylene. *Atmospheric Environment* **20,** 821.

Sayer, J. M., Yagi, H., van Bladeren, P. J., Levin, W., and Jerina, D. M. (1985). Stereoselectivity of microsomal epoxide hydrolase toward diol epoxides and tetrahydroepoxides derived from benz[a]anthracene. *J. Biol. Chem.* **260,** 1630–1640.

Schmiedel, G., Filser, J. G., and Bolt, H. M. (1983). Rat liver microsomal transformation of ethene to oxirane *in vitro*. *Toxicol. Lett*. **19,** 293–297.

Schulte, P. A., Walker, J. T., Boeniger, M. F., Tsuchiya, Y., and Halperin, W. E. (1995). Molecular, cytogenetic, and hematologic effects of ethylene oxide on female hospital workers. *J. Occup. Environ. Med.* **37,** 313–320.

SCOEL (2009). Recommendation from the Scientific Committee on Occupational Exposure Limits. Risk assessment for ethylene oxide. European Commission's DG for Employment, Social Affairs and Inclusion. Brussels, Belgium.

Seaton, M. J., Follansbee, M. H., and Bond, J. A. (1995). Oxidation of 1,2-epoxy-3-butene to 1,2:3,4-diepoxybutane by cDNA-expressed human cytochromes P450 2E1 and 3A4 and human, mouse and rat liver microsomes. *Carcinogenesis* **16,** 2287–2293.

Sega, G. A., Brimer, P. A., and Generoso, E. E. (1991). Ethylene oxide inhalation at different exposure-rates affects binding levels in mouse germ cells and hemoglobin. Possible explanation for the effect. *Mutat. Res.* **249,** 339–349.

Segerbäck, D. (1983). Alkylation of DNA and hemoglobin in the mouse following exposure to ethene and ethene oxide. *Chem. Biol. Interact.* **45,** 139–151.

Segerbäck, D. (1990). Reaction products in hemoglobin and DNA after *in vitro* treatment with ethylene oxide and *N*-(2-hydroxyethyl)-*N*-nitrosourea. *Carcinogenesis*, **11,** 307–312.

Shaik, S. and de Visser, S. P. (2005). Computational approaches to cytochrome P450 function. In: Cytochrome P450: Structure, Mechanism, and Biochemistry (Ortiz de Montellano P. R., ed.), pp. 531–535, Kluwer Academic/Plenum Publishers, New York.

Shaik, S., de Visser, S. P., Ogliaro, F., Schwarz, H., and Schröder, D. (2002). Two-state reactivity mechanisms of hydroxylation and epoxidation by cytochrome P-450 revealed by theory. *Curr. Opin. Chem. Biol.* **6,** 556–567.

Shen, J., Kessler, W., Denk, B., and Filser, J. G. (1989). Metabolism and endogenous production of ethylene in rat and man. *Arch. Toxicol. Suppl.* **13,** 237–239.

Snellings, W. M., Weil, C. S., and Maronpot, R. R. (1984). A two-year inhalation study of the carcinogenic potential of ethylene oxide in Fischer 344 rats. *Toxicol. Appl. Pharmacol.* **75,** 105–117.

Stayner, L., Steenland, K., Greife, A., Hornung, R., Hayes, R. B., Nowlin, S., Morawetz, J., Ringenburg, V., Elliot, L., and Halperin, W. (1993). Exposure–response analysis of cancer mortality in a cohort of workers exposed to ethylene oxide. *Am. J. Epidemiol*. **138,** 787–798.

Steenland, K., Stayner, L., and Deddens, J. (2004). Mortality analyses in a cohort of 18235 ethylene oxide exposed workers: follow up extended from 1987 to 1998. *Occup. Environ. Med.* **61,** 2–7.

Summer, K. H. and Greim, H. (1980). Detoxification of chloroprene (2-chloro-1,3-butadiene) with glutathione in the rat. *Biochem. Biophys. Res. Commun.* **96,** 566–573.

Tardif, R., Goyal, R., Brodeur, J., and Gérin, M. (1987). Species differences in the urinary disposition of some metabolites of ethylene oxide. *Fundam. Appl. Toxicol*. **9,** 448–453.

Tates, A. D., Grummt, T., Törnqvist, M., Farmer, P. B., van Dam, F. J., van Mossel, H., Schoemaker, H. M., Osterman-Golkar, S., Uebel, C., Tang, Y. S., Zwinderman, A. H., Natarajan, A. T., and Ehrenberg, L. (1991). Biological and chemical monitoring of occupational exposure to ethylene oxide. *Mutat. Res.* **250,** 483–497.

The Jackson Laboratory (2009). *http://jaxmice.jax.org/protocolsdb/f?p=116:2:2320994040584437::NO:2:P2_MASTER_PROTOCOL_ID,P2_JRS_CODE:569,002910* (downloaded on May 3, 2009).

Törnqvist, M. (1994). Is ambient ethene a cancer risk factor? *Environ. Health Perspect.* **102** (Suppl. 4)**,** 157–160.

Törnqvist, M. A., Almberg, J. G., Bergmark, E. N., Nilsson, S., and Osterman-Golkar, S. M. (1989b). Ethylene oxide doses in ethene-exposed fruit store workers. *Scand. J. Work Environ. Health* **15,** 436–438.

Törnqvist, M., Gustafsson, B., Kautiainen, A., Harms-Ringdahl, M., Granath, F. and Ehrenberg, L. (1989a). Unsaturated lipids and intestinal bacteria as sources of endogenous production of ethene and ethylene oxide. *Carcinogenesis* **10,** 39–41.

Törnqvist, M., Osterman-Golkar, S., Kautiainen, A, Jensen, S., Farmer, P. B., and Ehrenberg, L. (1986). Tissue doses of ethylene oxide in cigarette smokers determined from adduct levels in hemoglobin. Carcinogenesis **7,** 1519–1521.

van Sittert, N. J., Beulink G. D. J., van Vliet E. W. N., and van der Waal, H., (1993). Monitoring occupational exposure to ethylene oxide by the determination of hemoglobin adducts. *Environ. Health Perspect.* **99,** 217–220.

Van Sittert, N. J., Boogaard, P. J., Natarajan, A. T., Tates, A. D., Ehrenberg, L. G., and Törnqvist, M. A. (2000). Formation of DNA adducts and induction of mutagenic effects in rats following 4 weeks inhalation exposure to ethylene oxide as a basis for cancer risk assessment. *Mutat. Res.* **447,** 27–48.

Veech, R. L., Eggleston, L. V., and Krebs, H. A. (1969). The redox state of free nicotinamide-adenine dinucleotide phosphate in the cytoplasm of rat liver. *Biochem. J.* **115,** 609–619.

Vergnes, J. S. and Pritts, I. M. (1994). Effects of ethylene on micronucleus formation in the bone marrow of rats and mice following four week of inhalation exposure. *Mutat. Res*. **324,** 87–91.

Victorin, K., and Ståhlberg, M. (1988). A method for studying the mutagenicity of some gaseous compounds in Salmonella typhimurium. *Environ. Mol. Mutagen.* **11,** 65–77.

Walker, V. E., Fennel, T. R., Upton, P. B., MacNeela, J. P., and Swenberg, J. A. (1993). Molecular dosimetry of DNA and hemoglobin adducts in mice and rats exposed to ethylene oxide. *Environ. Health Perspect.* **99,** 11–17.

Walker, V. E., MacNeela, J. P., Swenberg, J. A., Turner, M. J., and Fennell, T. R. (1992a). Molecular dosimetry of ethylene oxide: Formation and persistence of N-(2-hydroxyethyl)valine in hemoglobin following repeated exposures of rats and mice. *Cancer Res*. **52,** 4320–4327.

Walker, V. E., Fennell, T. R., Upton, P. B., Skopek, T. R., Prevost, V., Shuker, D. E. G., and Swenberg, J. A. (1992b). Molecular dosimetry of ethylene oxide: Formation and persistence of 7-(2-hydroxyethyl)guanine in DNA following repeated exposures of rats and mice. *Cancer Res*. **52,** 4328–4334.

Walker, V. E., Wu, K. Y., Upton, P. B., Ranasinghe, A., Scheller, N., Cho, M. H., Vergnes, J. S., Skopek, T. R., and Swenberg, J. A. (2000). Biomarkers of exposure and effect as indicators of potential carcinogenic risk arising from *in vivo* metabolism of ethylene to ethylene oxide. *Carcinogenesis* **21,** 1661–1669.

Walsh, C. (1982). Suicide substrates: mechanism-based enzyme inactivators. *Tetrahedron* **38,** 871–909.

Walsky, R. L. and Obach, R. S. (2004). Validated assays for human cytochrome P450 activities. *Drug Metab. Dispos.* **32,** 647–660.

WHO (2003). *Ethylene Oxide* (Concise International Chemical Assessment Document 54), Geneva, World Health Organization. http://*www.who.int/entity/ipcs/publications/cicad/en/cicad54.pdf* (downloaded on Sept. 12, 2011).

WHO (2010). Characterization and application of physiologically based pharmacokinetic models in risk assessment (IPCS Harmonization project document 9). ISBN 978 92 4 150090 6. Geneva, World Health Organization 2010. *http://www.who.int/entity/ipcs/methods/harmonization/areas/pbpk_models.pdf* (downloaded on Oct. 19, 2011).

Wistuba, D. and Schurig, V. (1992). Enantio- and regioselectivity in the epoxide-hydrolase-catalyzed ring opening of simple aliphatic oxiranes: Part I: Monoalkylsubstituted oxiranes. *Chirality* **4,** 178–184.

Wu, K. Y., Chiang, S. Y., Shih, W. C., Huang, C. C., Chen, M. F., and Swenberg, J. A. (2011). The application of mass spectrometry in molecular dosimetry: ethylene oxide as an example. *Mass Spectrom. Rev.* **30,** 733–756.

Wu, K.-Y., Ranasinghe, A., Upton, P. B., Walker, V. E., and Swenberg, J. A. (1999b). Molecular dosimetry of endogenous and ethylene oxide-induced N7-(2-hydroxyethyl) guanine formation in tissues of rodents. *Carcinogenesis* **20,** 1787–1792.

Wu, K.-Y., Scheller, N., Ranasinghe, A., Yen, T.-Y., Sangaiah, R., Giese, R., and Swenberg, J. A. (1999a). A gas chromatography/electron capture/negative chemical ionization high-resolution mass spectrometry method for analysis of endogenous and exogenous N7-(2-hydroxyethyl)guanine in rodents and its potential for human biological monitoring. *Chem. Res. Toxicol.* **12,** 722–729.

Yong, L. C., Schulte, P. A., Wiencke, J. K., Boeniger, M. F., Connally, L. B., Walker, J. T., Whelan, E. A., and Ward, E. M. (2001). Hemoglobin adducts and sister chromatid exchanges in hospital workers exposed to ethylene oxide: effects of *glutathione S-transferase T1* and *M1* genotypes. *Cancer Epidemiol. Biomarkers Prev.* **10,** 539–550.

Yong, L. C., Schulte, P. A., Kao, C. Y., Giese, R. W., Boeniger, M. F., Strauss, G. H., Petersen, M. R., and Wiencke, J. K. (2007). DNA adducts in granulocytes of hospital workers exposed to ethylene oxide. *Am. J. Ind. Med.* **50,** 293–302.

Zimmermann, H. and Walzl, R. (2007). Ethylene. Ullman's Encyclopedia of Industrial Chemistry, Wiley-VCH, Weinheim.